

AD-A157 485

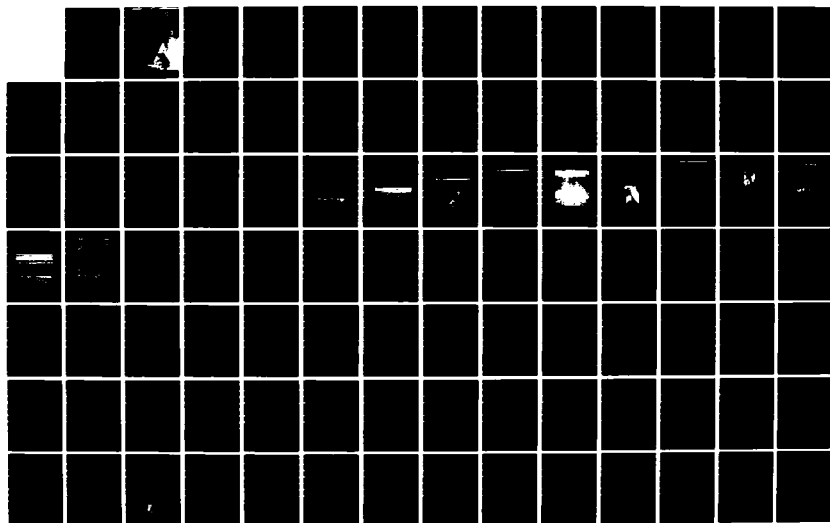
WORKSHOP ON PERMAFROST GEOPHYSICS HELD AT GOLDEN
COLORADO ON 23-24 OCTOBER 1984(U) COLD REGIONS RESEARCH
AND ENGINEERING LAB HANOVER NH J BROWN ET AL. MAY 85
CRREL-SR-85-5

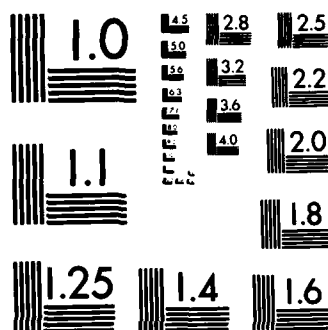
1/2

UNCLASSIFIED

F/G 8/12

NL





MICROCOPY RESOLUTION TEST CHART
NBS-1963-A

Special Report 85-5

May 1985

AD-A157 485



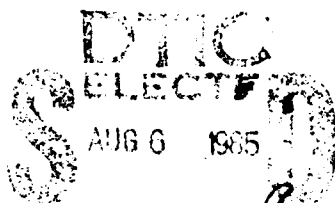
**US Army Corps
of Engineers**

Cold Regions Research &
Engineering Laboratory

Workshop on permafrost geophysics Golden, Colorado, 23-24 October 1984

J. Brown, M.C. Metz and P. Hoekstra, Editors

DTIC FILE COPY



Prepared in cooperation with
COMMITTEE ON PERMAFROST
POLAR RESEARCH BOARD
NATIONAL RESEARCH COUNCIL
WASHINGTON, D.C.



Approved for public release; distribution is unlimited.

85 : 7 30 064

Committee on Permafrost

Polar Research Board

National Research Council

Jerry Brown (Chairman), Cold Regions Research and Engineering Laboratory

Bernard Hallet, University of Washington

James A. Hunter, Geological Survey of Canada

Christopher E. Heuer, Exxon Production Research Company

Douglas L. Kane, University of Alaska

Raymond A. Kreig, R.A. Kreig and Associates

Michael C. Metz, GeoTec Services, Inc.

Ied S. Vinson, Oregon State University

David C. Esch, Liaison, Transportation Research Board

George Gryc, Liaison, U.S. Geological Survey

John Haugh, Liaison, Bureau of Land Management

C.W. Lovell, Liaison, American Society of Civil Engineers

Froy L. Péwé, Ex Officio, Arizona State University

Stuart E. Rawlinson, Liaison, Alaska Division of Geological and Geophysical
Surveys

Cover: Illustration courtesy of Geo-Physi-Con Co. Ltd.,
Calgary, Alberta, Canada.

PROGRAM*
WORKSHOP ON PERMAFROST GEOPHYSICS
Marriott Denver West Hotel
Golden, Colorado
23-24 October 1984

23 October (8:30 a.m.-Noon)

DEEP ONSHORE AND OFFSHORE PERMAFROST METHODS

Opening Remarks	Pieter Hoekstra
Permafrost Distribution in Northern Canada: Interpretation of Well-Logs	A. Judge, A. Taylor
Transient Electromagnetic Detection of Subsea Permafrost	G.G. Walker, K. Kawasaki, T.E. Osterkamp
Some Aspects of Interpreting Seismic Data for Information on Shallow Subsea Permafrost	K.G. Neave, P.V. Sellmann
Some Aspects of Transient Electromagnetic Soundings for Permafrost Delineation	G. Rozenberg, J.D. Henderson, A.N. Sartorelli, A. Judge
Subsea Permafrost: Field Mapping and Numerical/ Physical Modeling of Its Spatial Distribution in the Canadian Beaufort Sea	S.M. Blasco, D.L. Lewton

23 October (1:30-5:30 p.m.)

DEEP ONSHORE AND OFFSHORE PERMAFROST METHODS (Continued)

Deep Transient EM Sounding in the Mackenzie Delta, NWT, Canada	A.K. Sinha
Velocity-Depth Structure of Offshore Permafrost, Canadian Beaufort Sea	H.A. MacAulay, S.E. Pullan, J.A. Hunter
Some Aspects of Interpretation of Transient EM Data for Mapping Frozen Ground on the North Slope of Alaska	L.E. Evans
Galvanic Methods for Mapping Resistive Seabed Features	P.V. Sellmann, A.J. Delaney, S.A. Arcone
A Summary of Field Operations and Results of Three Years of Transient Surveys on the North Slope of Alaska	M.W. Blohm
Marine Permafrost Studies Related to Develop- ment of the Alaskan Beaufort Sea	L.J. Toimil
Well Logging in Permafrost	J.K. Peterson, K. Kawasaki, T.E. Osterkamp, J.H. Scott
Obtaining Precise Temperature Measurements in Abandoned Offshore Petroleum Exploration Wells	A. Taylor, A. Judge

*In this report the abstracts and papers are arranged alphabetically by senior author

24 October (8:30 a.m. - Noon)

SHALLOW GEOPHYSICAL AND BOREHOLE METHODS

Guest Speaker	George Keller
Monitoring Permafrost Ground Conditions with Ground Probing Radar (G.P.R.)	J.A. Pilon, A.P. Annan, J.L. Davis
Impulse Radar Sounding of Frozen Ground	A. Kovacs, R.M. Morey
Analysis of Wide-Angle Reflection and Refraction Measurements*	R.M. Morey, A. Kovacs
Shallow Induction Measurements in Permafrost Terrain	K. Kawasaki, T.E. Osterkamp
Dielectric Studies of Permafrost Using Cross-Borehole VHF Pulse Propagation	S.A. Arcone, A.J. Delaney
Thermal Properties from Borehole Heating: Experience in the Canadian Beaufort Sea, 1984	W.D. Harrison, J.L. Morack

24 October (1:00-4:30 p.m.)

SHALLOW GEOPHYSICAL METHODS AND TERRAIN ANALYSIS

Borehole Monitoring of Permafrost Electrical Properties	R.F. Corwin
Permafrost Temperature Measurements in an Alaskan Transect: Preliminary Results	T.E. Osterkamp, J.P. Gosink, K. Kawasaki
Medium Scale Maps of Permafrost and Ground Ice Conditions, Tuktoyaktuk and Illisarvik Areas, Western Arctic Coast, Canada	J.A. Heginbottom
Unfrozen Permafrost and Other Taliks	R.O. van Everdingen
Shallow Geophysical Borehole Logging in Permafrost: A Case History	R. Miller
Suggested Legend Terminology for Permafrost Mapping*	R.A. Kreig
A Digital Information System for Delineation of Discontinuous Permafrost*	H.B. Granberg

* Not formally presented.

OPENING REMARKS

Pieter Hoekstra
The Earth Technology Corporation
Golden, Colorado

The workshop is a good opportunity to review the progress that has been made in mapping permafrost by geophysical methods. Scanning papers and presentations at technical meetings, it is quite evident that progress never follows a smooth, consistent path, but comes in leaps and bounds as a result of real engineering needs.

The first critical demands on geophysical methods came during the initial designs of various proposed arctic gas pipelines. The preliminary designs called for chilled, buried lines. There was great reluctance to place even small sections of those lines above ground. The last point of cold flow was generally well into the discontinuous permafrost zone. It became evident that major mitigating measures needed to be adopted to prevent frost heaving where a chilled line was buried in a section of unfrozen ground. In fact the permafrost distribution needed to be delineated meter by meter. Experience on the Alyeska line had shown that permafrost mapping could not be satisfactorily accomplished by airphotos and drilling alone, but that an intermediate step in the exploration program was necessary. The geophysical method to a large extent developed in response to this need was magnetic induction profiling with the Geonics EM 31 and EM34. That method, when closely integrated with airphoto analysis and drilling, proved reliable and was used along several hundreds of miles of route (Sartorelli and French 1982). Although these methods were successful in delineating boundaries of frozen and unfrozen ground, they failed in mapping ice content.

The second need for permafrost mapping was late in coming. Seismic profiles on the North Slope frequently traverse water bodies, lakes, rivers and coastlines. It is common to observe rapid changes in permafrost distribution at these locations requiring corrections in seismic processing. The thickness of permafrost on the North Slope can be in excess of 2,000 feet. During this workshop several papers will show transient electromagnetic soundings applied to this problem. This is a development of the last few years (Ehrenbard et al. 1983).

With construction of offshore pipelines not far away, development and testing of marine towed direct current and high resolution seismic reflection

methods, for mapping the top of permafrost offshore, is in high gear (Corwin and Conti 1983).

One large requirement remains unsatisfied and that is a geophysical technique for measuring ice content of frozen soils. An obstacle to solving that problem is the fact that no consistent relation exists between ice content and electrical resistivity or seismic velocity. Such relations are also influenced by temperature and soil type.

REFERENCES

- Corwin, R.F. and U. Conti (1983) Sea-floor electrical resistivity measurements using a diver-operated system. Proceedings, Offshore Technology Conference, Vol. 1, p. I-637.
- Ehrenbard, R.L., P. Hoekstra and G. Rozenberg (1983) Transient electromagnetic soundings for permafrost mapping. Proceedings, Fourth International Conference on Permafrost. Washington, D.C.: National Academy Press, p. 272.
- Sartorelli, A.N. and R.B. French (1982) Electro-magnetic induction methods for mapping permafrost along northern pipeline corridors. Proceedings, Fourth Canadian Permafrost Conference (H.M. French, Ed.), National Research Council of Canada, Ottawa, p. 283-295.

DIELECTRIC STUDIES OF PERMAFROST USING CROSS-BOREHOLE
VHF PULSE PROPAGATION

Steven A. Arcone and Allan J. Delaney
Cold Regions Research and Engineering Laboratory
Hanover, New Hampshire

Cross-borehole pulse propagation studies of permafrost electromagnetic properties were begun in March 1984 in the Fairbanks, Alaska, area. The objective of this program is to measure in situ the complex index of refraction of frozen silts, sands and gravels and correlate it with temperature, grain size and ice content. The signals propagated are short pulses transmitted from commercially available borehole antennas and are similar in waveform to those of impulse radar systems. The pulse frequency bandwidth is centered near 100 MHz.

Two sites were initially chosen, one in a deep, frozen silt and the second in a frozen alluvium. Our intentions were to core each of at least three boreholes to approximately 15 m depth and later place thermocouple strings in at least one borehole at each site. Each borehole was to be cased with plastic piping and capped for future use. This plan ran into serious difficulties:

1) The silt site located at Glenn Creek in Fox above the CRREL permafrost tunnel proved to be only marginally frozen for a few feet below the active layer, probably due to recent warm summers and winters. Consequently, the coring auger frequently froze back as it was being raised through this section since we were unable to maintain rotation while the drill rods were being removed. Attempts to just auger a hole also failed.

2) Coring was not possible in the gravelly alluvium. Therefore we could only auger holes and collect grab samples. The auger depth was limited to 12.2 m, at which point the holes began to slump and had to be immediately cased.

An alternate silt site was chosen at the CRREL Farmer's Loop facility in Fairbanks. Six holes were augered and cased to 12.2 m depth. Their spacings ranged from 5 to 30 m. For all holes only grab samples were obtained, allowing only gravimetric water content to be measured.

The experimental procedure was as follows. Antennas were elevated simultaneously from the bottom in 1-m intervals. All antenna depths were referred to a datum plane so that the antenna pair was always at the same absolute

height. Pulses were recorded digitally in a 32 stack which greatly eliminated incoherent noise. Time of flight was calibrated from air measurements with the antennas at a measured distance apart. Attenuation measurements were made using the calibrated gain settings of the control unit. These measurements were relative values, with the shortest hole spacing used as a reference. A magnetic induction technique was used at the surface to give an approximate value of the ground DC conductivity. These values plus spatial attenuation calculations were then used as an adjustment to calculate ground attenuation in dB/m due only to dielectric absorption and scattering.

The first silt site at Glenn Creek was not a total loss because we were able to obtain over 20 m of core from which we could make an excellent volumetric ice versus gravimetric water calibration curve. Thus we could correlate our Farmer's Loop dielectric data indirectly with volumetric ice content since only the frozen cuttings were available at Farmer's Loop. Volumetric ice content from the Farmer's Loop site ranged from 48 to 78%. A thermistor string has been placed at Glenn Creek for future ground temperature measurements. At the alluvial site, the gravimetric water content was much less. A loose application of our silt calibration curve suggests volumetric water contents ranging from 10 to 48%.

The Farmer's Loop silt measurements were surprisingly low but consistent with our past laboratory work. We are certain that temperatures throughout the depth of our boreholes were no lower than -4°C . This led us to expect relative dielectric values (real part K' , imaginary part K'') of between 10 and 15. Instead the K' values were generally between 4.3 and 6.1, with the higher values usually at greater depth. The K'' values generally ranged between 0.08 and 0.22. No values were calculated above 3 m as the signals were too highly attenuated relative to the high level of noise near the surface. The attenuation rates which determined the K'' values generally ranged between 1 and 4 dB/m, with the higher values occurring at the greater depths. DC resistivity values ranged between 740 and 2040 ohm-meters as measured with a Geonics EM-31 magnetic induction device (40 kHz).

The alluvium measurements made on Ft. Wainwright were more predictable. K' ranged from 4 to 6 and K'' from 0.09 to 0.45. The EM-31 consistently indicated resistivity values at greater than 10,000 ohm-m. Attenuation was never greater than 1.5 dB/m and these values occurred near the surface, which was all sand to about 2 m depth. Measurements were made at all depths to

12.2 m and at borehole spacings of 22 m. The strong signals recorded at this separation showed that much wider spacings could be attained.

In almost all cases only one event was observed, which we have assumed to represent a wavefront propagating horizontally. The one exception occurred at the alluvial site for the closest hole spacing of 9.02 m. Here, secondary events occurred, the time delays of which could be predicted by ray paths refracting along the surface. In all the alluvial cases, the attenuation was low enough so that the index of refraction n could be excellently approximated by $n = \sqrt{k'} (1 - i \tan \Delta/2)$.

Our provisional conclusions are that these K' values on high-ice-content frozen silt, although surprisingly low, are consistent with the theoretical and laboratory values. However, we cannot be sure until we obtain temperature profiles with depth. Delaney and Arcone* (Figure 8) have shown that a curve of K' versus volumetric water content is double-valued in that the same value of K' can occur for two different volumetric water contents. For example, a value of $K' = 5$ can occur at 10% water content where the value is determined by the combination of dry silt, air and adsorbed water, and also at 65% where the value is determined mainly by the adsorbed water and high ice content. A peak in K' is reached at about 40% water content where values might reach as high as 10 to 15 at -2°C . Since our volumetric water contents ranged as high as 78% and averaged 66%, these low values of K' are consistent.

* A. Delaney and S. Arcone (1984) Dielectric measurements of frozen silt using time domain reflectometry. Cold Regions Science and Technology, 9:39-46.

SUBSEA PERMAFROST: FIELD MAPPING AND NUMERICAL/PHYSICAL MODELING OF ITS
SPATIAL DISTRIBUTION IN THE CANADIAN BEAUFORT SEA

S.M. Blasco
Geological Survey of Canada, Bedford Institute of Oceanography
Dartmouth, Nova Scotia, Canada

D.L. Lewton
Department of Geology and Geophysics, University of Calgary
Calgary, Alberta, Canada

Through the correlation of high-resolution analog reflection seismic profiles with geotechnical borehole data from the Canadian Beaufort Continental Shelf, four types of subsea permafrost have been identified in the upper 100 m of sediment. These include laterally and vertically discontinuous hummocky patches, stratigraphically controlled layers, partially to marginally ice-bonded zones, and infrequent ice lensing and/or massive ice. In general, the regional distribution of this shallow permafrost varies laterally and vertically in extent and in degree of ice-bonding. The permafrost is primarily found within late-Wisconsin glacially related sediments lying unconformably beneath a thin veneer of transgressive and recent marine sediments.

Reverberations, side echoes and static shifts resulting from shallow water and shallow permafrost conditions combine to disrupt the lateral continuity of reflectors on high-resolution shallow multichannel data, making the interpretation of stratigraphy, structure and permafrost between 100 and 600 m difficult. To improve these sections an integrated program involving reprocessing and numerical and physical modeling has been established at the University of Calgary. Ray tracing analysis and reprocessing of sections indicate that in the presence of shallow high-velocity layers energy becomes critically refracted for angles of incidence greater than 25 degrees. This implies the use of short arrays, or possibly split spreads for long arrays are required to enhance shallow reflectors.

A physical seismic scale modeling facility including a large water-filled tank, movable transducer arrays and a high-speed data recorder has recently been constructed. Known and assumed permafrost distributions will be formed out of epoxy and Plexiglass and submerged in the tank. These models will be profiled to produce synthetic sections for comparison with numerical and field data and to test developments in the acquisition and processing of high-resolution shallow multichannel reflection seismic data in areas of severe shallow velocity anisotropy.

A SUMMARY OF FIELD OPERATIONS AND RESULTS OF THREE YEARS OF TRANSIENT SURVEYS ON THE NORTH SLOPE OF ALASKA

Mark W. Blohm
The Earth Technology Corporation
Golden, Colorado

For a period of over three years transient surveys with the Geonics EM-37 have been performed along seismic lines and over wells onshore and offshore on the North Slope of Alaska. Over these three years more than 500 soundings along approximately 150 miles have been conducted. The lines cover the area from Cape Halkett on the west to Flaxman Island on the east.

The logistics and productivity of transient surveying also have been continuously improved over the years.

The ground truth available to compare with the interpretation of the transient data consists of approximately a dozen wells. The agreement between information from induction logs at the well and the geoelectric section derived from the transient data is good.

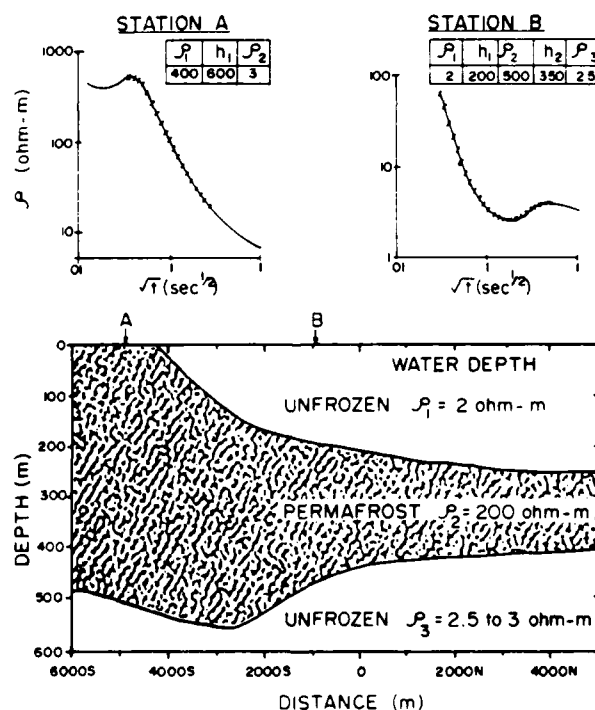


Figure 1. Permafrost profiles.

Figure 1 shows a section derived from transient surveys in Prudhoe Bay previously published.* The data illustrate the ability of transient surveys to map frozen ground under large thicknesses (up to 800 ft) of brine-saturated unfrozen material.

* Ehrenbard, R.L., P. Hoekstra and G. Rozenberg (1983) Transient electromagnetic soundings for permafrost mapping. In Proceedings, Fourth International Conference on Permafrost. Washington, D.C.: National Academy Press, p. 272-277.

BOREHOLE MONITORING OF PERMAFROST ELECTRICAL PROPERTIES

Robert F. Corwin
Harding Lawson Associates
Novato, California

Borehole temperature measurements are commonly used to monitor the degree of ice-bonding of arctic soils as a function of time and depth. However, because the degree of bonding at a given temperature also is affected by other soil properties such as pore water salinity, porosity, and grain size and shape, temperature measurements alone cannot fully determine the degree of bonding.

The electrical resistivity of a soil or rock usually increases rapidly with increasing degree of ice-bonding. Thus borehole measurements of the electrical resistivity of arctic soils provide a valuable supplement to temperature measurements in determining the distribution of bonded soils with depth. Using a probe consisting of wire electrodes wrapped around plastic pipe, measurements of both electrode contact resistance and bulk soil resistivity as a function of depth can be made with standard instruments.

Measurements of this type have been made on an offshore gravel island built for petroleum production near Prudhoe Bay, Alaska. Both the contact resistance and the bulk resistivity data defined the nature of the transition zones from unbonded marine sediments beneath the island to unbonded gravel at the sea floor, and from unbonded to fully bonded gravel with decreasing depth. Changes of the island's resistivity profile with depth were monitored over a period of two years, beginning shortly after construction of the island. The resistivity of the material below the sea floor was seen to remain constant at about 1 ohm-m, but the resistivity profile within the gravel changed considerably. The resistivity of fully bonded gravel above sea level ranged from about 200 up to 10,000 ohm-m, depending on its salinity, temperature and porosity. Seasonal resistivity changes in the active surface layer also were clearly evident.

Borehole resistivity systems of the type described above are relatively inexpensive to construct, install and monitor, especially if this is done in conjunction with borehole thermistor installations. The resistivity data should prove useful in monitoring time-varying bonding conditions, both in natural areas and beneath engineering structures in permafrost regions.

SOME ASPECTS OF INTERPRETATION OF TRANSIENT EM DATA FOR
MAPPING FROZEN GROUND ON THE NORTH SLOPE OF ALASKA

Lauren E. Evans
The Earth Technology Corporation
Golden, Colorado

In this presentation the interpretation techniques used on three geoelectric sections typical of permafrost on the North Slope of Alaska were discussed. The first section consists of highly resistive frozen ground underlain by brine-saturated unfrozen ground at a depth of about 2000 ft. This section, for example, would be typical of the thick frozen gravels encountered on land near Prudhoe Bay. The second section is offshore in an area where as much as 800 ft of brine-saturated material overlies several hundred feet of frozen ground. The range of equivalence in interpreting this section was evaluated. The third section is an example of the complex frozen ground distribution encountered offshore in the deltas. The importance of using two transmitter loop sizes was illustrated for several soundings.

A DIGITAL INFORMATION SYSTEM FOR
DELINEATION OF DISCONTINUOUS PERMAFROST

H.B. Granberg
Department of Geography, McGill University
Montreal, Quebec, Canada

Since 1954, when mining was begun by the Iron Ore Company of Canada at Schefferville, Quebec, the effect of permafrost on open-pit mining of iron ore has stimulated efforts to develop methods for delineating the permafrost. Simple digital terrain models were first used in 1970 to predict spatial variations in snow depth as an aid in permafrost prediction (Granberg 1972, 1973).

Through a grant from the Defence Research Establishment Suffield it was possible to establish a large digital terrain model in the Timmins-Barney area, some 25 km northwest of Schefferville (Parry et al. 1982). The digital terrain model was used for further development of the snow prediction method and the development of the predecessor to the digital geographic information system described here.

Grants from the Department of Energy, Mines and Resources, Canada made it possible to collect most of the information that has accumulated throughout the 25 years of permafrost research in the Schefferville area. The resulting two reports (Granberg et al. 1983, 1984), totalling some 42 volumes of papers, theses, reports, correspondence and data, include digital data from over 200 thermocable installations and numerous soundings of active layer depth. They also contain auxiliary information on topography and geology in the form of detailed maps, cross sections and stereo models. An additional set of information currently being retrieved consists of the thermal properties of the different rock types at Schefferville using drill cores from Iron Ore Company collections. A set of aerial photographs, taken sequentially at approximately weekly intervals throughout several snowmelt seasons, provide excellent information about the spatial distribution of the seasonal snow cover, which is one of the main factors controlling the spatial variations in surface energy balance.

To cope with this large and varied data base a digital geographic information system is being developed. The information system consists of a series of programs which manage the data base and facilitate retrieval, manipu-

lation and display of information that is either stored in the data base or derived from it.

REFERENCES

- Granberg, H.B. (1972) Snow depth variations in a forest-tundra environment, Schefferville, P.Q., winter 1968-69. McGill University, Montreal, Unpublished M.Sc. Thesis, 134 p.
- Granberg, H.G. (1973) Indirect mapping of the snowcover for permafrost prediction at Schefferville, Quebec. In Permafrost: The North American Contribution to the Second International Conference. Washington, D.C.: National Academy Press, p. 113-120.
- Granberg, H.B., J.E. Lewis, T.R. Moore, P. Steer and R.K. Wright (1983) Schefferville permafrost research. Final Report, DSS Contract No. 20SU 23235-2-1030, 26 Volumes.
- Granberg, H.B., D.T. Derochers, J.E. Lewis, R.K. Wright and L. Houston (1984) Annotations, error analysis and addenda to the Schefferville permafrost data file. Final Report, DSS Contract No. OST83-00302, 16 Volumes.
- Nicholson, F.H. and H.B. Granberg (1973) Permafrost and snowcover relationships near Schefferville. In Permafrost: The North American Contribution to the Second International Conference. Washington, D.C.: National Academy Press, p. 151-158.
- Parry, J.T., W.G. Howland, H.B. Granberg, P. MacLean and L. Houston (1982) Mobility model development: Terrain characteristics. Interim Summary Report, DSS Contract No. 8SU81-00094, 108 p.

THERMAL PROPERTIES FROM BOREHOLE HEATING:
EXPERIENCE IN THE CANADIAN BEAUFORT SEA, 1984

W.D. Harrison and J.L. Morack
Geophysical Institute and Physics Department, University of Alaska
Fairbanks, Alaska

The University of Alaska was invited to participate in the 1984 Geological Survey of Canada (GSC) spring drilling program in the Beaufort Sea. A series of 22 sub-bottom boreholes was drilled northwest of Richards Island. Two of these holes (45+00 and 36+00) were electrically heated and their temperature responses were monitored.

The difficulty of obtaining thermally and mechanically undisturbed soil samples during subsea permafrost investigations has led the University of Alaska to the development of a method of in-situ measurement.* The approach is particularly valuable in reconnaissance jet-drilling and probing investigations when no soil samples are obtained at all. A unique problem in subsea materials is that it is often difficult to tell from the drilling or from samples taken whether ice is present in situ. If the borehole is repeatedly logged for temperature after completion, this question can sometimes be resolved by an interpretation of the rate of return of the hole to temperature equilibrium, but clearly a better approach is desirable.

The method used is to supply a known amount of energy per unit length in the borehole, using a long, electrically heated wire, and to study the temperature response. The interpretation is simplest if the heating is carried out after temperature equilibrium has become reestablished following drilling, but in some cases this is not essential. If no ice is present, the approach to equilibrium after heating can usually be interpreted to give the thermal conductivity as a function of depth. The presence of ice is indicated by a different temperature response. The method is most effective in small diameter boreholes, because the time required to obtain interpretable results varies approximately as the square of the hole diameter.

This in-situ method is still in its developmental phase, and it is therefore of special interest to compare thermal conductivity measured by this technique with that measured on samples by laboratory methods. The GSC sam-

* Osterkamp, T.E. and W.D. Harrison (1980) Subsea permafrost: Probing, thermal regime and data analysis. OCSEAP Annual Report, 1 April, p. 9-10.

ples taken in this study provide an ideal opportunity for this comparison because they appear to be relatively undisturbed.

Theory shows that the temperature response, ΔT , on the axis of a linear heat source after the heat is turned off is:

$$\Delta T = \frac{P}{4\pi k} \ln\left(\frac{t}{t-s}\right)$$

where P is the power per length, s is the time of heating, k is the thermal conductivity, and t is the time, measured from the time the heating begins.

Analysis of the data from hole 45+00 indicates the utility of the method for a borehole containing no ice. The hole was heated for 7.0 hours with an average power of 33 ± 3 watts/m. The data near the bottom of the hole (Fig. 1) follow the theory after approximately 1 hour. Data taken at shallower depths, where the material is more disturbed by the drilling, take longer to fit the theory. Thermal conductivities for the materials were calculated using the theory and gave values in the range from 1.4 to 1.8 W/m °C. These values agree well with those measured in the laboratory for samples taken from the holes.

Analysis of the data from hole 36+00 was complicated by the presence of ice, which is clearly indicated by the cooling curves (Fig. 2). In this case the utility of the method seems to be in its sensitivity to amounts of ice that were too small to be detected during drilling or sampling, rather than in a determination of thermal conductivities. The cooling curves are quite different from those observed at Prudhoe Bay where the ice content is known to be high, suggesting that further analysis may be able to determine quantitatively the amount of ice present.

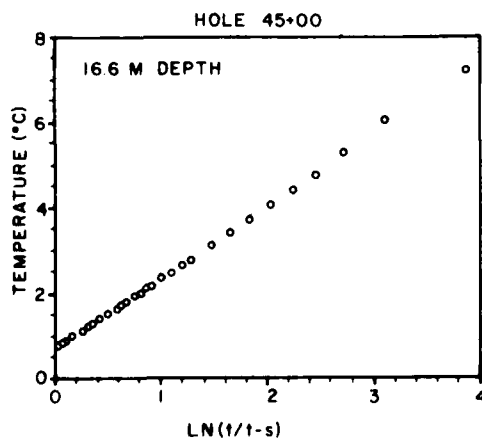


Figure 1. Data from borehole containing no ice.

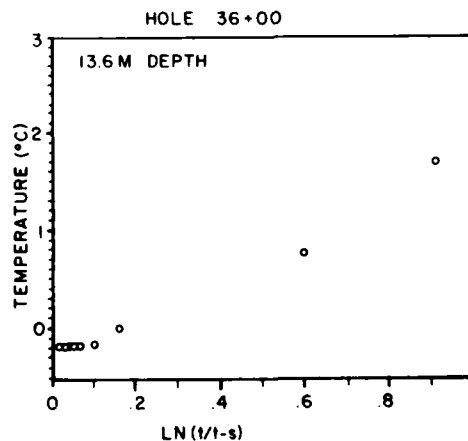


Figure 2. Data from borehole with ice present.

MEDIUM SCALE MAPS OF PERMAFROST AND GROUND ICE CONDITIONS,
TUKTOYAKTUK AND ILLISARVIK AREAS, WESTERN ARCTIC COAST, CANADA

J.A. Heginbottom
Terrain Sciences Division, Geological Survey of Canada
Ottawa, Ontario, Canada

A general knowledge of ground ice conditions is important in planning many forms of industrial and developmental activity within permafrost regions. This information is required in addition to the data on topography, surficial geology, drainage and groundwater conditions traditionally demanded of geologists. In Canada, the Geological Survey has been attempting to fill these needs for some two decades by producing maps of surficial geology and terrain conditions in areas where developmental activity is most intense. Many of these maps have been accompanied by extended tabular legends which include information on permafrost and ground ice conditions, wherever the extent of subsurface information is sufficient. These maps are generally at scales of between 1:100 000 and 1:250 000.

There are two small areas of the western arctic coast of Canada for which detailed information is available and for which larger scale maps (1:25 000) of the surficial geology have been produced. These are the areas around the settlement of Tuktoyaktuk, on the east side of Kugmallit Bay, and around Illisarvik, on northern Richards Island (Fig. 1). Detailed mapping of the surficial geology of these areas was done in 1971-1973 at Tuktoyaktuk (Rampton

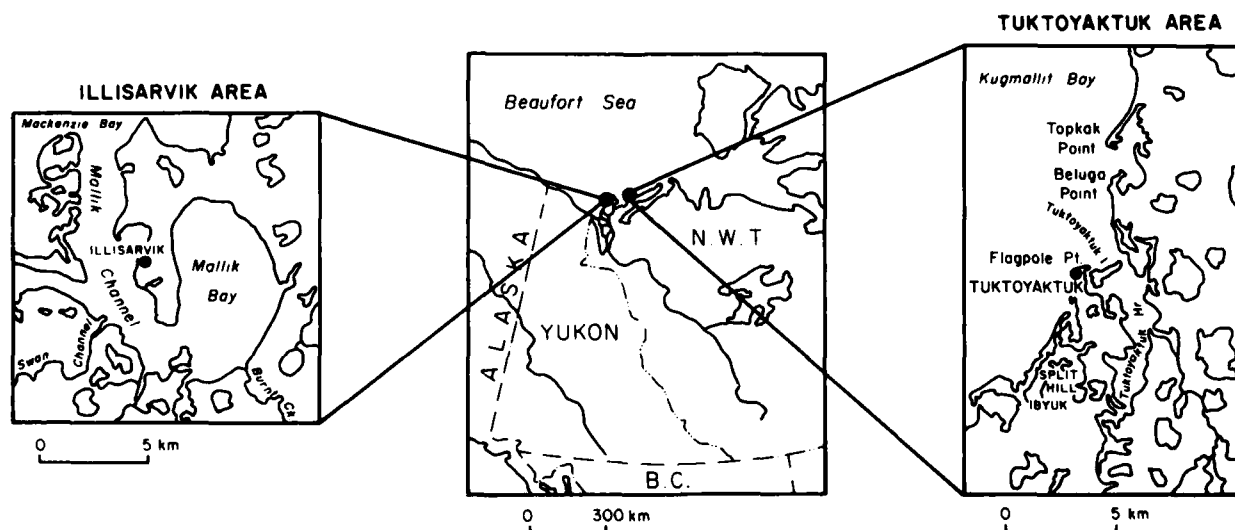


Figure 1. The Illisarvik and Tuktoyaktuk areas, northwest Canada.

and Bouchard 1975) and in 1982 at Illisarvik (Hardy Associates 1983). Furthermore, substantial subsurface investigations have been done, by means of drilling and sampling programs undertaken by various agencies. In addition to the detailed surficial geology maps, reports describing surficial deposits, geomorphic processes, Quaternary history and engineering considerations are available for both areas. The data base for these two areas is thus sufficient to allow the compilation of maps of the permafrost and ground ice conditions.

These new maps are being compiled at a scale of 1:50 000, using a common legend and permafrost classification developed specifically for this task. The map areas are in similar geologic settings and are only 60 km apart. Permafrost conditions are described in order of decreasing extent and decreasing ice content for each of the map units. The legend presents information on the extent and continuity of frozen ground, the general location of taliks, the quantity of ground ice and its configuration. A summary of the surficial geology conditions for each map unit is also included. It should be emphasized that, as with all earth science maps, local variations in the extent, thickness and ice content of the materials occur in many map units. Ice content is described in a semi-quantitative way, using the terms low, medium, high and very high. These terms can be defined only generally, for extensive, detailed subsurface data on ice contents are unavailable. On this basis, six major permafrost and ground ice environments are defined with respect to their geomorphic and geologic conditions. These are described briefly in the following paragraphs.

Permafrost is most extensive in areas of morainal and colluvial diamictons, overlying sandy glaciofluvial and pre-Holocene marine deposits, and in areas of fine-grained lacustrine deposits overlying glaciofluvial sands. The diamictons are found to the south, southwest and northeast of Tuktoyaktuk Harbour and around Mallik Bay near Illisarvik. Ice contents are low to medium, with the ice occurring as wedges, lenses and reticulate veins. Pore ice is ubiquitous. Bodies of massive ice are common at the base of the diamictons. Massive ice also underlies an area of lake terraces east of Tuktoyaktuk Harbour; here growth of the massive ice has resulted in topographic reversal, with the lake terraces standing above adjacent deposits (Rampton and Bouchard 1975). Infrequent taliks are found below thermokarst depressions.

To the east of Mallik Bay (Illisarvik map) is an area of pre-Holocene, sandy, marine-deltaic deposits. These are characterized by extensive perma-

frost, with rare taliks below deep lakes and thaw depressions, and generally low ice content. At Tuktoyaktuk, a broad zone of glaciofluvial sands and gravels runs from southeast to northwest across the northern part of Tuktoyaktuk Harbour, including Flagpole Point, Tuktoyaktuk Island and Beluga Point. These deposits are characterized by continuous permafrost with infrequent taliks beneath deep lakes and thermokarst depressions. Ice contents are low near the surface, where ice occurs in wedges and lenses, but locally there are high to very high contents, with ice lenses and bodies of massive ice. Pore ice is again ubiquitous.

Scattered throughout the units just described are numerous drained lake basins, many containing residual ponds. These are underlain by lacustrine deposits of interbedded silty clay and fine sand, often organic-rich, and locally underlain by diamictons. In the Illisarvik area, southeast of Swan Channel, is an area where the lacustrine deposits are veneered with Holocene deposits. Permafrost is continuous in these materials, but with more extensive and more frequent taliks beneath channels, thaw lakes and recently drained basins, such as Illisarvik itself. Ice content is generally high in the upper several meters of permafrost, with ice in the form of wedges and reticulate veins; low to medium ice content is found at greater depths, in reticulate veins. Pingos occur exclusively in this map unit; they are largely confined to drained lake basins within the areas of morainal deposits, to the southwest and northeast of Tuktoyaktuk and to the south of Mallik Bay. Massive ice of segregation and intrusive origin is found in the cores of the pingos.

Discontinuous permafrost is found in association with marine and alluvial deposits. A complex distribution of frozen and unfrozen ground, reflecting changing hydraulic conditions, is found beneath areas of recent and modern alluvial, deltaic and marine deposits in tidal flats, floodplains and terraces. The materials are stratified silts, fine sands and clays, frequently organic-rich, locally overlying diamictons or sands. Taliks are found beneath channels, ox-bows and thaw lakes. Where the ground is frozen, ice content is medium to high in the form of reticulate veins, wedges and lenses plus pore ice. Permafrost is aggrading in areas of active sedimentation. Near Illisarvik, this map unit occurs along the southeast side of Mallik Bay, alongside Swan Channel and beneath the alluvial islands west of Mallik Channel. The map unit is less extensive near Tuktoyaktuk; it occurs around bays

between Topkak Point and Beluga Point, south of Tuktoyaktuk Island and around Split Hill and Ibyuk Pingos.

Thin, sporadically distributed permafrost with low ice content is found in marine beach deposits, primarily along the shore of Kugmallit Bay.

Organic deposits overlie lacustrine deposits and also occur in small areas of poor drainage on other deposits. The peats are generally 1 to 2 m and locally up to 4 m in thickness and grade into the underlying deposits. Ice content is very high, with ice occurring in numerous small lenses.

REFERENCES

- Hardy Associates Ltd. (1978, 1983) Surficial geology of the area around Illisarvik, Richards Island, N.W.T. Canada Geological Survey, Open File Report No. 941, 55 p., and 115 p. and map.
- Rampton, V.N. and M. Bouchard (1975) Surficial geology of Tuktoyaktuk, District of Mackenzie. Canada Geological Survey, Paper 74-53, 17 p.

PERMAFROST DISTRIBUTION IN NORTHERN CANADA:
INTERPRETATION OF WELL LOGS

A. Judge and A. Taylor
Earth Physics Branch, Department of Energy, Mines and Resources
Ottawa, Ontario, Canada

DATA BASE

Through three contracted studies (D&S Group 1983, Hardy and Associates 1984a,b) the base of permafrost has been determined using the conventional well logs from 530 wells drilled for hydrocarbon exploration in northern Canada. Of the wells examined, 220 were in the Mackenzie Valley and the Yukon, 100 in the Mackenzie Delta - Beaufort Sea region and 150 in the Arctic Islands. For each well the suite of logs was examined using the techniques outlined by Walker and Stuart (1976), Hnatiuk and Randall (1977), Hatlelid and Macdonald (1979) and Osterkamp and Payne (1981). The values determined are strictly the base of ice-bearing permafrost as revealed by changes in the physical properties, in particular the electrical and acoustic properties. In coarse-grained sediments the base may coincide closely with the 0°C isotherm, the difference dependent on depth and pore water salinity alone. In fine-grained soils the freezing characteristics of the soil or rock predominate and the base of the ice-bearing layer may be as much as 100 m above the 0°C isotherm, with a transition layer below (Osterkamp and Payne 1981, Taylor and Judge 1981). The bottom of the ice-bearing sediments is in fact determined by a very complex set of soil characteristics, both static and dynamic, whose relationships remain poorly understood.

Over the past 15 years precise temperature measurements have been made at successive times since completion in 120 wells drilled for hydrocarbon exploration (Taylor et al. 1982). The base of ice-bearing permafrost, the 0°C isotherm and indications of zones of high ice content as derived from this data set were used to develop criteria for (essentially to calibrate) the interpretation of the geophysical well logs.

THICKNESS OF PERMAFROST

The most detailed picture of permafrost distribution emerges for the Beaufort Sea and Mackenzie Delta regions. In Figure 1, the pick of permafrost base has been plotted and the values contoured at 100-m intervals where

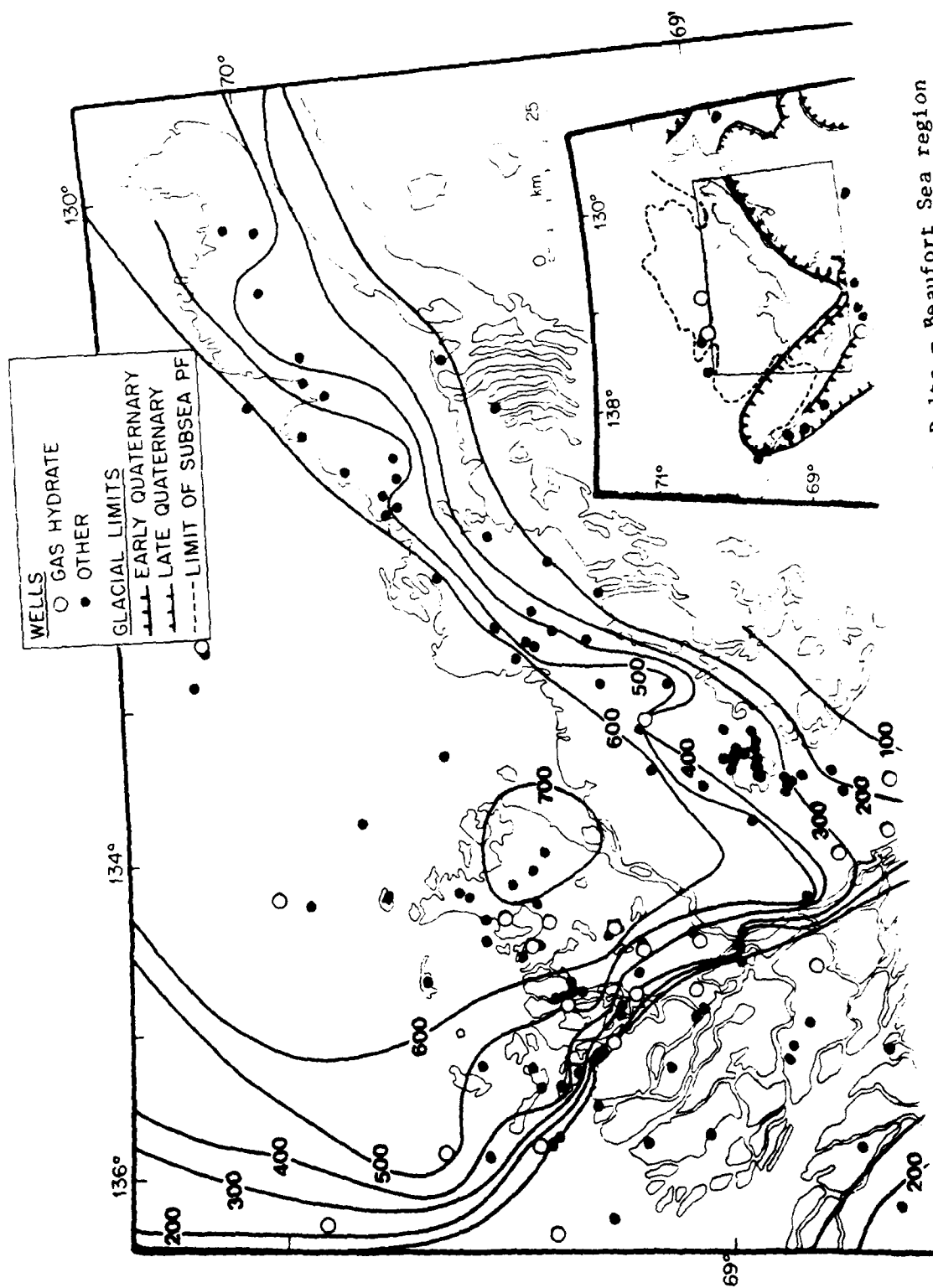


Figure 1. Depth to base of permafrost in the Mackenzie Delta - Beaufort Sea region by industry well logs and government temperature surveys. Contours of bottom of ice-bonded permafrost in metres.

data permit. The greatest depth, as much as 740 m, to the base of permafrost on land is in the northern part of the Mackenzie Delta on northern Richards Island, but depth exceeds 500 m in the northern half of the entire Tuktoyaktuk Peninsula between the east channel of the delta and the northeastern tip of the Tuktoyaktuk Peninsula. Offshore, depth to the permafrost base reaches 700 m beneath the sea-floor. Almost the entire shelf between longitude 129°W and 136°W is characterized by thick occurrences of permafrost in and below the seabed. The seaward boundaries of permafrost determined from the well-log analysis coincide closely with the boundaries of permafrost inferred from seismic refraction velocities on the upper permafrost table. Seismic interpretation (Neave et al. 1978) suggests an additional portion of the northeastern shelf, extending southwesterly in a belt 15-20 km wide, to be without this frozen substrate. Lack of well information in the area prevents confirmation of the total absence of permafrost throughout the belt.

Thickness of permafrost decreases in the southern portion of the Mackenzie Delta, and possibly on the Yukon Coastal Plain. The offshore area west of 136°W is largely characterized by thin or absent permafrost. A few limited observations onshore to the east of the study region again indicated thick permafrost, e.g. 300 m at 68°51'N, 126°47'W, and 450 m at 67°44'N, 126°50'W (Taylor et al. 1982). Similar increases in permafrost thickness might be expected west of the Mackenzie Delta with a boundary either in or to the south of the Yukon coastal areas. However, well data are not available to confirm this. West of the Mackenzie Trough, offshore permafrost may again thicken, although again the little well data that are available do not confirm the supposition. Sediment characteristics are akin to those encountered in the Alaskan Beaufort, where thick permafrost is encountered offshore (Osterkamp and Payne 1981).

As shown in Figure 2 the interpretation of well logs from 150 exploratory wells in the Arctic Islands yields a wide range of results, from a base of permafrost of 131 m on Linckens Island to 860 m at Cornwallis Central Dome. In a general sense the permafrost thickness exceeds 600 m in the interior of Banks, Devon, Cornwallis, Melville, Prince Patrick and King Christian Islands, and generally ranges between 300 and 600 m throughout much of the rest of the onshore areas. The shallowest permafrost in onshore areas appears to occur in the Sabine Peninsula of Melville Island, close to the present shorelines of many of the islands and in the more southerly parts of the region.

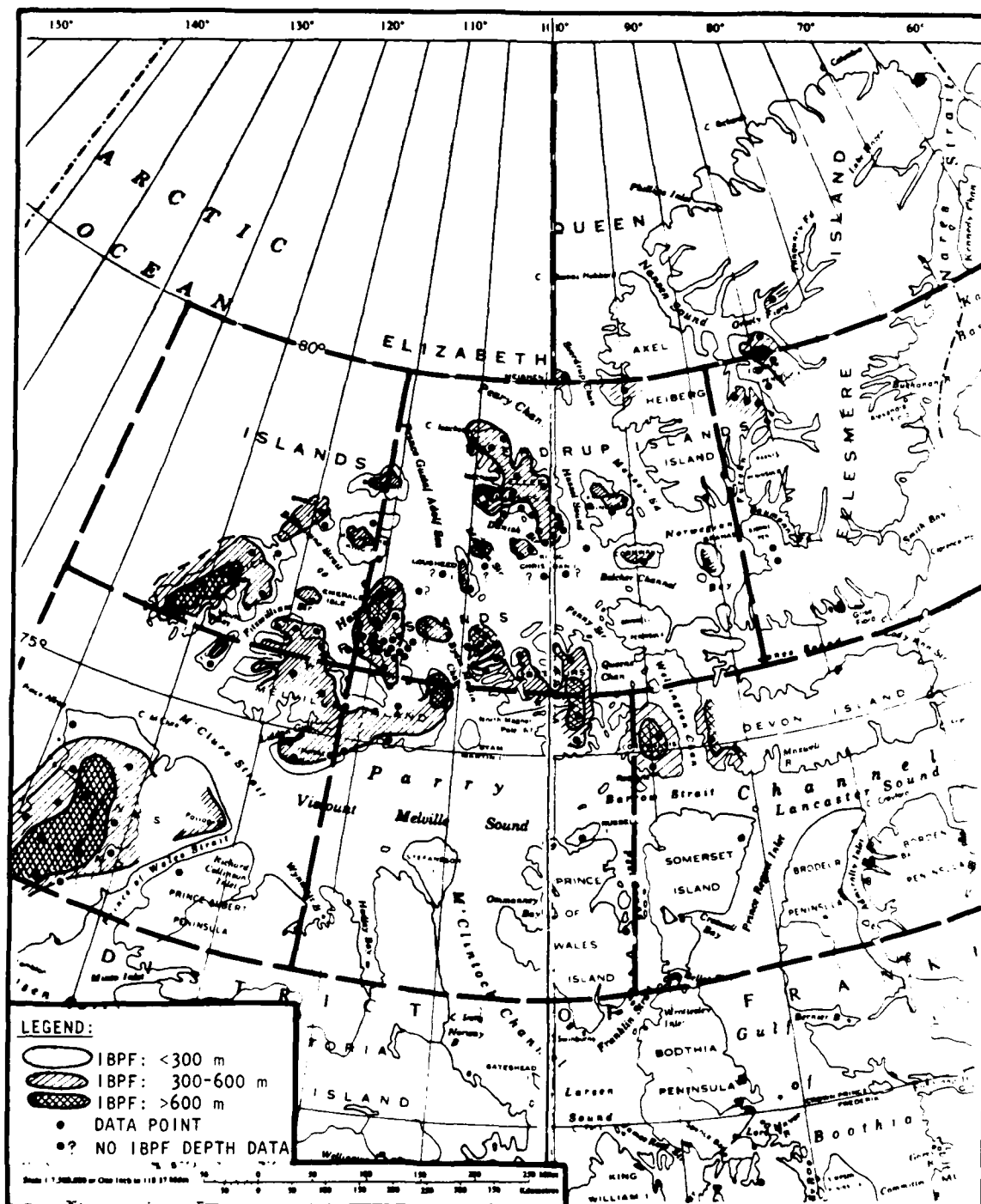


Figure 2. Depth to base of permafrost in the Arctic Islands.

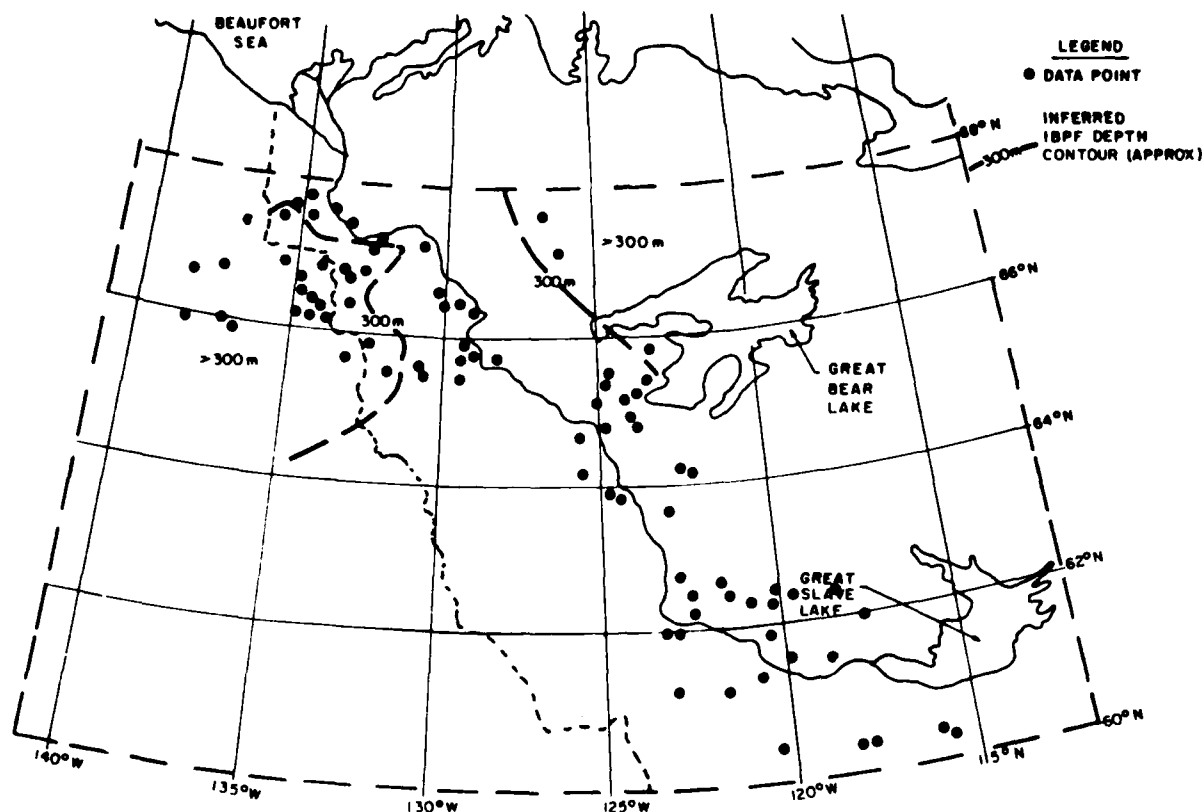


Figure 3. Depth to base of permafrost in the western Northwest Territories and Yukon. Approximate division shown between less than and more than 300 m to base of ice-bonded permafrost.

Unfortunately, many of the logs in the offshore wells were commenced at too great a depth to determine the absence or presence of permafrost.

Permafrost thickness, as evidenced in 220 wells between the Beaufort region and the Alberta provincial border, is highly variable in this more southerly area. The overall trend shown in Figure 3 is of permafrost greater than 300 m in thickness in the northwest part of the region and north of Great Bear Lake, a general increase away from the Mackenzie Valley, and a decrease in thickness from 600 m in the north to sporadic or nonexistent in the south. Locally, permafrost becomes highly variable in thickness.

REFERENCES

- D&S Group (1983) Study of well logs in the Mackenzie Delta - Beaufort Sea to outline permafrost thickness and/or gas hydrate occurrence. Department of Energy, Mines and Resources, Ottawa, Earth Physics Branch Open-File Report 83-10, 242 p.
- Hardy and Associates (1984a) Study of well logs in the Arctic Islands to outline permafrost thickness and/or gas hydrate distribution. Department of Energy, Mines and Resources, Ottawa, Earth Physics Branch Open-File Report 84-8, 374 p.
- Hardy and Associates (1984b) Study of well logs in the western N.W.T. and Yukon to outline permafrost thickness and/or gas hydrate distribution. Department of Energy, Mines and Resources, Ottawa, Earth Physics Branch Open File Report 84-27, 290 p.
- Hatlelid, W.G. and J.R. Macdonald (1979) Permafrost determination by seismic velocity analysis. In Proceedings of Symposium on Permafrost Field Methods and Permafrost Geophysics, Assoc. Comm. Geotech. Res., Tech. Memo 124, p. 146-147.
- Hnatiuk, J. and A.G. Randall (1977) Determination of permafrost thickness in wells in northern Canada. Canadian Journal of Earth Science, 14:375-383.
- Osterkamp, T.E. and M.W. Payne (1981) Estimates of permafrost thickness from well logs in northern Alaska. Cold Regions Science and Technology, 5:-13-27.
- Neave, K.G., A.S. Judge and J.A. Hunter (1978) Offshore permafrost distribution in the Beaufort Sea as determined from temperature and seismic observations. Geological Survey of Canada, Paper 78-1C, p. 13-18.
- Taylor, A.E. and A.S. Judge (1981) Measurement and prediction of permafrost thickness, arctic Canada. 51st Annual Meeting, Society of Exploration Geophysicists, Vol. 6, p. 3964-77.
- Taylor, A.E., M. Burgess, A.S. Judge and V.S. Allen (1982) Canadian geothermal data collection - northern wells, 1981. Department of Energy, Mines and Resources, Ottawa, Earth Physics Branch, Geothermal Series, No. 13, 154 p.
- Taylor, A.E., A.S. Judge and D. Desrocher (1983) Shoreline regression: Its effect on permafrost and the geothermal regime. In Proceedings of Fourth International Conference on Permafrost, Washington, D.C.: National Academy Press, p. 1239-1244.

Walker, J.D. and A.J. Stuart (1976) Permafrost investigation by crystal cable surveys, Mackenzie Delta, N.W.T. Transactions SPWLA, 17th Annual Logging Symposium.

SHALLOW INDUCTION MEASUREMENTS IN PERMAFROST TERRAIN

K. Kawasaki and T.E. Osterkamp
Geophysical Institute, University of Alaska
Fairbanks, Alaska

With three-fourths or more of the land surface of Alaska and its continental shelf underlain by permafrost, problems arising from the thaw instability of permafrost will probably be as frequently encountered in the future development of the resources of this region and supporting infrastructure (such as roads and houses) as they have been in the past. As an example, it is estimated that one-fourth to one-fifth of the more than 100-million-dollar maintenance budget for Alaskan highways is attributable to permafrost-related problems. Thus, any techniques that remotely and rapidly provide knowledge of subsurface permafrost conditions which would allow avoidance and/or specialized construction methods to be used could be of great benefit to the orderly and cost-effective development of the arctic regions.

A number of geophysical exploration techniques have been applied to permafrost detection in Alaska and elsewhere. In particular, electromagnetic induction (EM) has been used extensively for this purpose, especially in geotechnical problems. We have made some selected EM surveys to evaluate the effects of terrain type and season with the fixed-frequency, fixed-loop-separation Geonics EM-31.

As has been demonstrated by previous studies, our results indicate, generally speaking, that the most favorable time for detecting ice-rich soils and ground ice is the late winter - early spring months. However, under some circumstances of temperature and moisture profiles with depth, ground ice may not show a detectable resistivity contrast from surrounding frozen ground even during periods considered favorable. An example of this situation has been modeled using a layered earth.

For many surveys, made during the late summer - early fall period when the active layer above permafrost is thawed, the apparent conductivity σ_{av} obtained in the vertical coplanar loop mode was larger than the σ_{ah} obtained in the horizontal coplanar mode. Modeling of this situation indicates this result is an artifact of the cumulative response functions (R_v and R_h) in the two modes. (The response function R_h for the horizontal mode falls off faster than that of the vertical mode for a certain range of depths.)

Terrain and vegetative cover are important factors in determining where frozen ground will occur in interior Alaska. Measurements made over poorly drained and well-drained flatlands indicate that drainage patterns significantly determine where frozen ground will occur, with drainage channels associated with unfrozen zones.

IMPULSE RADAR SOUNDING OF FROZEN GROUND

A. Kovacs and R.M. Morey
Cold Regions Research and Engineering Laboratory
Hanover, New Hampshire

VHF electromagnetic impulse sounding is currently being used by a number of organizations for probing into frozen ground. During the past decade, we have used an impulse radar system in the Arctic and Antarctic to study the electromagnetic properties and thickness variation of lake, sea and shelf ice. However, as a side activity to our work we have used the system to explore various subsurface ground features in Alaska. One of our first results was the mapping of massive ice along a segment of the Alyeska Pipeline and the pump station feeder gas pipeline. In this study we used a dual antenna configuration in which one antenna was a transceiver and the second a receiver only. This configuration generated wavelet flight time information which allowed us to delineate the thickness and lateral variation of the buried massive ice.

An example of the profile results is shown in Figure 1. In this record the top and bottom of massive ice as revealed by the radar are indicated by the dark line. The location of ice as found during drilling of the vertical support member (pile) holes is also indicated. While the drill holes at any

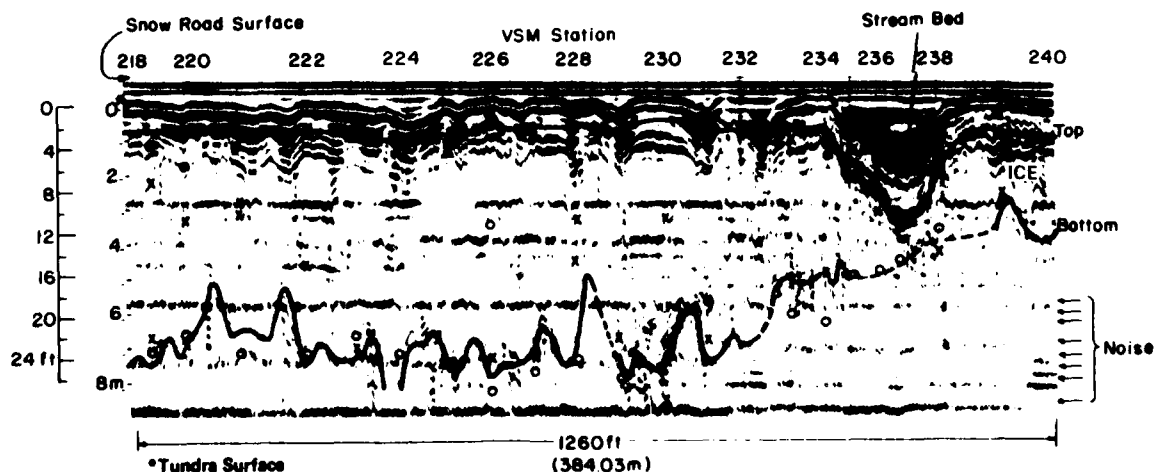


Figure 1. Graphic record of impulse radar data collected along the Alyeska Pipeline from VSM Stations 218 to 240. Lines labeled Top and Bottom denote field interpretation of massive ice horizon. The O's on the record represent top and bottom of ice found in the west VSM borehole and the X's top and bottom logged at the east VSM borehole.

one station were only about 3 m apart, the depth to the ice encountered in each hole, and its thickness, varied significantly, as indicated, for example, by the logs for the east and west drill holes at station 221. Even though the radar profile was run about 8 m away from the east boreholes, the correlation between the drill log and radar massive ice positions is quite good. Further information on the results of this survey can be found in Kovacs and Morey (1979).

In May 1982, the ice depth in several pingos near Prudhoe Bay, Alaska, was profiled. In this study we used antennas with center frequencies in air of about 80 MHz, 120 MHz, 300 MHz and 500 MHz. We found that the information provided by each antenna highlighted different internal features of the pingos. Examples of the radar profiles made over Weather Pingo are shown in Figures 2-5. These profiles were made perpendicular to the long axis of the pingo. The records reveal internal layering in the subsurface ice. Some of these layers are shown in Figure 6, which depicts the cross section of the

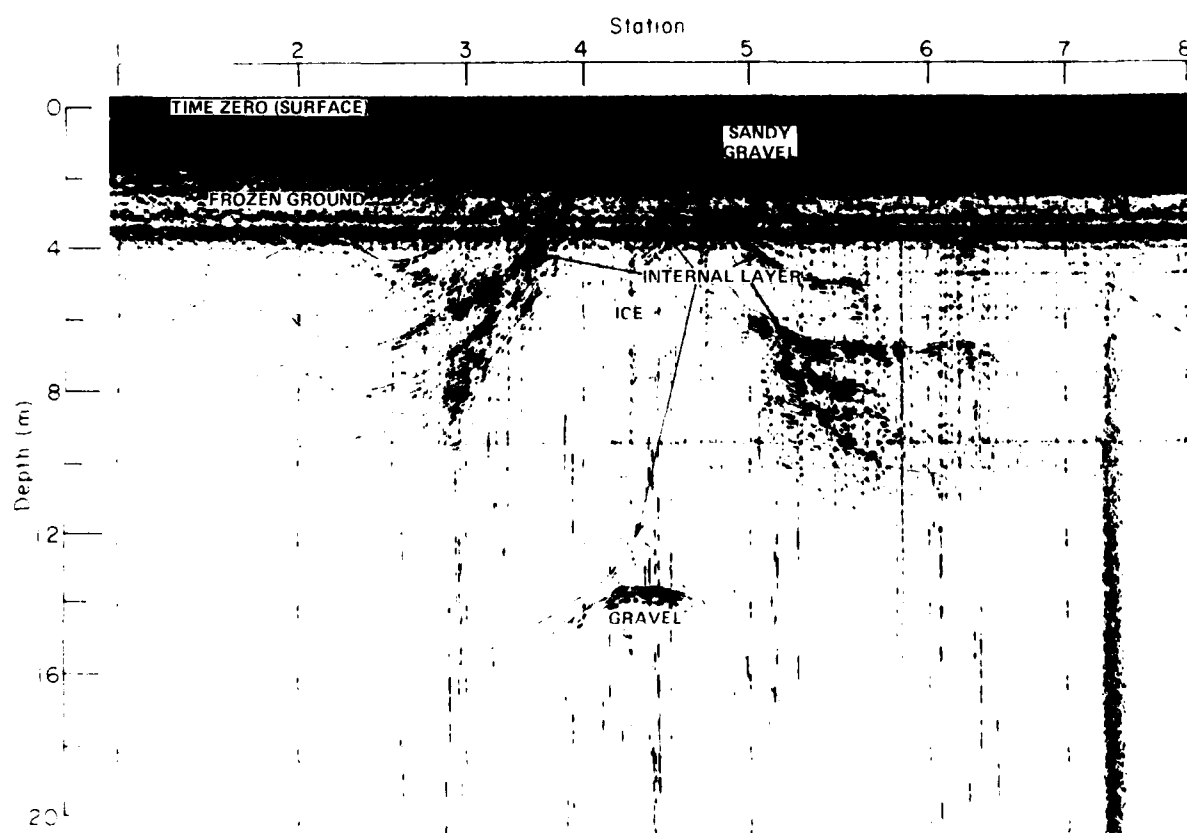


Figure 2. Ground-penetrating radar profile made from south to north over Weather Pingo using a 500-MHz antenna. Distance between stations is 10 m. Note internal layering within the ice core of the pingo.

pingo as constructed from elevation surveys and the radar sounding data. A core through the pingo revealed that the ice in it was composed of bands containing different bubble arrangements and geometries as well as sandy ice layers up to 0.7 m thick (Fig. 6)(pers. comm., Bruce Brockett, CRREL). The depth to the bottom of the ice and to the various internal layers was estimated by using an effective velocity of the radiated impulse wavelet in the bubbly ice and overburden of 0.172 m/ns. Using this value, and the wavelet time of flight, the calculated ice depth agreed within 2% with the drill-hole-measured depth of 13.1 m.

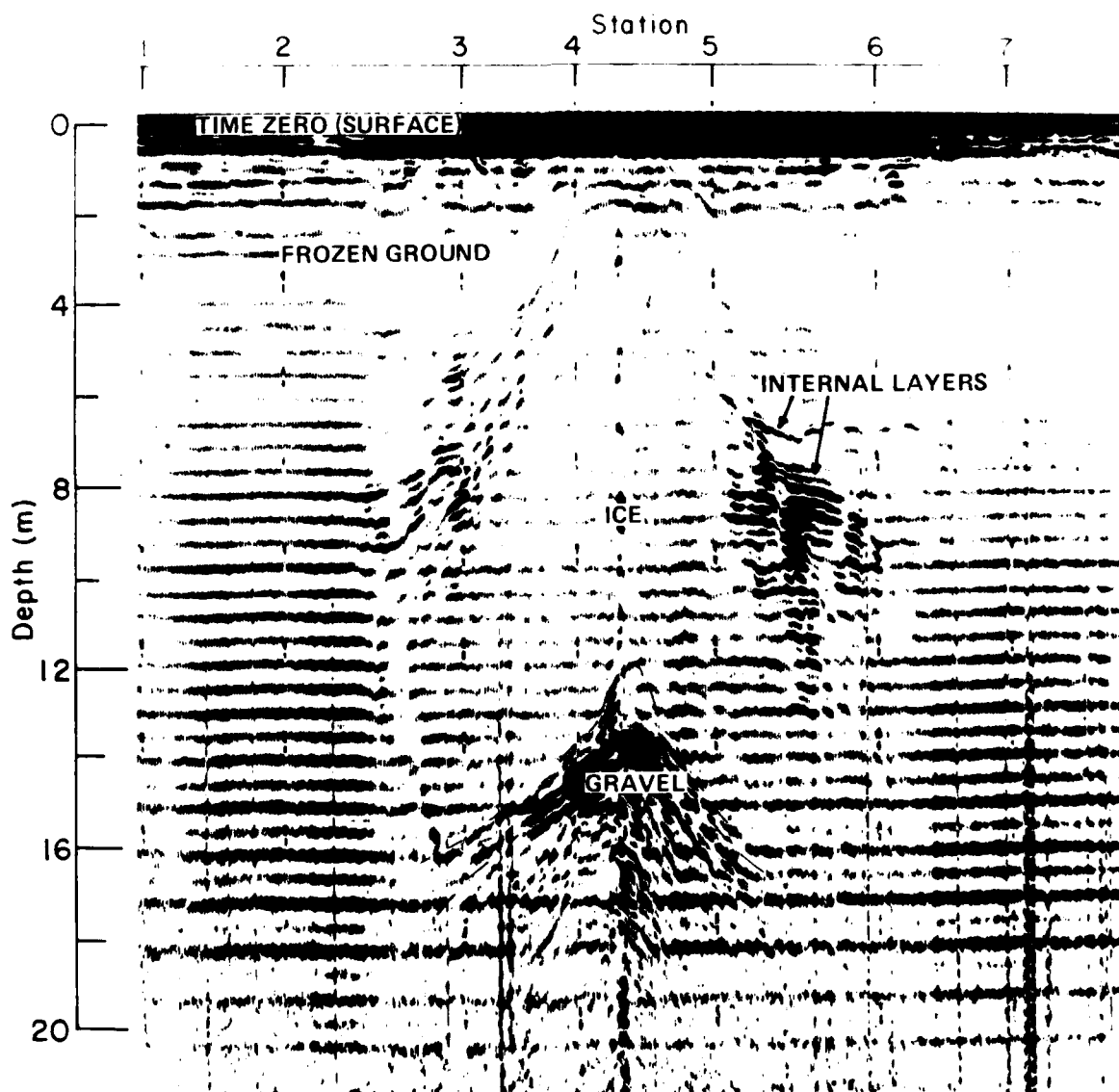


Figure 3. Second radar profile over Weather Pingo using a 300-MHz antenna. Horizontal banding is noise.

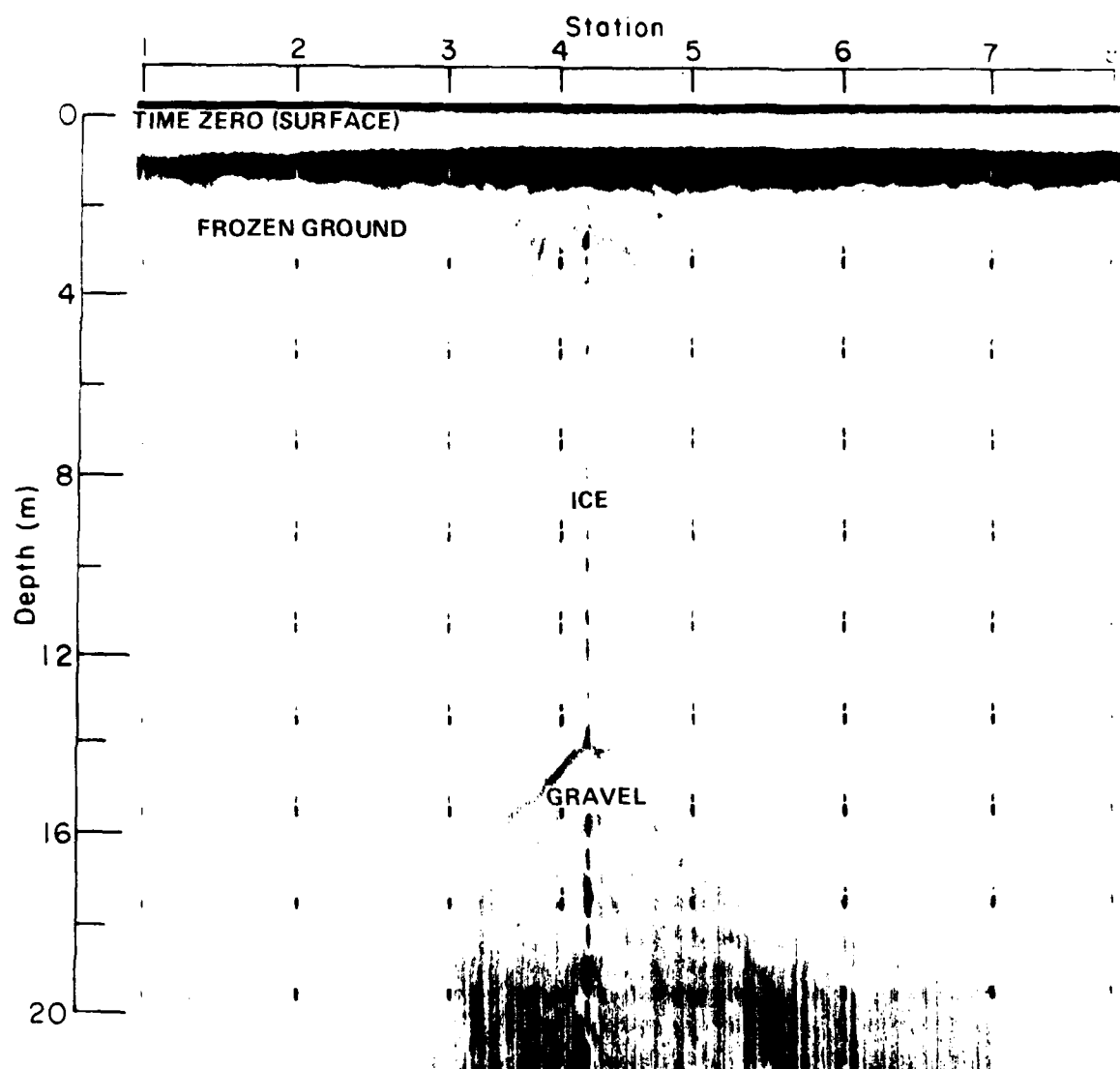


Figure 4. Fourth radar profile over Weather Pingo using a 120-MHz antenna.

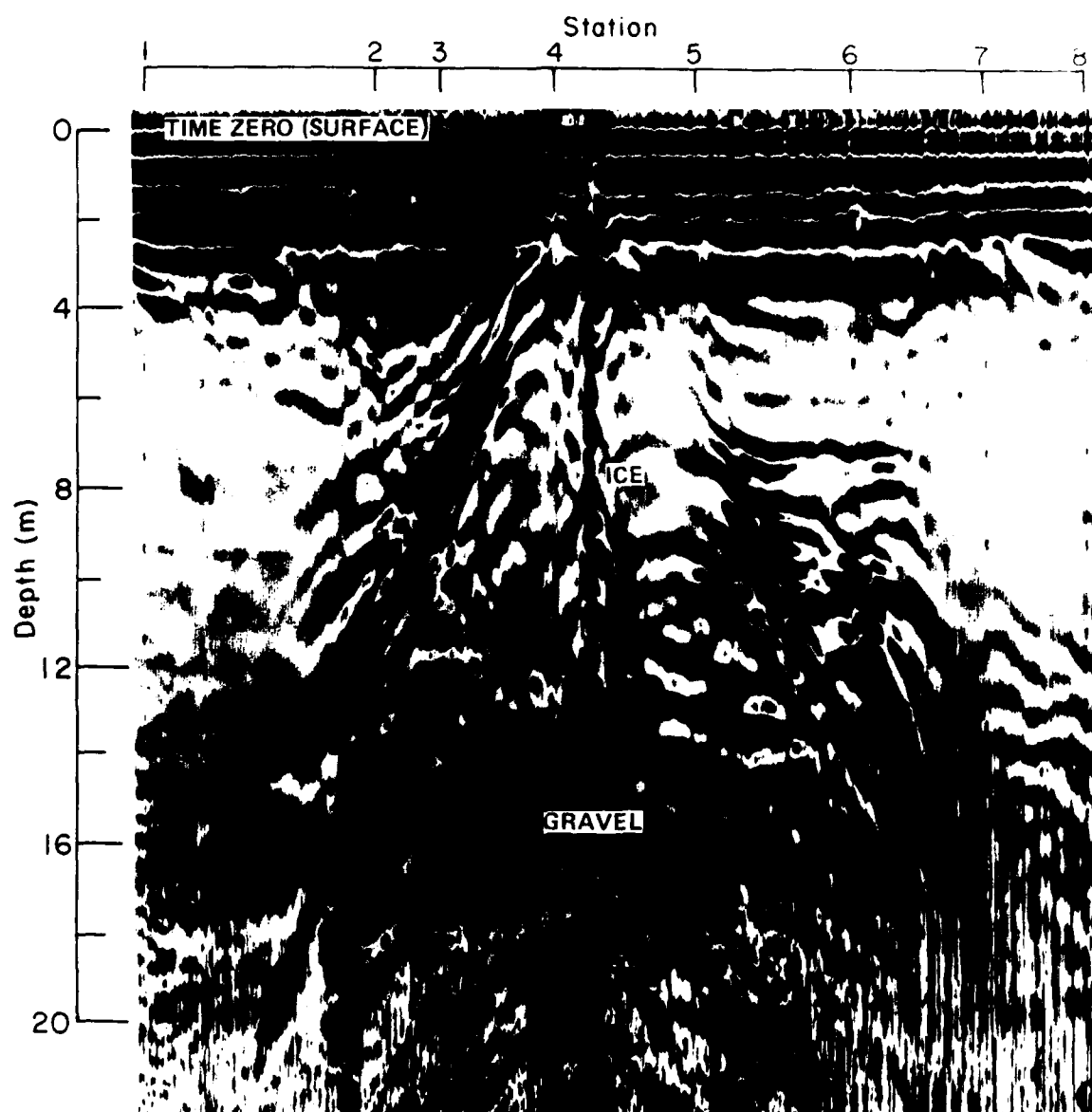


Figure 5. Fifth radar profile over Weather Pingo using an 80-MHz antenna.

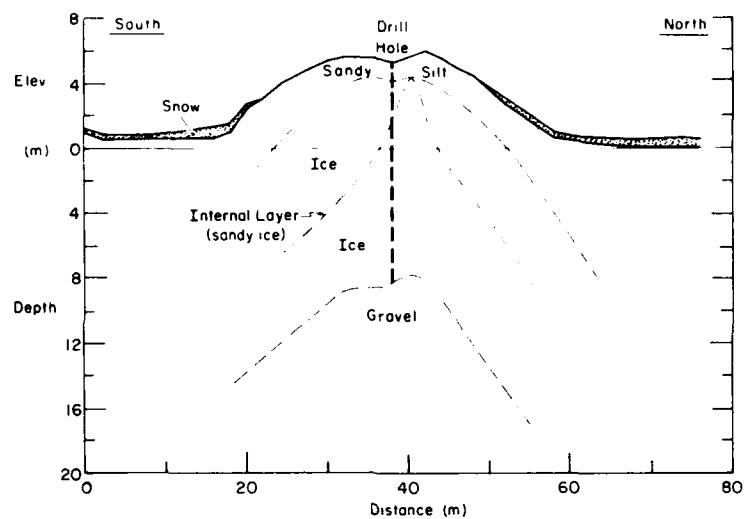


Figure 6. Cross section of Weather Pingo. Drill hole data from B. Brockett (pers. comm., CRREL).



Figure 7. Ice core from Weather Pingo showing sand layer at about 4.75 m (courtesy of B. Brockett, CRREL).

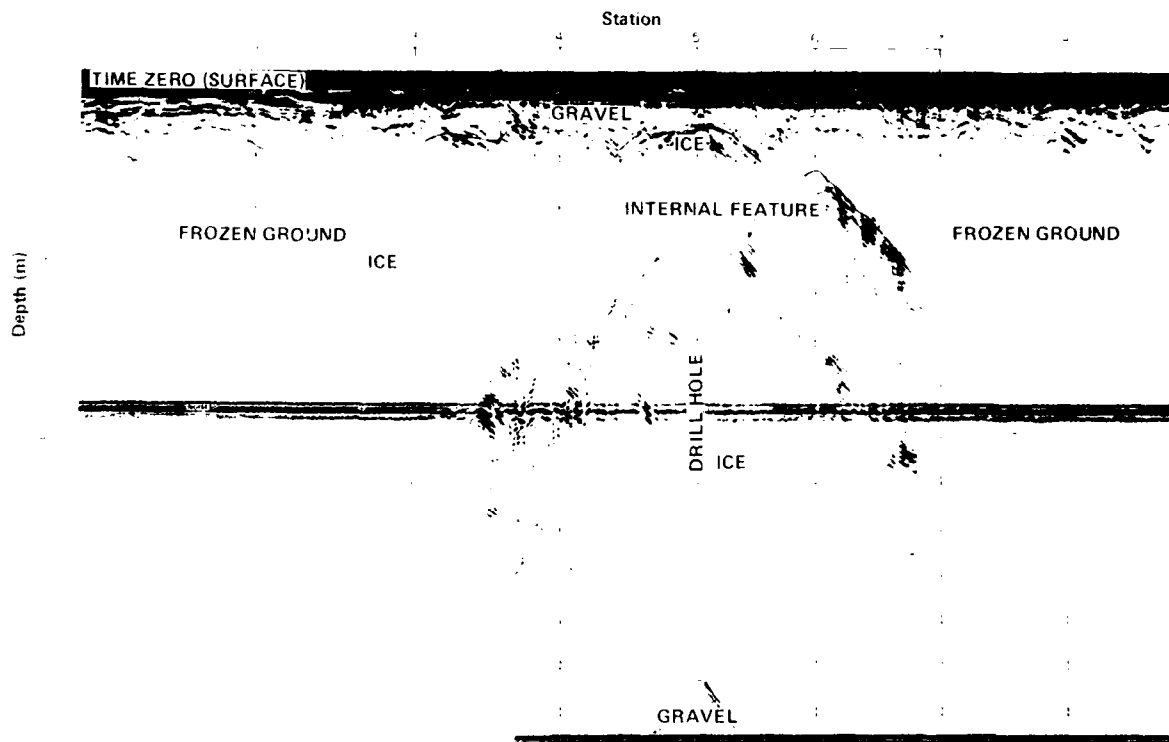


Figure 8. Radar profile made over Prudhoe Mound (pingo) using a 500-MHz antenna. Distance between stations is 25 ft (7.6 m).

The radar profile data revealed a rising interface under the pingo. We are uncertain as to whether this feature is an artifact of wavelet time-of-flight variation or refraction in the pingo, sensing angle distortion, or indeed the relative configuration of the gravel feature encountered at the bottom of the borehole. A similar feature was observed in the radar profile data taken over the Prudhoe Mound pingo (Fig. 8-10). We believe that the gravel layer under both pingos is "flat," and the indicated rise in the gravel layer is a profile artifact.

Coring at the toe and on the slope of Weather Pingo would provide information on the slope of the ice/gravel interface and the internal layers within the pingo ice.

A radar profile was made on the relatively level surface at the top of Weather Pingo. The profile was run along the long axis of the mound, perpendicular to the profiles in Figures 2-5. It indicated that the ice/gravel interface was relatively flat as shown in Figure 11. There is also indication of layering in the gravel just below the ice/gravel interface.

Wide-angle reflection and refraction (common depth point) measurements were also made on the top of Weather Pingo. Analysis of the two-way wavelet

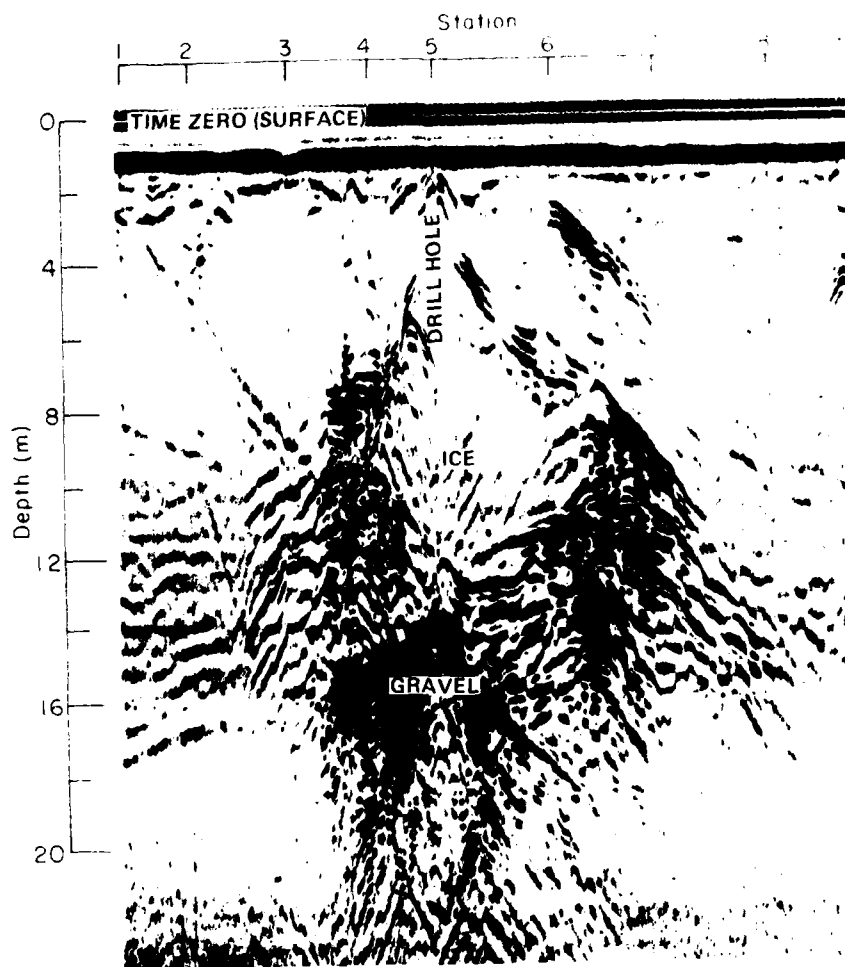


Figure 9. Radar profile made over Prudhoe Mound (pingo) using a 120-MHz antenna.

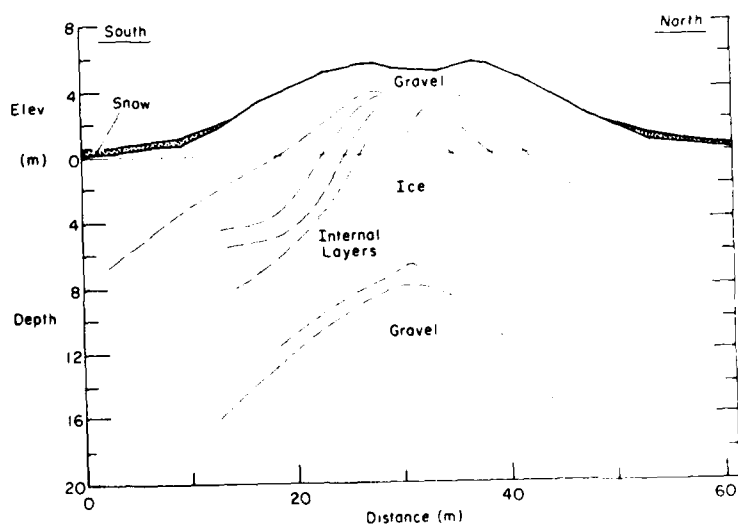


Figure 10. Cross section of Prudhoe Mound (pingo) as constructed from elevation survey and radar flight time data.

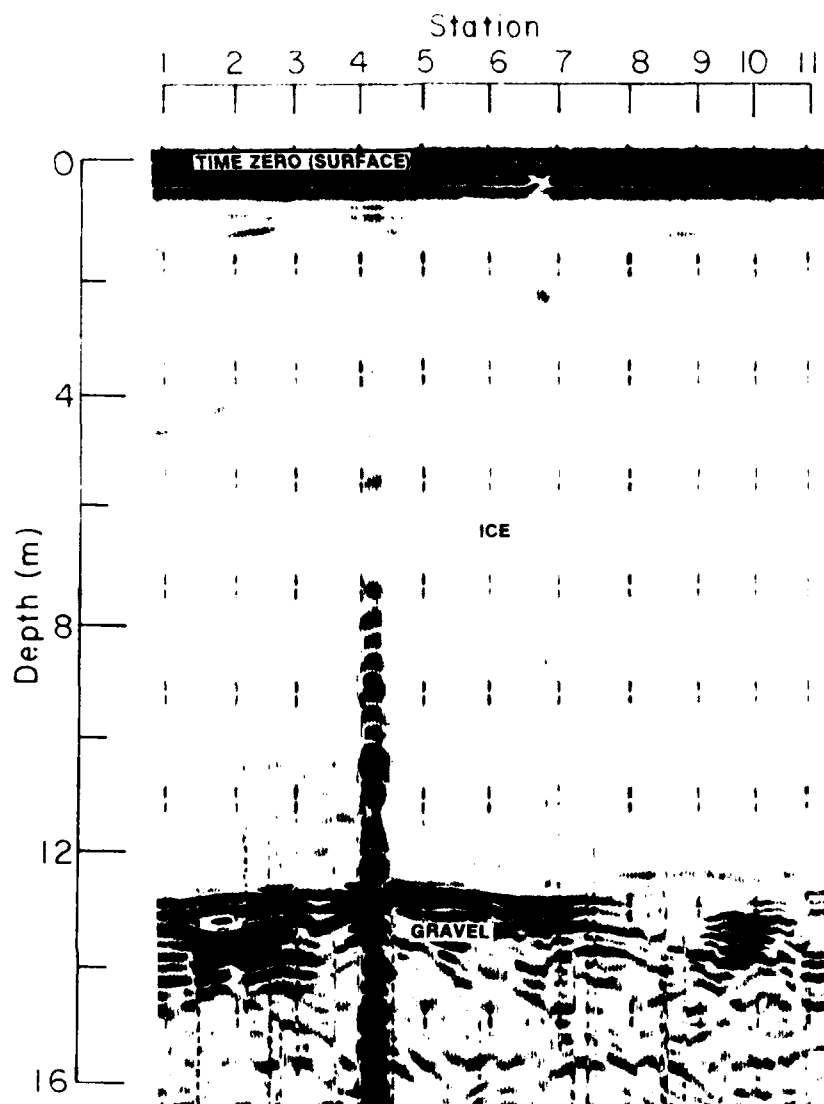


Figure 11. Radar profile along east-west axis of Weather Pingo. Stations are 1 m apart.

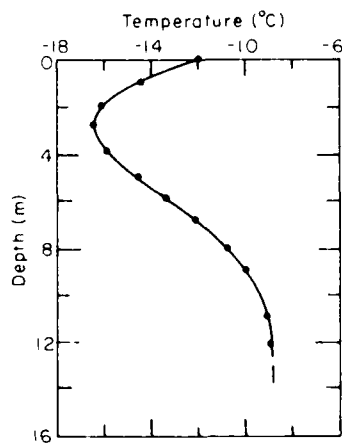


Figure 12. Temperature profile in Weather Pingo.

travel time (t) versus antenna separation distance (x) in a t^2 versus x^2 plot gave an apparent wavelet velocity to the gravel interface of 0.161 m/ns. As with virtually all radio echo wide-angle reflection and refraction sounding results when the dielectric constant varies with depth (see paper by Morey and Kovacs, p. 53 of this report), this velocity did not agree with the value calculated from the wavelet travel time obtained in vertical sounding and the drill-hole-measured gravel depth. At Weather Pingo the velocity was found to be about 0.172 m/ns.

Temperature measurements made in the borehole one year after drilling are shown in Figure 12. At a depth of 13 m, the temperature in the pingo is

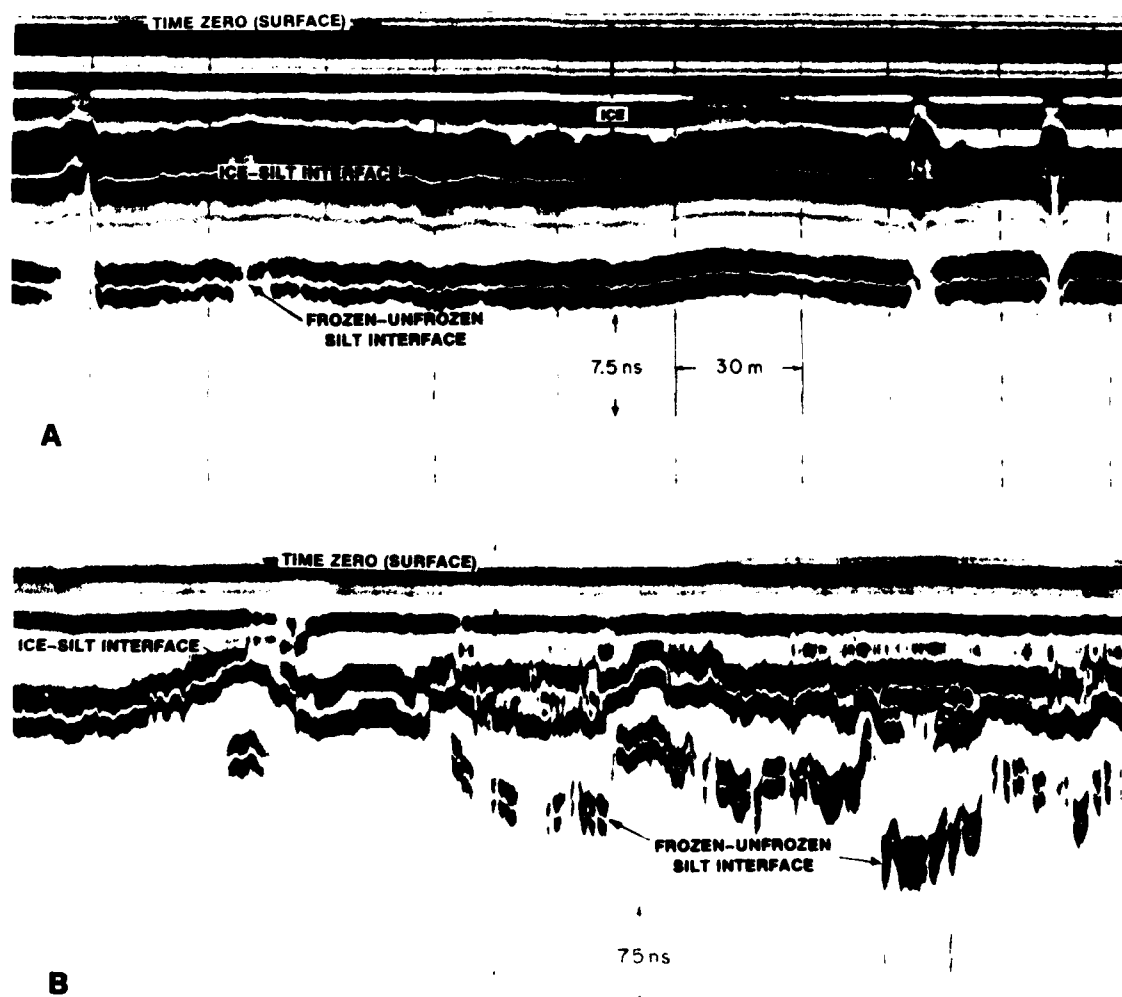


Figure 13. Graphic records of radar profiles made on surface of grounded fast ice.

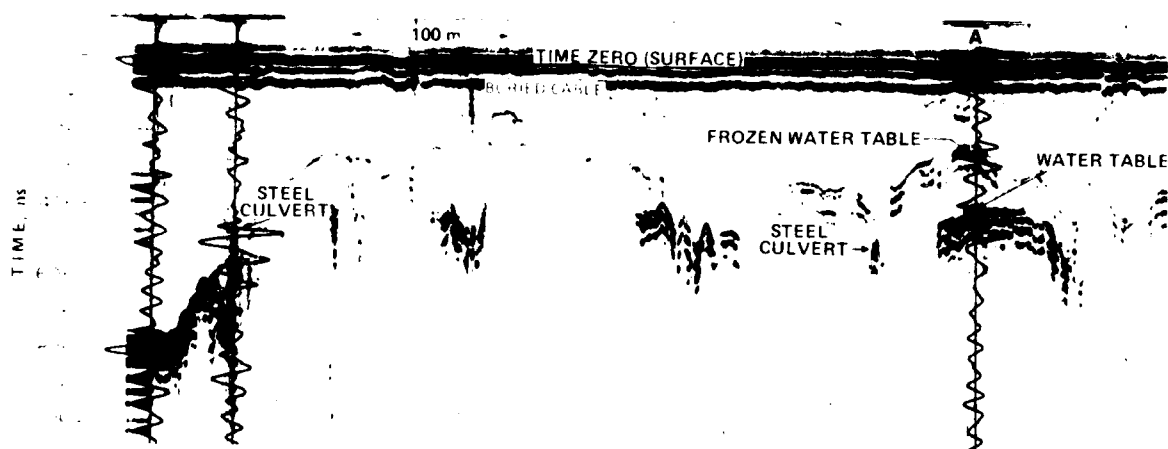


Figure 14. Radar profile made on dredge tailings. Superimposed on the record are three x-y plots of the reflected EM wavelet. Note that the higher voltage amplitudes of the wavelets appear as darker bands on the record. The ordinate is the two-way travel time. Velocity to top of steel culvert on left was 0.155 m/ns (ϵ' about 3.7). Frozen water table at position A was at about 1.9 m and the free water at about 3.3 m. Water table on extreme left was at about 5.9 m.

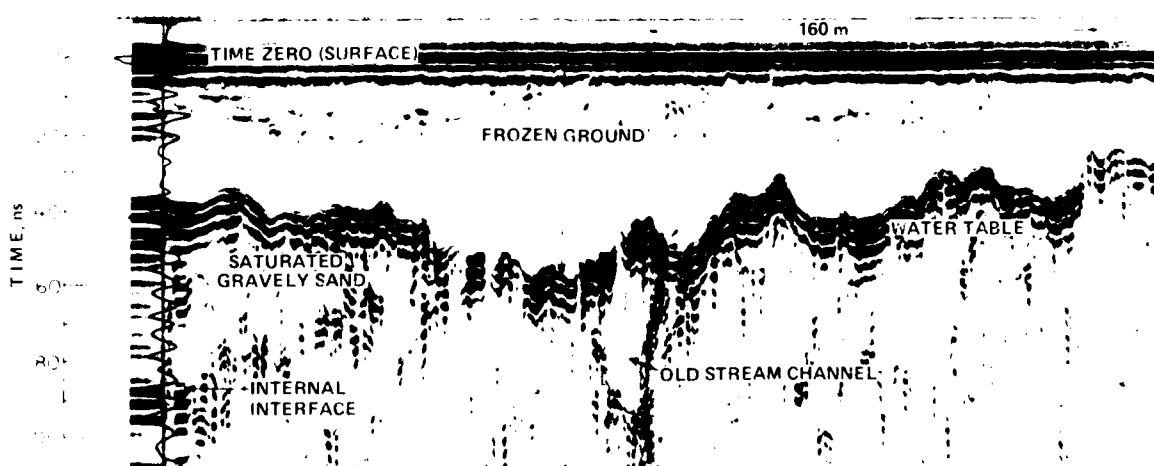


Figure 15. Radar profile along road on Duck Island. A drill hole at the location of the superimposed reflected EM wavelet on left side of figure revealed frozen sandy gravel to about 0.4 m, then a thin frozen silt band at about 18 ns on the ordinate followed by frozen gravelly sand. The water table at the bottom of the frozen ground was located at about 2.90 m (V about 0.153, ϵ' about 3.8).

approaching the relatively stable temperature of the surrounding ground, which is about -8.5°C at a depth of about 20 m.

Impulse radar subsurface profiling was used on the ice surface off the Sagavanirktok River Delta in 1978 to detect the frozen sea ice/seabed interface. The bottom-fast ice at our study site consisted of 0.35 m of brackish water ice having a salinity of 0.1 to $0.7^{\circ}/_{00}$ followed by about 0.57 m of sea ice having a salinity of 2 to $6^{\circ}/_{00}$. The seabed below the ice was found to consist of frozen silt. Drilling into this material revealed it to be frozen to a depth of about 0.5 m. Below this interface the silt was found to be moist. Graphic records of two profile runs are presented in Figure 13. These records show the sea ice/silt interface and, intermittently, the frozen/unfrozen silt interface.

In 1980 at Fox, Alaska, we were able to detect the frozen water table in dredged gravel tailings and the free water below this interface (Fig. 14). Along a segment of the Tanana River bank by the Fairbanks Airport the depth of the seasonal frost table (about 3 m) was profiled as was the depth to the bottom of the nearby permafrost, which varied from 4 to 8 m. The water table in the thawed ground was again detectable. On Duck Island in the Tanana River impulse radar profiling revealed subsurface soil layering and the seasonal frost - water table boundary (Fig. 15).

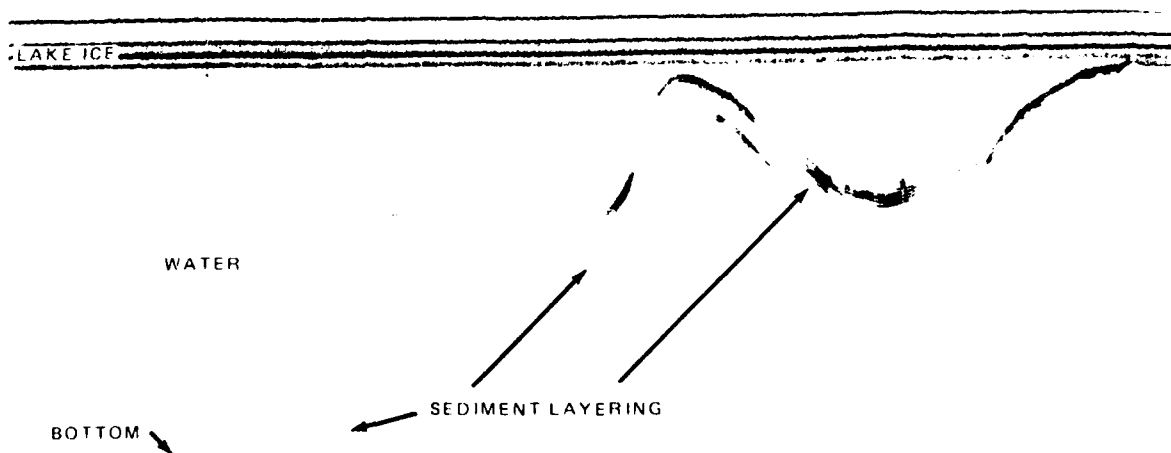


Figure 16. Profile of pond bottom and internal sediment layering. Pond was about 12 m deep on left side of profile.

The depths of lakes and rivers have also been profiled from the ice surface, and internal sediment layering observed (Fig. 16).

The above findings represent positive sounding results. We have also had many negative results where the soils were highly conductive, thus limiting electromagnetic penetration. Where the internal ground structure was very disordered the source of the reflected wavelets could not be determined. Unsatisfactory surveys have also resulted from various equipment malfunctions.

REFERENCE

- Kovacs, A. and R.M. Morey (1979) Remote detection of massive ice in permafrost along the Alyeska Pipeline and the pump station feeder gas pipeline. Proceedings of the Specialty Conference on Pipelines in Adverse Environments, ASCE, New Orleans, 15-17 January.

SUGGESTED LEGEND TERMINOLOGY FOR PERMAFROST MAPPING

R.A. Kreig
R.A. Kreig & Associates, Inc.
Anchorage, Alaska

INTRODUCTION

This discussion is concerned with the terminology used for mapping the areal extent of permafrost (as opposed to the mapping of frozen soil types or ground ice content). It is not concerned with whether the permafrost is defined by temperature (cryotic) or the degree of ice bonding (van Everdingen 1976). The mapping of permafrost has recently been reviewed and discussed by Heginbottom (1984) (see also paper on p. 15). That review touched on the different legends and terminology that have been used in the past to prepare such maps. This paper will treat this subject in more detail and present a suggested legend for discussion.

SCALE CATEGORIES FOR PERMAFROST MAPS

Permafrost maps can be divided into four broad-scale categories:

Very Small Scale	1:1,000,000 or smaller--includes the "miniature maps" and "national maps" of Heginbottom (1984, p. 78)
Small Scale	1:100,000 to 1:1,000,000
Medium Scale	1:24,000 to 1:100,000
Large Scale	1:24,000 or larger--includes the detailed geotechnical and terrain unit maps prepared for recent petroleum transportation projects in Alaska (TAPS and ANGTS at 1:12,000 scale)

PREVIOUSLY USED TERMINOLOGY

Most small and very small scale maps call their permafrost subdivisions zones, while others describe them as units (as noted in the following description of individual maps).

Small and Very Small Scale maps: Black (1950) used a legend with the terms continuous, discontinuous and sporadic permafrost zones on a 1:60,000,000-scale map of world permafrost distribution. If the permafrost-free areas are considered to also be a zone, this map has a total of four units. Ferrians (1965) used a legend which first subdivided the state on the

basis of physiography for a 1:2,500,000-scale map of permafrost in Alaska. At the second level in the legend, he further subdivided on the basis of five units. These units were named, in decreasing order of permafrost extent (based on the percentage of permafrost in the different mapping units): continuous, discontinuous, numerous isolated masses, isolated masses, and free of permafrost. Four different permafrost zones are shown on the 1:25,000,000-scale permafrost map of Canada by Brown (1970). The permafrost region was first divided into continuous and discontinuous zones; the latter zone was then subdivided into the widespread and southern fringe zones; there is also an implied permafrost-free zone. For onshore, latitudinal permafrost Péwé (1983) used only the terms continuous and discontinuous permafrost for a total of three zones if the permafrost-free areas of his map are implied to also be a zone. While Brown (as did Péwé 1983) avoided use of the term sporadic, Ives (1974) and Heginbottom (1984) restored Black's use of it for their 1:80,000,000-scale maps of Northern Hemisphere permafrost distribution.

Large Scale maps: On numerous terrain assessment projects in Alaska performed in the past 14 years, I have used a permafrost mapping terminology concept that is based solely on the percentage areal extent of permafrost. These projects include the highly detailed geotechnical investigations required for design of the Trans-Alaska Pipeline System (TAPS) and the Alaskan Northwest Natural Gas Transportation System (ANGTS), which involved mapping based on airphoto analysis, extensive field work, and approximately 25,000 boreholes. Mapping scales were typically 1:12,000. The legend used had four units:

<u>Symbol</u>	<u>Unit name</u>	<u>Permafrost extent</u>
F	Generally frozen	90-100% frozen
D	Discontinuously frozen	50- 89% frozen
S	Sporadically frozen	11- 49% frozen
U	Generally unfrozen	0- 10% frozen

PROPOSAL FOR A NEW LEGEND TERMINOLOGY

With increasing interest in the mapping of ground ice and permafrost in Canada and the U.S., this may be a good time to discuss ideas for a new legend. It is my belief that such a legend should ideally attempt to satisfy the following criteria:

1. The same basic legend should be suitable for use with all the different scales used for permafrost mapping (from Very Small to Large).

2. The same legend should be suitable for use whether large or small amounts of field information are available to prepare the map. Numerous borings and field observations, including ground temperature sites, are available to the terrain analyst doing mapping on mammoth projects like TAPS, ANGTS, Polar Gas, etc. In contrast, other mapping may have to be prepared from very limited field data or image interpretation alone.
3. The legend should be based on the percentage (by area) of a given map unit that is underlain by permafrost. Permafrost can be defined as either cryotic (temperature below 0°C , also termed climatic) or ice-bonded (phase change of water fraction to ice). In the past, some maps have been based on air temperature data because of the absence of any available subsurface information. Other map legends have used permafrost ground temperatures as the basis for defining zones (for example, the Soviet Union has used the -5°C zero amplitude temperature to differentiate the continuous and discontinuous zones). The use of either of these criteria leads to imprecise and unreliable permafrost maps. Zero amplitude ground temperatures can vary by more than 6°C over distances of less than 2 km in interior Alaska (depending on soil textures, ground-mat characteristics, slope, aspect and vegetation types). It is clearly no longer necessary to rely on climate data or ground temperatures to define the legend units for permafrost mapping. Synoptic views of terrain are now possible from enhanced Landsat imagery and high altitude color infrared photography. Subsurface data that are available can now be much better applied and extended in a mapping process because of the continuing improvement of photointerpretation techniques combined with more complete utilization of existing low-altitude airphoto coverage.
4. It should be possible to express uncertainties on the map that result from either lack of information or conflicting information.
5. The criteria defining the breaks between units in the legend should relate as much as possible to units that can be mapped from airphotos and Landsat images and/or field work.
6. The unit breaks should have significance for the needs of the users of these maps, especially engineering and geotechnical users.
7. The legend approach should include the concept of a control section (i.e. the depth below the surface used to include permafrost bodies on the map).

Generalized Mapping (typically with little or no field data)			Detailed Mapping (typically with extensive field data)		
Map Symbol	Unit Name	Percent of Unit Frozen		Unit Name	Map Symbol
F	Generally Frozen	100		Continuously Frozen	F'
		95-100		Generally Frozen	F
D	Discontinuously Frozen	50-94		Discontinuously Frozen	D
S	Sporadically Frozen	6-49		Sporadically Frozen	S
U	Generally Unfrozen	0-5		Generally Unfrozen	U
		0		Unfrozen	U'

Figure 1. Proposed legend for mapping the extent of permafrost on maps of Large to Very Small scale.

I would like to propose for discussion a legend for permafrost mapping (Fig. 1). I believe it satisfies most of the ideal features enumerated above for such a legend.

This legend is a refinement of the one I have previously used on other projects. It has proven to work well for large and medium scale permafrost mapping and I have experimented with it successfully for small scale mapping on enhanced Landsat imagery. I have not tried it for very small scale maps.

Uncertainties can be expressed with this legend by adding question marks to the symbols F, D, S, or U thus: F?, D?, S?, U?. Question marks should not be used with units F' and U' because, by definition, they are known to be either respectively frozen or unfrozen (at whatever confidence level is required for a given purpose).

I propose that a control depth of 50 ft (15 m) be used because the occurrence of permafrost anywhere within this depth can potentially have a significant impact on engineering structures

COMMENTS ON INDIVIDUAL UNITS

F': Continuously Frozen

This unit should be used only where either 1) sufficient field information is available to conclusively demonstrate that the mapping unit is con-

tinuously frozen, or 2) the identification characteristics of the permafrost-terrain relationships (vegetation, airphoto pattern, etc.) are sufficiently straightforward to make a confident interpretation with minimal field data (with due regard to the skill and experience of the permafrost mapper). Note that for most engineering purposes, it will not be necessary to prove that the generally frozen unit (F - 95-100% frozen) has no unfrozen zones. The mapping of a unit as simply "F" will generally suffice. However, for applications where frost heave is of prime concern (such as chilled gas pipelines) the F' unit has distinct engineering significance because heave can occur in any wet, unfrozen, fine-grained taliks that might be present.

F: Generally Frozen

Ninety percent was previously used as the break between the generally frozen and discontinuously frozen legend units on the detailed large-scale terrain studies for ANGTS and TAPS. For most units that would be mapped as "generally frozen," I feel that the permissible inclusions of unfrozen ground in the "F" unit can be confidently reduced from 10% to 5% because of the quality of airphotos and imagery now available and the advancement of skills in terrain analysis of permafrost regions. This would place the break between the generally frozen and discontinuous units at 95% rather than the previous 90%. Mapping unit variability in the "F" unit would be substantially reduced, while that in the "D" unit would not be significantly changed. Any classification changes that increase the uniformity of mapping units will tend to help geotechnical engineers that plan site investigations. They frequently have to make decisions on the commitment of funds for more field exploration in a given area by evaluating the chances of success in reducing the costs of a conservative design necessitated by uncertain site conditions.

D: Discontinuously Frozen

The use of 50% as the break between this unit and S (sporadically frozen) is arbitrary and without obvious engineering significance. It could probably be changed to any number between 30 and 60% without impairing the use of the maps by engineers. The break at 50% is proposed solely for reasons of symmetry. This would subdivide the large middle ground, between 5% and 95% frozen, into two equal units. Geotechnical engineers often must locate a site that satisfies given criteria such as a minimum area and uniform permafrost conditions--either frozen or unfrozen. A subdivision of this large

unit is necessary to help establish the most prudent intensity level of cost-ly field site investigation work.

S: Sporadically Frozen

I favor retention of the term sporadic in permafrost mapping. It is simple and conveys in one word its meaning to nontechnical users. The other terms recently used for the sporadic zone on very small scale maps (i.e. "discontinuous permafrost zone - southern fringe" and "widespread discontinuous permafrost zone") are wordy and awkward in usage. They do not significantly improve the communication of field permafrost conditions. Sporadic is a better term than those similar to "permafrost islands," "insular permafrost zone," etc. However, isolated specific occurrences of permafrost could be considered as "islands" for discussion (not mapping) purposes. It should be noted that the term sporadic is considered by some (especially on the older maps) to be a very thin zone at the southern limits of permafrost. Expanding its definition to include up to 49% frozen extent could lead to confusion (J. Brown, pers. comm.). Additionally, sporadic was dropped as a recognized permafrost zone in the Permafrost Terminology prepared by the National Research Council of Canada (Brown and Kupsch 1974). On the other hand, Soviet workers continue to use it for mapping and regional studies (Fotiev et al. 1978, p. 106, and other papers in the same proceedings volume).

U: Generally Unfrozen

The boundary between sporadic and generally unfrozen should be moved from 10% to 5% for the same reasons discussed under F above (better imagery and terrain analysis skills; more useful to geotechnical users).

U': Unfrozen

This unit is used only when evidence is clear (from drilling, field inspection, geophysics, etc.) that no permafrost occurs within the mapped unit, for reasons similar to those discussed for the F' unit. In contrast to the F' unit, for most engineering purposes, it will be necessary to prove that the generally unfrozen unit (U - 0-5% frozen) has no frozen zones. The mapping of units as simply "U" will not generally suffice for location of facilities requiring unfrozen terrain in otherwise thaw-unstable soil types.

REFERENCES

- Black, R.F. (1950) Permafrost. In Applied Sedimentation (P.D. Trask, Ed.). New York: John Wiley & Sons, Inc., p. 247-273.
- Brown, R.J.E. (1970) Permafrost in Canada. Toronto: University of Toronto Press, 234 pp.
- Brown, R.J.E. and W.O. Kupsch (1974) Permafrost terminology. Associate Committee on Geotechnical Research, National Research Council of Canada, Technical Memorandum No. 111, 62 pp.
- Ferrians, O.J., Jr. (1965) Permafrost map of Alaska. U.S. Geological Survey Miscellaneous Geological Investigations Map, I-445.
- Fotiev, S.M., N.S. Danilova, and N.S. Sheveleva (1978) Zonal and regional characteristics of the permafrost in central Siberia. In USSR Contribution, Permafrost: Second International Conference (F.J. Sanger, Ed.), Washington: National Academy of Sciences, p. 104-110.
- Heginbottom, J.A. (1984) The mapping of permafrost. Canadian Geographer, 28(1): 78-83.
- Ives, J.D. (1974) Permafrost. In Arctic and Alpine Environments (J.D. Ives and R.G. Barry, Ed.). London: Methuen & Co. Ltd., p. 159-194.
- Péwé, T.L. (1983) The periglacial environment in North America during Wisconsin time. In Late-Quaternary Environments of the United States (H.E. Wright, Jr., and S.C. Porter, Ed.). Minneapolis: University of Minnesota Press, vol. 1, 407 pp.
- van Everdingen, R.O. (1976) Geocryological terminology. Canadian Journal of Earth Science, 13(6): 862-867.

VELOCITY-DEPTH STRUCTURE OF OFFSHORE PERMAFROST,
CANADIAN BEAUFORT SEA

H.A. MacAulay, S.E. Pullan and J.A. Hunter
Geological Survey of Canada
Ottawa, Ontario, Canada

Over the past decade, the Geological Survey of Canada has acquired the front ends of thousands of oil company records shot in the Canadian Beaufort Sea. Many of these records show high-velocity first-arrivals which indicate the presence of high-ice-content frozen sediments beneath the sea floor. The depths of these high-velocity refractors have been calculated for over 5000 records, which show refraction velocities ≥ 2200 m/s. It is assumed that velocities in this range almost certainly indicate frozen materials. Because of the strong dependence of seismic velocity on the ice content of unconsolidated sediments, the occurrence of high velocities depends on both temperature and lithology. By confining this analysis to velocities ≥ 2200 m/s we are dealing only with materials in which the fraction of ice exceeds 0.15 (King 1984).

Earlier work on selected lines of these data (Morack et al. 1983) has shown that across much of the shelf there appear to be two distinct layers of high-velocity material. There is considerable irregularity in the structure of the shallow high-velocity material, while the deeper layer may be continuous over large areas. As the occurrence of separate layers might be related to the sea-level history of the Beaufort Sea, we have analyzed the depth of the high-velocity lenses or layers below sea bottom as a function of water depth.

As a first step, 5147 records showing high refraction velocities (≥ 2200 m/s) have been analyzed as a single group, with no account taken of the areal distribution of the data. The results are presented in the form of a contour plot showing the percentage of measurements as a function of both water depth and depth of the high-velocity refractor below sea bottom (Fig. 1). This plot shows the occurrence of a large number of high-velocity refractors within 20 m of the bottom for water depths between 45 and 70 m. There are very few high velocities found within 80 m of the seabed at water depths of 30-40 m, but between 15 and 30 m water depth there were many high-velocity measurements in the range of 30-50 m below bottom. Near shore, very few shallow high velocities were found. The plot also shows a deep layer of high-

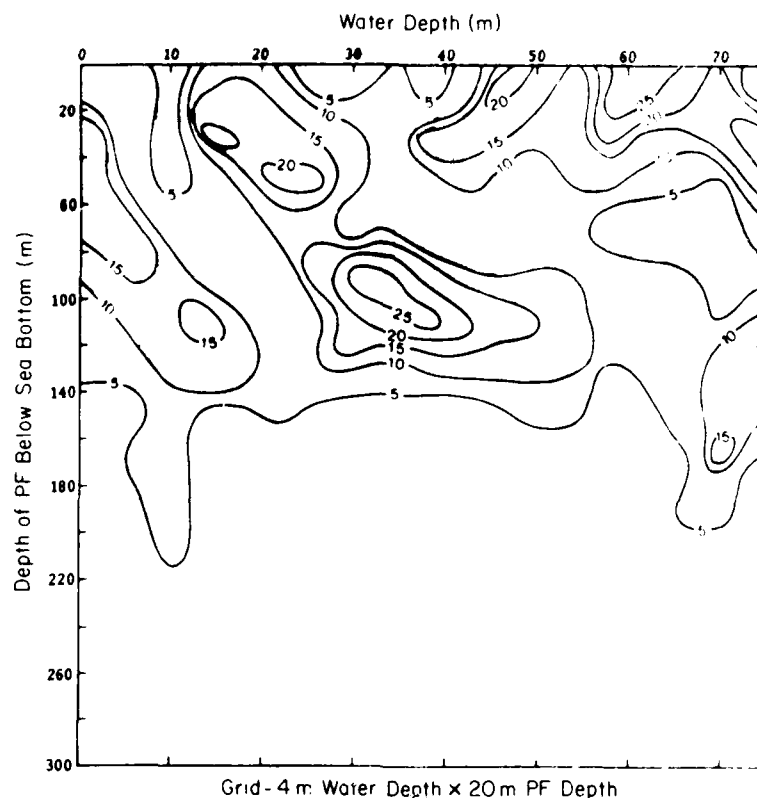


Figure 1. Contour plot of percentage of high refraction velocities (> 2200 m/s) as a function of water depth and depth of refraction below sea bottom.

velocity material which drops off quickly from the shoreline. This layer is found approximately 100 m below the sea bottom and may be essentially continuous over the Beaufort Shelf east of longitude 135°W . The lack of data indicating this deep layer for water depths of 15-25 m and 50-70 m could be due to the masking effect of shallower high-velocity layers/lenses.

As yet we have no satisfactory explanation for the distribution of shallow high-velocity materials except in the near-shore region. Sub-bottom temperature data collected over several spring seasons along near-shore lines clearly indicate a warm bulb due to Mackenzie River outflow that extends out to water depths of 12 m and down to depths of 30 m below bottom. Beyond that, sub-bottom temperatures are continuously subzero and shallow high velocities begin to occur.

The next step in this work is to take into account the areal distribution of these data, and to look at the depths to high-velocity refractors as

a function of water depth on a more regional basis. This work is ongoing at the present time.

REFERENCES

- King, M.S. (1984) The influence of clay-sized particles on seismic velocity for Canadian Arctic permafrost. *Canadian Journal of Earth Sciences*, 21: 19-24.
- Morack, J.L., H.A. MacAulay and J.A. Hunter (1983) Geophysical measurements of sub-bottom permafrost in the Canadian Beaufort Sea. *Proceedings of the Fourth International Conference on Permafrost*. Washington, D.C.: National Academy Press, p. 866-871.

SHALLOW GEOPHYSICAL BOREHOLE LOGGING IN PERMAFROST: A CASE HISTORY

R. Miller
TSA Systems Inc.
Boulder, Colorado

The construction of the Trans-Alaska Pipeline System involved the placement of approximately 77,000 vertical support members for the elevated portion of the hot oil pipeline. While the average length of each was calculated to be approximately 30 ft, the actual length was to be dependent on the dry density of the permafrost soils. Conditions assumed in the original design required field checking to confirm the design or adjust the design in the field (by increasing VSM length) for conditions identified as worse than anticipated. Critical breakpoints in dry density were established to be 70 lb/ft³ and 40 lb/ft³. A need was therefore established for a geophysical tool capable of rapid determination of dry density to be used as an aid to VSM field engineers conducting sample logging of all holes drilled. Alyeska Pipeline Service Company contracted with Holosonics of Richland, Washington, to develop a logging system employing the simultaneous reading of gamma-gamma density and neutron-thermal-neutron logs and thus provide a means of determining these key engineering parameters. Work on the project was initiated in the fall of 1973, initial field testing done in the fall of 1974, and 12 units constructed for the 1975-76 construction season.

A literature search and lab work were undertaken by Holosonics to define the optimum source types, source strengths, and source-detector distances for the neutron and density tools to be designed. For the neutron-thermal-neutron tool, it was determined that optimum source-detector spacing should be < 2 in. or > 12 in.; probe construction dictated the shorter spacing, and the neutron probe was constructed using a 0.250-curie AmBe source, with one BF₃ tube placed above and one below the source. Output of the two tubes was combined. The gamma-gamma density tool used a 0.250-curie Cs137 source and a 3/4 x 1-1/2-in. NaI(Th) detector coupled to a photomultiplier tube, with the source-detector distance set at 12 in.

The probe array consisted of three separate detector assemblies: two gamma-gamma density tools and one neutron tool. They were mounted on arms, spaced at 120° intervals, which could be extended outward from the probe body to contact the wall of the borehole.

Since both the neutron and gamma-density tools measure bulk density, although in different fashion, the neutron (moisture) density and the bulk den-

sity were electronically subtracted by means of an on-board analog computer. The resultant curve - dry density - was plotted along with the basic bulk density and moisture curves on the analog output. Calibration curves were derived from both test borings on site and from test pits constructed of materials of known density and moisture content. Both precision and accuracy were found to be in the $\pm 4 \text{ lb/ft}^3$ range.

In operation, the probe assembly, with detector retracted, was lowered into the hole. The arms, spring-loaded with the source-detector arrays, were put in contact with the sides of the borehole, and the probe pulled up at approximately 20 ft/min. This somewhat rapid probe velocity was dictated by poor hole conditions, and the inability of the probe assembly to stabilize at lower velocities. Since the entire exercise was designed to yield on-site engineering data, a cross-plot chart relating moisture content (lb/ft^3), percent moisture, and dry density (lb/ft^3) was constructed, using a matrix density (specific gravity) of 2.65 as typical of the formation expected to be encountered.

Results were generally very good, with samples from the hole correlating well with log results. Due to a high degree of horizontal variability in the large diameter holes, no point-to-point correlation was demonstrated. The major source of problems encountered was associated with hole wall irregularity, as hole diameter changes of as little as 1 in. skewed the data. Engineering data initially were reported to be less than satisfactory on dry densities of less than 70 lb/ft^3 (60% moisture), and it was found necessary to generate a separate set of curves for dry densities in the 40- to 70-lb/ft^3 material.

It certainly appears that the field program was a success, and validated the method of using a combination of neutron and bulk density measurement to evaluate specific sites for engineering purposes. It proved more than adequate for VSM design evaluation.

A case must be made for the use of multiple small diameter (3-5 in.) holes for these same purposes. We are currently developing a small-hole logging system for use in permafrost soils. In this application, however, it would be possible to use combination tools which offer more definitive density and moisture measurements, as well as temperature, caliper, resistance, and natural gamma. The entire logging package -- winch, probes, power, and electronics -- can be made helicopter-portable (< 300 lb) and thus adaptable to a far greater range of usage.

ANALYSIS OF WIDE-ANGLE REFLECTION AND REFRACTION MEASUREMENTS

R.M. Morey and A. Kovacs
Cold Regions Research and Engineering Laboratory
Hanover, New Hampshire

The analysis of subsurface radar surveys sometimes depends on knowing the velocity of propagation of the radar signal in the ground. This velocity information is then used to calculate the depth to subsurface targets and interfaces. For layered earth, velocity data can be estimated by performing wide-angle reflection and refraction (WARR) surveys. Examples of radar equipment, procedures and WARR profiles are given in Morey (1974), Davis et al. (1976) and Arcone (1984), among others. Basically, a WARR survey is performed by continuously increasing the separation between a transmitting antenna and a receiving antenna. The antenna separation, x , is recorded along with the travel time, t , of the radar wavelet from the transmitting antenna to a reflecting layer and back to the receiving antenna. A horizontal reflecting layer will produce a hyperbolic pattern on the resulting time-distance plots, but only if a constant velocity exists in the subsurface medium to the reflector. The time-distance information can be plotted on a t^2-x^2 graph (Jezek et al. 1978). The slope of the line through the data points is the velocity of propagation to the reflecting layer. From the velocity value, the dielectric constant can be calculated.

Some investigators, using WARR data, have calculated dielectric constants lower than expected. This paper presents one possible reason for the underestimation of dielectric constants determined from WARR surveys.

Wide-angle reflection and refraction measurements are used to determine the dielectric properties of earth materials and the depth to an interface. The evaluation of the resultant t^2-x^2 plots assumes that the radar ray path is a straight line from the transmitter to the reflector and back to the receiver. However, there are many instances where the dielectric constant changes with depth. This variation causes the rays to bend (be refracted) instead of following a straight ray path to the subsurface interface. For example, in polar ice shelves the dielectric constant of the firn increases with depth; this causes a negative velocity gradient which bends the ray towards the vertical. A simple two-layer model showing this effect is given in Figure 1. Snell's law governs this process of refraction:

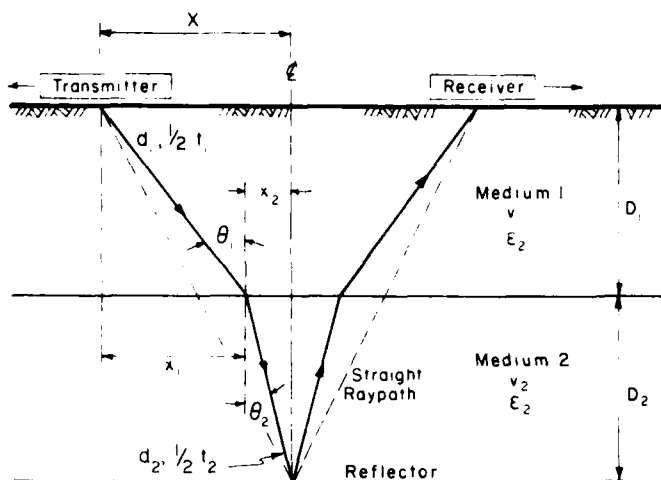


Figure 1. Model example of WARR common-depth-point impulse radar antenna configuration showing EM wavelet ray path in two materials.

$$\frac{\sin \theta_1}{v_1} = \frac{\sin \theta_2}{v_2}$$

where v_1 , v_2 = velocity of propagation in media 1 and 2 respectively (see Fig. 1). The following shows the error which can exist in the calculated apparent dielectric constant when refraction is not taken into account in analyzing the WARR data. We demonstrate this by calculating x_1 (see Fig. 1) when the dielectric constants of medium 1 (ϵ_1) and medium 2 (ϵ_2) along with the depth (D_1 and D_2) of each layer and the antenna separation ($2X$) are given. The ray path lengths in each layer, d_1 and d_2 , are calculated and then the total time of flight determined. This refracted (or actual) travel time will always be less than the straight line ray path travel time. The total distance traveled by the ray will be greater than the straight line distance, thus giving a total or bulk apparent dielectric constant ϵ_a less than the actual value. The errors are greatest at large antenna separations. Listed are the formulas used:

$$D = \frac{t \cdot c}{2 \sqrt{\epsilon_r}}$$

$$v = \frac{c}{\sqrt{\epsilon}}$$

$$t_1 = \frac{2 d_1}{v_1}$$

$$t_2 = \frac{2 d_2}{v_2}$$

We want $t_1 + t_2 =$ the minimum value. Thus

$$\sin \theta_1 = \frac{x_1}{d_1}$$

$$\sin \theta_2 = \frac{x_2}{d_2}$$

$$\frac{x_1}{d_1} v_2 = \frac{x_2}{d_2} v_1 \text{ or } x_1 d_2 v_2 = x_2 d_1 v_1$$

Squaring both sides gives $x_1^2 d_2^2 v_2^2 = x_2^2 d_1^2 v_1^2$.

Substituting for x_2 ($x_2 = X - x_1$) yields:

$$(v_2^2 - v_1^2) X^4 - 2X (v_2^2 - v_1^2) x_1^3 + [X^2(v_2^2 - v_1^2) + v_2^2 D_2^2 - v_1^2 D_1^2] x_1^2 + 2X v_1^2 D_1^2 x_1 - X^2 v_1^2 D_1^2 = 0$$

or:

$$a x_1^4 + b x_1^3 + c x_1^2 + d x_1 + e = 0$$

where:

$$a = (v_2^2 - v_1^2),$$

$$b = -2X (v_2^2 - v_1^2)$$

$$c = [X^2 (v_2^2 - v_1^2) + v_2^2 D_2^2 - v_1^2 D_1^2]$$

$$d = 2X v_1^2 D_1^2$$

$$e = -X^2 v_1^2 D_1^2$$

Solving for the roots we arrive at

$$x_1^4 + \frac{b}{a} x_1^3 + \frac{c}{a} x_1^2 + \frac{d}{a} x_1 + \frac{e}{a} = 0$$

There are four roots; only one root is reasonable.

If we take an extreme case as an example, we find that the error in the bulk ϵ_a can be substantial. Figure 2 shows 2 m of fresh ice ($\epsilon_1 = 3$) over 4 m of fresh water ($\epsilon_2 = 88$). The calculated ray paths are indicated. Beyond an X of about 5 m the ray leaving the water will be beyond the critical angle and will not return to the ice surface. However, for illustrative purposes, X was taken out to 16 m. The total two-way transit time for vertical sounding ($X = 0$) is about 273 ns, giving a bulk $\epsilon_a = 47$ and $v_m = 0.044$ m/ns. The two-way travel times along the ray paths (Fig. 2) are plotted versus antenna separation in Figure 3. Note that rather than being a straight

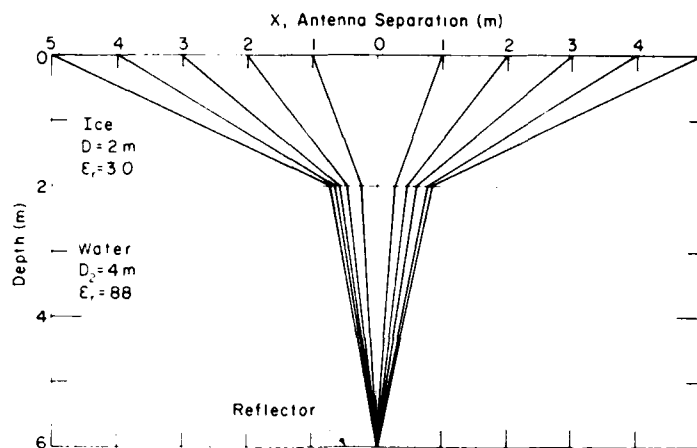


Figure 2. Model example for WARR common-depth-point EM ray path through ice and water media.

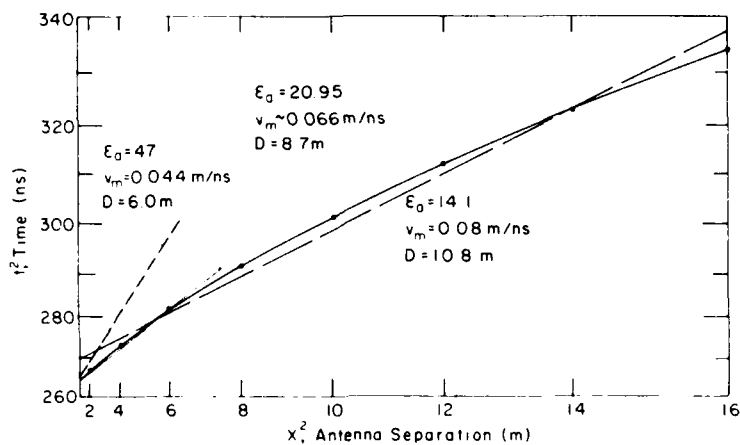


Figure 3. t^2 - X^2 plot of model results depicted in Figure 2.

line the data points form a curve. The data points are what would actually be measured in a WARR survey. The normal procedure would be to calculate the linear least squares fit to the data. In this case the calculated bulk ϵ_a would be 14.1, which is about 3 times lower than the correct value of 47. Even if we run a line through just the first three points, at antenna separations of 2, 4 and 6 m, the bulk ϵ_a would be calculated to be about 21, or less than half the actual bulk ϵ_a value of 47. Therefore, if there is any velocity gradient, positive or negative, a standard WARR analysis will always give a lower apparent dielectric constant.

Another example is fresh water over a lake bottom. Figure 4 shows 2 m of water ($\epsilon_1 = 81$) over 4 m of saturated soil ($\epsilon_2 = 20$), while Figure 5 pre-

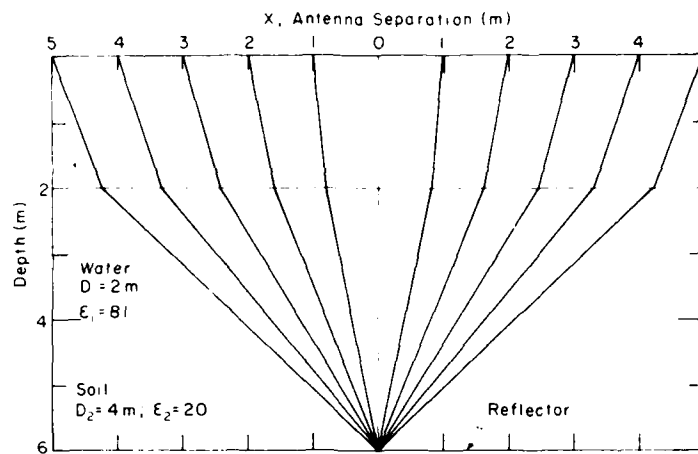


Figure 4. Model example for WARR common-depth-point EM ray path through water and saturated soil media.

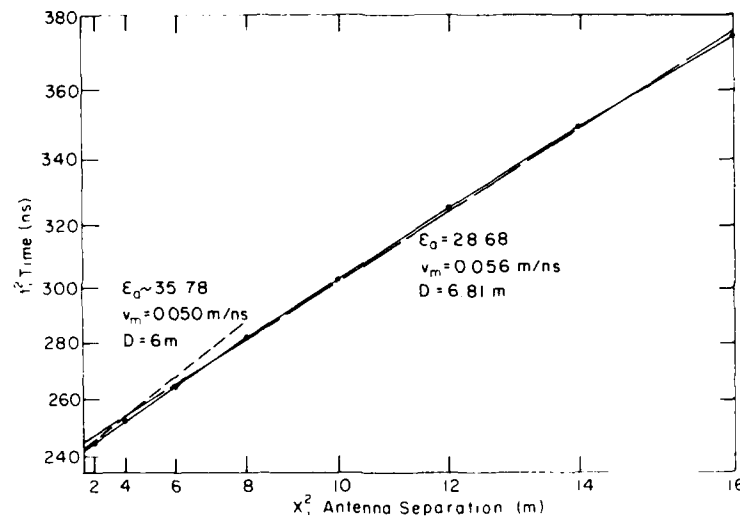


Figure 5. t^2-X^2 plot of model results depicted in Figure 4.

sents the t^2-X^2 plot. Again the type of curvature is the same as that in Figure 3. The actual bulk apparent dielectric constant is 35.78, whereas the WARR calculated value is 28.68. Both Figures 3 and 5 show that the linear least squares fit line intersects the time axis above the "measured" vertical two-way travel time. Along with the lower calculated bulk apparent dielectric constant and higher two-way travel time, the calculated depth to the reflector will always be greater than the measured depth when the raw time-distance data are used in a standard WARR analysis (Hughes 1984).

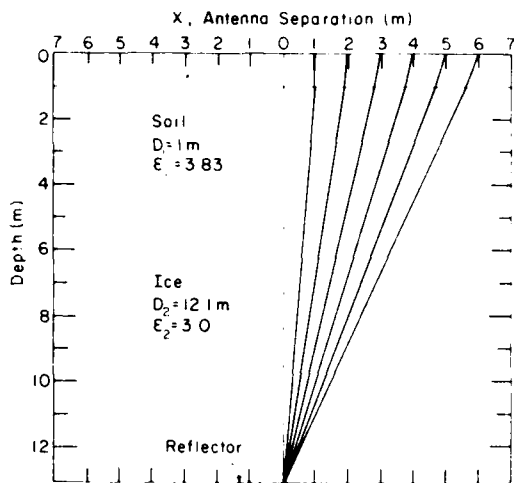


Figure 6. Model example for WARR common-depth-point EM ray path in Weather Pingo.

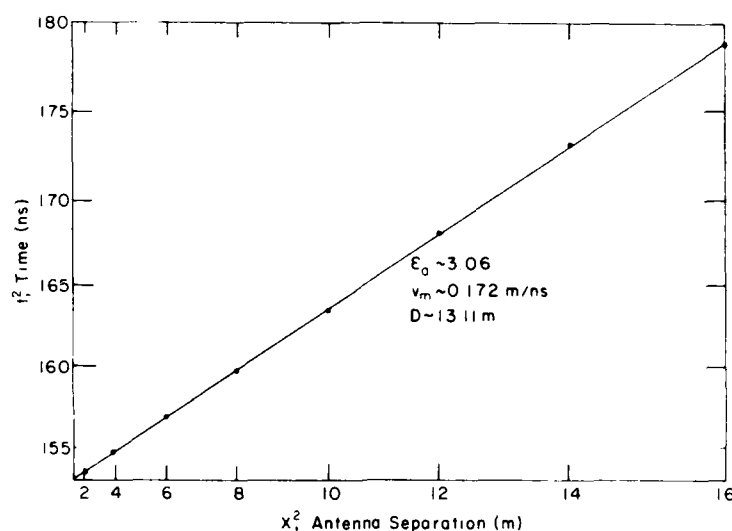


Figure 7. t^2-X^2 plot of model results depicted in Figure 6.

A WARR (common depth point) profile was made on top of Weather Pingo, Prudhoe Bay, Alaska. Drilling indicated 1 m of frozen soil over 12.1 m of ice. The vertical two-way EM wavelet travel time at this drill hole site was used to calculate a bulk apparent dielectric constant of 3.06. If the bubbly ice had an $\epsilon_a = 3.0$, then the 1 m of frozen soil would have had an $\epsilon_a = 3.83$ in order for the bulk ϵ_a to be 3.06. This situation is modeled in Figure 6. Since the velocity gradient in the model is relatively small, the time-distance plot (Fig. 7) for the model gives a bulk ϵ_a of 3.06 and a depth of 13.1 m, which is in agreement with the depth measured in the drill hole. However, the WARR common-depth-point measured time-distance data shown

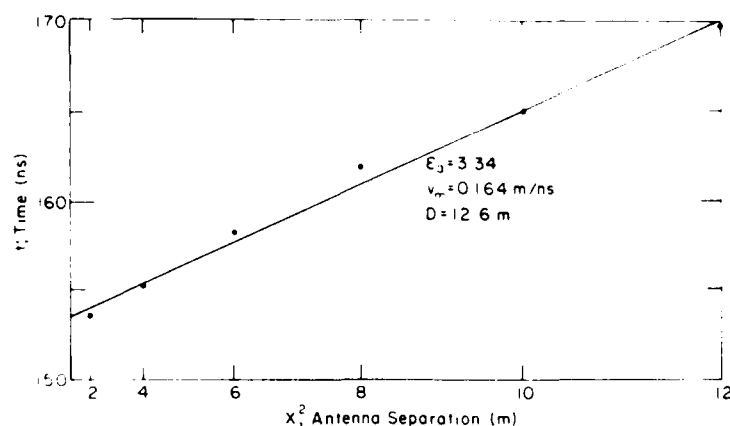


Figure 8. t^2 - X^2 plot of WARR common-depth-point survey data obtained on Weather Pingo.

in Figure 8 have the characteristic curve of a greater velocity gradient. For some reason, the bulk ϵ_a as determined from the slope of the curve passing through the WARR data is 3.34, which is higher than the value of 3.06 calculated from the measured vertical two-way travel time over the borehole. In addition, the ice bottom as determined from the WARR data was about 12.6 m, or 0.5 m less than the borehole-determined depth. From the previous analyses we would not have expected the WARR-determined bulk ϵ_a to be higher than that determined from the vertical sounding data. However, it should be pointed out that the center of the WARR common-depth-point measurement array was about 6 m away from the borehole site. Therefore, the reason why the WARR bulk ϵ_a is higher than that determined by vertical sounding at the borehole location may be a thicker layer of frozen ground at the WARR common-depth-point site or a system timing error of as little as 3%.

Our past experience with WARR common-depth-point profiling on the McMurdo Ice Shelf, Antarctica, always gave lower values for the apparent dielectric constant than those determined from vertical soundings to a known target depth. The reason was a dielectric constant gradient in the firn, ϵ_a , that increased with depth. The effect of such a gradient can be inferred from the preceding analysis and has been discussed by Jezek and Roeloffs (1983). In short, the use of WARR data to infer horizon depth and the electromagnetic properties of the subsurface environment may result in very erroneous information.

REFERENCES

- Arcone, S.A. (1984) Field observations of electromagnetic pulse propagation in dielectric slabs. *Geophysics*, 49: 1763-1773.
- Davis, T.L., W.T. Scott, R.M. Morey and A.P. Annan (1976) Impulse radar experiments on permafrost near Tuktoyaktuk, Northwest Territories. *Canadian Journal of Earth Sciences*, 13(11): 1584-1590.
- Hughes, D. (1985) V w/o T: Velocity without tears. *Geophysica: The Leading Edge*, 4(2).
- Jezek, K.C., J.W. Clough and C.R. Bentley (1978) Dielectric permittivity of glacier ice measured in situ by radar wide-angle reflection. *Journal of Glaciology*, 21(85).
- Jezek, K.C. and E.A. Roeloffs (1983) Measurements of radar wave speeds in polar glaciers using a down-hole radar target technique. *Cold Regions Science and Technology*, 8(2).
- Morey, R.M. (1974) Continuous subsurface profiling by impulse radar. American Society of Civil Engineers Specialty Conference on Subsurface Exploration for Underground Excavation and Heavy Construction, Henniker, New Hampshire.

SOME ASPECTS OF INTERPRETING SEISMIC DATA FOR INFORMATION ON SHALLOW SUBSEA PERMAFROST

K.G. Neave
Northern Seismic Analyses
Echo Bay, Canada

P.V. Sellmann
Cold Regions Research and Engineering Laboratory
Hanover, New Hampshire

Refraction analysis of oil-industry seismic records has been able to delineate the boundary of cold relict permafrost near the coast (Neave and Sellmann 1982). An example is shown in Figure 1 for Prudhoe Bay. A more elusive target has been to outline the top and extent of the warmer subsea permafrost.

There are three problems associated with finding the extent of warmer ice-bonded sediments. First, the boundary is not sharp; it is often gradational, with strong contrasts in seismic velocity seldom observed offshore (Neave and Sellmann 1983). This implies that temperature and salinity usually change gradually and produce gradients in ice content and ice bonding. The second problem is that shallow gas shifts the velocity ranges for both

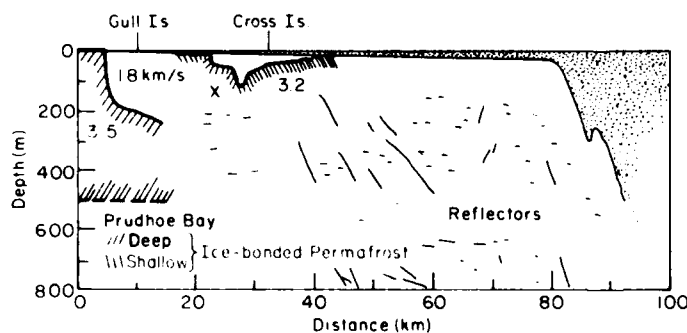


Figure 1. Cross section of the Beaufort Shelf at Prudhoe Bay. A high-velocity refractor outcrops at the shoreline and slopes northward to more than 200 m depth under the bay. Shallow refractors with lower velocity occur farther offshore. The base of permafrost is plotted at the depth indicated in Osterkamp and Payne (1981).

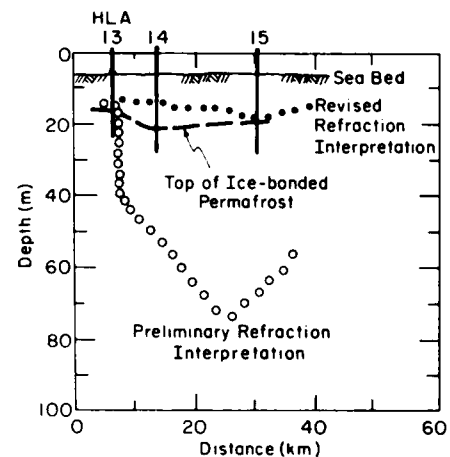


Figure 2. Preliminary and corrected refraction interpretation for Foggy Island Bay and Mikkelsen Bay along a line of Harding Lawson Associates boreholes. The top of ice-bonded permafrost is plotted as reported in Miller and Bruggers (1980).

thawed and bonded sediments (Gregory 1976, Domenico 1977) and makes interpretation of velocity and depth much more uncertain. The third problem is that the signal-to-noise ratios are poor on the records, partly because of attenuation due to the shallow gas, which often makes identification of first arrivals for refraction interpretation difficult.

An example of coping with the shallow gas problem is provided using data from an area west of the Sagavanirktok River Delta. We propose that a "hidden layer," a gassy, thawed Holocene stratum with a velocity as low as 0.3 km/s, can be invoked to make the seismic interpretation agree with the published drilling results (Fig. 2). A correction of 80 m (90 ms of delay time) is required to compensate for the gas "push-down" that occurred in our preliminary refraction interpretation. Similar corrections are anticipated for parts of Harrison Bay where shallow gas is also present (Fig. 3).

Another approach to the gas problem comes from surface wave analysis. Surface waves have the distinct advantage that they are not affected by shallow gas to the same extent as compressional waves (Domenico 1977). Therefore, changes in surface wave velocity may be attributed to variations in other material properties such as degree of ice bonding and overconsolidation. Surface waves are invariably lower frequency signals and are not usually recorded on marine seismic surveys, but they do appear on the nearshore oil industry records (Fig. 4). The surface wave velocity readings for Harrison Bay, Foggy Island Bay and Mikkelsen Bay are approximately 0.6 times the observed values on land (i.e. the dynamic rigidity drops to about one-third for the subsea materials in these areas).

Normal mode dispersion analysis has been used with some success to overcome the signal-to-noise problem that shallow gas and ice-bonded permafrost create (Fig. 5). Compressional wave velocities for the seabed have been de-

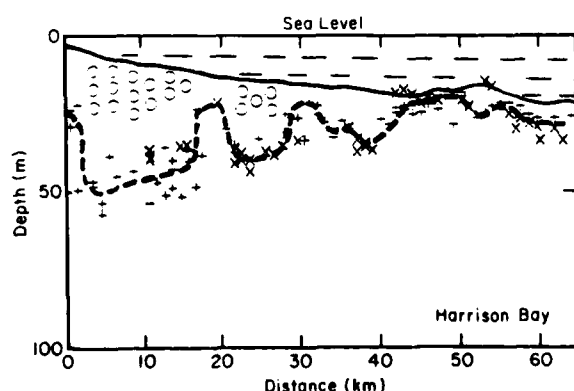


Figure 3. A north-south cross section situated near the Colville Delta. The circles represent shallow gas detected by strong seismic attenuation (Neave and Sellmann 1982). The seismic depth interpretation is "pushed down" by 20 m under the gassy locations and should be corrected upward to show a relatively flat surface for the top of ice-bonded permafrost.

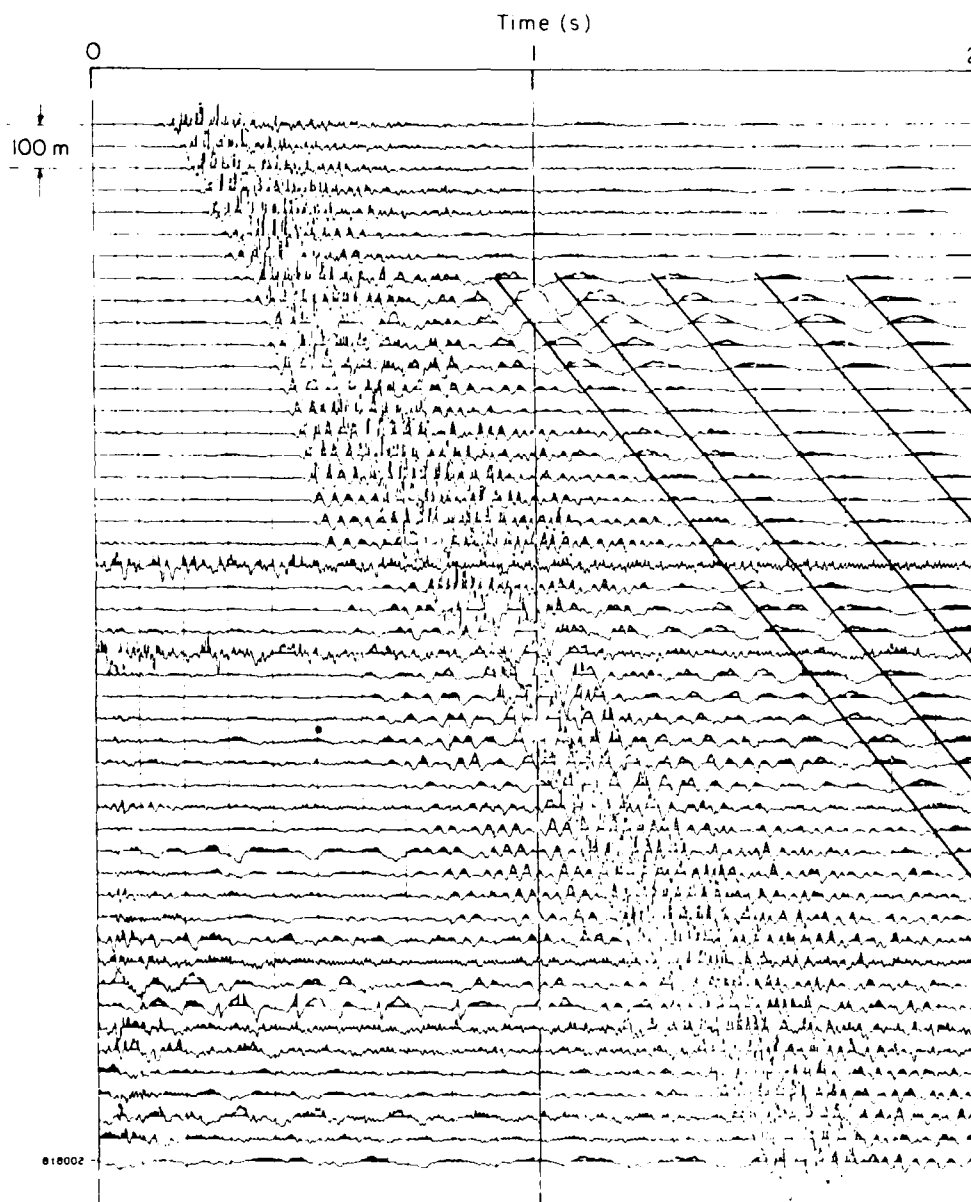


Figure 4. A shallow water marine seismic record with surface waves. The surface waves are the late-arriving low frequency signals marked with lines on the record.

terminated in a number of cases where the first-arrival refractions are not visible above the noise level. Drilling control has established that a dispersion interpretation has delineated the top of shallow ice-bonded permafrost at several locations, and elsewhere has located the top of unfrozen Pleistocene gravels.

Because of the complexity of the subsea permafrost environment, it appears that proper analysis of seismic data can be greatly enhanced when suf-

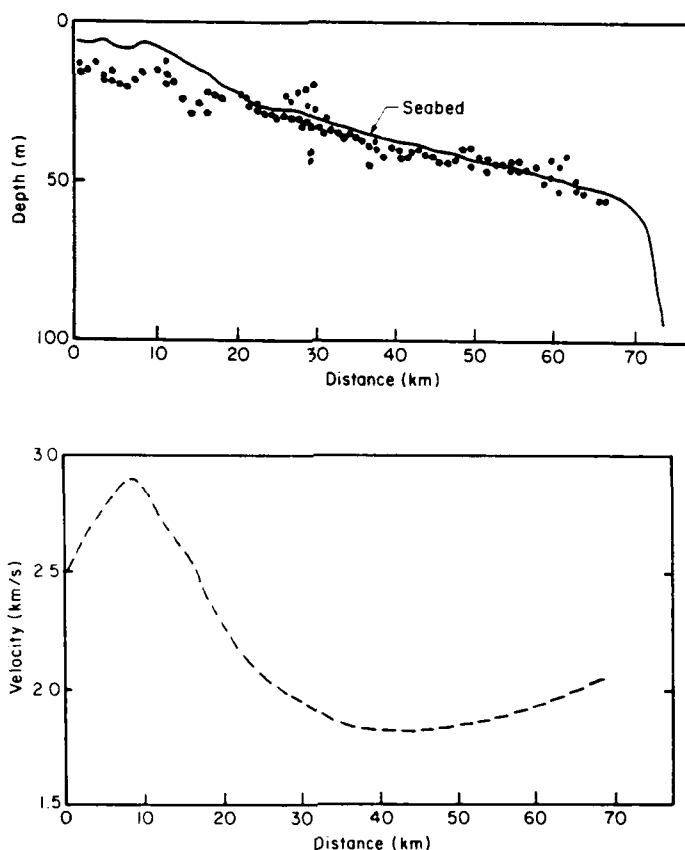


Figure 5. A cross section and velocity profile from dispersion analysis of seismic records. The section is located north of the Sagavanirktok River Delta where there is drilling control (Miller and Bruggers 1980). The top of ice-bonded permafrost is indicated by the top of the shading in the shallow water area. Dispersion depths agree with the drilling results and the high velocities are compatible with the presence of ice bonding in the sediments.

ficient control is available to establish an appropriate interpretation technique for a given region.

This study was funded wholly by the Bureau of Land Management through inter-agency agreement with the National Oceanic and Atmospheric Administration, as part of the Outer Continental Shelf Environmental Assessment Program. We would like to thank the geophysical companies for their cooperative spirit in providing necessary seismic data.

REFERENCES

- Domenico, S.N. (1977) Elastic properties of unconsolidated porous sand reservoirs. *Geophysics*, 42(7): 1339-1368.
- Gregory, A.R. (1976) Fluid saturation effects on dynamic elastic properties of sedimentary rocks. *Geophysics*, 41(5): 895-921.
- Miller, D.L. and D.E. Bruggers (1980) Soil and permafrost conditions in the Alaskan Beaufort Sea. *Proceedings 12th Annual Offshore Technology Conference*, p. 325.
- Neave, K.G. and P.V. Sellmann (1982) Subsea permafrost in Harrison Bay, Alaska: An interpretation from seismic data. *USA Cold Regions Research and Engineering Laboratory, CRREL Report 82-24*.
- Neave, K.G. and P.V. Sellmann (1983) Seismic velocities and subsea permafrost in the Beaufort Sea, Alaska. *Proceedings, Fourth International Conference on Permafrost*. Washington, D.C.: National Academy Press, p. 894-898.
- Osterkamp, T.E. and M.W. Payne (1981) Estimates of permafrost thickness from well logs in northern Alaska. *Cold Regions Science and Technology*, 5: 13-27.

PERMAFROST TEMPERATURE MEASUREMENTS IN AN ALASKAN TRANSECT:
PRELIMINARY RESULTS

T.E. Osterkamp, J.P. Gosink and K. Kawasaki
Geophysical Institute, University of Alaska
Fairbanks, Alaska

The trans-Alaska pipeline and nearby roads cross Alaska from north to south and thus transect continuous, discontinuous and non-permafrost regions. A number of investigators from the U.S. Geological Survey, the Cold Regions Research and Engineering Laboratory, the Alaska Department of Transportation and Public Facilities, and the University of Alaska have measured permafrost temperatures at various sites along this transect since the 1960's.

Unfortunately, these temperature measurements were made in permafrost that had suffered some degree of thermal disturbance. Consequently, the results, particularly near-surface permafrost temperatures, are difficult or impossible to interpret reliably. During the past few years, we have been systematically establishing drill holes along this north-south Alaskan transect at undisturbed permafrost sites. Nine holes in the 40-80 m depth range and over 20 shallower holes have been drilled. The purpose of this study is to determine the natural thermal regime of the permafrost and to relate it to surface temperature changes produced by present and past climates. This paper presents some preliminary results of these measurements and reviews some of the existing permafrost temperature data along this transect. It should be emphasized that the conclusions reached are tentative and subject to change with further interpretation of the data.

Permafrost temperature data along the general direction of this transect also exist for the offshore region to a water depth of about 17 m offshore from Reindeer Island. These data show that the permafrost thaws from the top and bottom after inundation by relatively warm and salty sea water. Where the soils are coarse-grained, thermal models give an approximate estimate of the amount of thawing.

There is a strong gradient in mean annual surface temperature (MAST) across the Arctic Coastal Plain and evidence for recent increases in MAST which appear to be related to recent climatic warming. This recent warming is superimposed on a longer-term climatic warming (over the past century) which appears to be greatest along the coast and to decrease southward. There is no evidence for climatic warming in the arctic foothills.

The drill holes of our transect in the southern Brooks Range are still recovering from the drilling disturbance. A drill hole at Livengood shows some evidence for recent climatic warming.

A number of drill holes near Chatanika, Fairbanks and Eielson Air Force Base have what appear to be anomalous thermal gradients and varying curvatures in the temperature profiles near the surface, suggesting a recent climatic warming superimposed on a century-long warming similar to that at Prudhoe Bay. Evidence for the recent warming is found in drill holes south of the Alaska Range.

Two drill holes on the north side of the Chugach Range did not encounter permafrost at sites where surface conditions suggested it should be present. Non-equilibrium temperature profiles from these holes showed that temperatures were strongly positive but that a negative thermal gradient may exist at these sites.

Interpretation of temperature data from the above-noted drill holes is just beginning. We expect to use the data to develop profiles of the permafrost, MAST, thermal gradients, etc. along this transect. The data are also being used to support other geophysical studies.

WELL LOGGING IN PERMAFROST

J.K. Peterson, K. Kawasaki and T.E. Osterkamp
Geophysical Institute, University of Alaska
Fairbanks, Alaska

J.H. Scott
U.S. Geological Survey
Denver, Colorado

INTRODUCTION

Exploration geophysics has proven to be very valuable for the detection and delineation of permafrost. Of the many geophysical methods used, well logging can be used not only for detection and delineation but also for the in-situ determination of many physical properties of permafrost. Well-log evaluation in permafrost can be conveniently divided into several classes of logs, two of which are logs from large diameter drill holes, usually drilled through the permafrost for oilfield development, and logs from holes that have been drilled specifically for the geophysical or geotechnical evaluation of the permafrost. Usually, the geophysical type of drill hole is of small diameter (< 15 cm) and is drilled and left dry.

PERMAFROST LOGGING IN OIL WELLS

Osterkamp and Payne (1981) examined well logs from northern Alaska and published a contour map showing the estimated depth to the base of the ice-bonded permafrost. For this present study, the logs from approximately 80 additional wells from northern Alaska were examined to determine the base of the ice-bonded permafrost. Most of these depths were used in addition to the depths determined by Osterkamp and Payne (1981) to create a series of three new maps of the depth to the base of the ice-bonded permafrost for different regions along Alaska's North Slope.

In determining these new data points, the dual induction log (DIL) was the primary log used. The bore hole compensated sonic (BHCS), self potential (SP), and bore hole geometry or caliper (BH Geo) logs were also used. Generally, the DIL log showed an increase in resistivity and the BHCS showed a decrease in travel time in the ice-bonded sections. The SP log sometimes showed a negative drift when going from unfrozen to frozen sections of the log and the BH Geo log showed severe caving of the borehole in the unconsoli-

dated frozen sands and gravels. The natural gamma ray log was used to interpret the lithology of the well.

Neutron and density porosity logs were difficult to interpret in the ice-bonded permafrost. This can be attributed to severe caving as indicated on the caliper log.

GEOTECHNICAL PERMAFROST LOGGING

A Mt. Sopris portable logger was calibrated for the low density, high moisture content soils typically found in permafrost well logging. This logging unit can log single-point sensitivity, SP, natural gamma, gamma-gamma with short and long source-to-detector spacings, and neutron-thermal-neutron. This logger was used to log numerous holes in permafrost. The calibrated logs were then used to estimate thaw consolidation.

Calibration of the Mt. Sopris system was accomplished by filling 65-gallon ABS plastic drums with soils from the Fairbanks vicinity. A 2-in. ABS plastic water pipe served as the drill hole in the barrels. This is the same material that was used to case some of the drill holes logged in actual permafrost for this study. These barrels have a radius of material of approximately 27 cm around the probes. This annulus of material can be shown to be sufficiently "infinite" for the gamma-gamma probes.

The materials used for these barrels were ice, water, saturated peat, saturated coal, dry silt, dry gravel, wet silt, and wet gravel, which have densities of 0.88, 1.00, 1.07, 1.20, 1.40, 1.63, 1.83, and 2.02 g/cm³ respectively. The low ice density is apparently due to air bubbles captured in the ice upon freezing. The count rates found in the coal barrel were not used for the actual calibration of the sondes.

The neutron tool was field-calibrated by comparing neutron count rates with a gamma-gamma density-derived porosity in an unfrozen, water-saturated section of a hole.

Calibration curves were fitted to the nuclear probes by the least squares technique. When fitting curves to the gamma-gamma probes, measured densities were used rather than the Z/A corrected densities.

RESULTS

Gamma-gamma-determined bulk densities agree fairly well with the bulk densities found in the drill holes as determined by sampling.

Logs of a hole drilled through a buried artificial ground ice mass showed that the natural gamma log count rate decreases significantly in the vicinity of the ice, indicating that the natural gamma log could prove very useful for the detection and delineation of massive ice.

Since the hydrogen density of ice is 92% that of water the neutron tool gives a porosity reading of approximately 72% in pure ice. This fact agrees with the theoretical work of Segesman and Liu (1971). By cross plotting gamma-gamma density and neutron porosity it is possible to determine both total porosity and volumetric unfrozen water content.

REFERENCES

- Osterkamp, T.E. and M.W. Payne (1981) Estimates of permafrost thickness from well logs in northern Alaska. Cold Regions Science and Technology, 5: 13-17.
- Segesman, F. and O. Liu (1971) The excavation effect. SPWLA Reprint, Volume, Gamma Ray, Neutron, and Density Logging (1978), Paper N.

MONITORING PERMAFROST GROUND CONDITIONS WITH
GROUND PROBING RADAR (G.P.R.)

J.A. Pilon
Department of Energy, Mines and Resources
Ottawa, Ontario, Canada

A.P. Annan and J.L. Davis
A-Cubed Inc.
Mississauga, Ontario, Canada

Ground-probing radar is a relatively new geophysical method for mapping and monitoring changes to subsurface geological structures. The method is gradually gaining acceptance in a marketplace where consumers of technology are extremely conservative as a result of the continuing efforts of research scientists, both in government laboratories as well as in the private sector. In the course of the last ten years we have watched the rise of G.P.R. from an unknown to an accepted, albeit underutilized, method in the geophysical arena. During this time we have come to realize the usefulness of G.P.R. as a tool to sort out relatively shallow subsurface geological features, subsurface hydrological characteristics and, last but not least, active layer and shallow permafrost characteristics.

One of the basic objectives of the permafrost group at the Earth Physics Branch is to develop new technology and methodology to study permafrost features and their evolution with time in order to better understand their nature and thus be better able to deal with the geotechnical problems they present to the development of northern lands. In the G.P.R. field we are carrying out the development in collaboration with A-Cubed Inc. from Mississauga.

We will attempt, through examples of previous and current studies, to demonstrate the capabilities of G.P.R. to study and monitor changes in permafrost characteristics.

The initial area where radar methods were applied successfully to geologic materials was in the sounding of the polar ice cap and glacier-covered areas. Permafrost engineering application is a natural evolution from the determination of ice thickness by radar.

G.P.R. is particularly sensitive and capable of detecting zones and interfaces with strong dielectric contrasts, such as dry/wet and unfrozen/frozen interfaces. Thus, wherever shallow structural features in a material are manifested by a change in electrical properties, G.P.R. is an applicable technique.

The first example we would like to use to demonstrate the capabilities of G.P.R. to study active layer and shallow permafrost characteristics is drawn from a series of experiments made in the Leaf Bay area in Mouveau, Quebec. We were looking for a means of confirming experimental data on active layer characteristics gathered in the various geomorphological units found in the area. Thus continuous profiles of the frost table for a series of traverses in unconsolidated sediments in the Leaf Bay area were obtained with a G.P.R. These were then correlated with shallow geothermal data obtained with temperature probes, and in this fashion we were able to confirm the accuracy of the radar data interpretation and its ability to profile active layer depth accurately.

The second example we want to present is some of the data obtained with G.P.R. at the Foothills Pipeline Frost Heave Test Facility in Calgary, Alberta. These experimental surveys were carried out as part of an EMR program to build up a data base on the applicability of geophysical methods for mapping and monitoring changes in ground conditions around pipelines buried in permafrost terrain. The field data collected in this ongoing study were utilized to develop and test digitization of analog radar data and of a variety of digital processing and plotting techniques used to enhance the data display.

Many advantages are derived by transforming the radar data into digital form. The primary benefit is that the data can be displayed in a variety of formats. In the past, data display format inhibited the comparison of radar data with control information and the inter-comparison of multiple frequency radar sections.

The ground probing radar method detected the presence of the buried pipe, the depth of burial, the depth of the frost table, and changes in the geological conditions in the vicinity of the pipe. The conclusion drawn from this experimental program is that ground probing radar is an extremely useful method for monitoring conditions around a buried pipeline.

In the course of our endeavors we have recently been called upon to design and implement a multi-departmental, joint government-industry, long-term monitoring program to study the impact of the construction and operation of a small diameter oil pipeline on active layer, permafrost and ground thermal regimes. G.P.R. will play a key role in this ground thermal behavior study in addition to the more standard monitoring methods. The program began last winter before the start of construction of the pipeline which stretches 860 km from Norman Wells, N.W.T., to Zama, Alberta.

We have now carried out three geophysical surveys of the sites established during the 1984 construction program carried out by Interprovincial Pipeline Limited. The six long-term monitoring sites are located near river crossings and other areas where ground stability may be questionable. Together with the seven sites to be established during the 1985 construction period this provides us with a complete cross section of terrain and permafrost characteristics, from continuous permafrost approximately 50 m thick to sporadic permafrost in peat plateaus at the southern terminal. The results obtained thus far have shown that the radar method can successfully detect and map interfaces between frozen and unfrozen soil as well as changes in soil type. G.P.R. has also shown itself very useful in mapping the evolution of thermal changes in soils. The results obtained from these surveys indicate that it offers excellent potential for economically monitoring changes to the thermal and hydrological regime in the ground surrounding the Norman Wells to Zama pipeline. This is confirmed by comparison with control measurements obtained through other means, such as a series of multi-thermistor cables installed at the sites and active layer profiles obtained with rigid ground thermal probes.

Based on the test cases and the experience acquired to date, the G.P.R. is starting to emerge as the most promising geophysical method for obtaining high-resolution data on near-surface thermal, hydrological and geological ground conditions via their impact on the soil electrical properties. G.P.R. possesses advantages in resolution and speed of survey; on the other hand, there are disadvantages of complexity. Until a greater body of experience is available it remains a geophysical system that requires careful analysis in order to extract the maximum useful information from the data produced. Ongoing studies by us and other government agencies and industries will eventually make G.P.R. a very common geophysical tool for the study of near-surface ground characteristics.

SOME ASPECTS OF TRANSIENT ELECTROMAGNETIC SOUNDINGS FOR PERMAFROST DELINEATION

G. Rozenberg, J.D. Henderson and A.N. Sartorelli
Geo-Physi-Con Co. Ltd.
Calgary, Alberta, Canada

A. Judge
Department of Energy, Mines and Resources
Ottawa, Ontario, Canada

INTRODUCTION

A variety of geophysical methods have been applied over the last few decades to map the top and bottom of permafrost. A good review of different geophysical techniques for permafrost investigation and a representative bibliography may be found in Scott et al. (1978). Among more recent papers, Hatlelid and MacDonald (1982) and Sartorelli and French (1982) can be recommended.

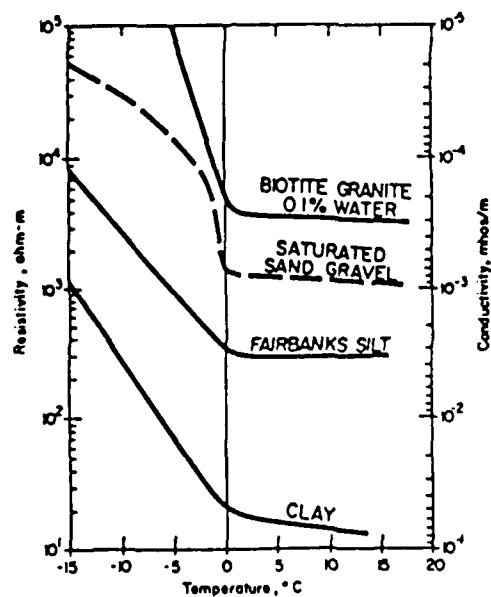
During the past three years, the method of transient electromagnetic (TEM) soundings has been successfully employed to delineate upper and lower permafrost surfaces in a number of arctic areas. Kaufman and Keller (1983) describe the theoretical basis of the method. Rozenberg and Hoekstra (1982) and Ehrenbard et al. (1983) describe the characteristics of the method which make it suitable for permafrost investigations and present case histories for surveys performed in the vicinity of the Alaskan Beaufort coast.

This paper illustrates the use of the TEM method for permafrost mapping under more complex conditions. Three of the four cases cited are taken from surveys in the western Canadian Arctic.

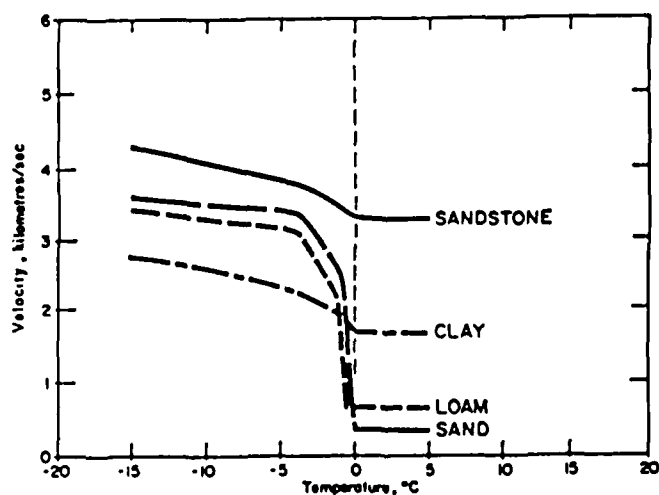
GENERAL PRINCIPLES

The physical basis for the delineation of permafrost using geophysical methods lies in the fact that the physical properties of subsurface materials vary with temperature. Figure 1 illustrates typical dependencies of electrical resistivity and velocity of compression waves on temperature and lithology. It is apparent that both electrical resistivity and compression wave velocity are similarly affected by temperature and tend to increase as temperature decreases for different lithologies.

Figure 2 shows the variations in resistivity and seismic velocity as ice content changes. Again the similarity is obvious.

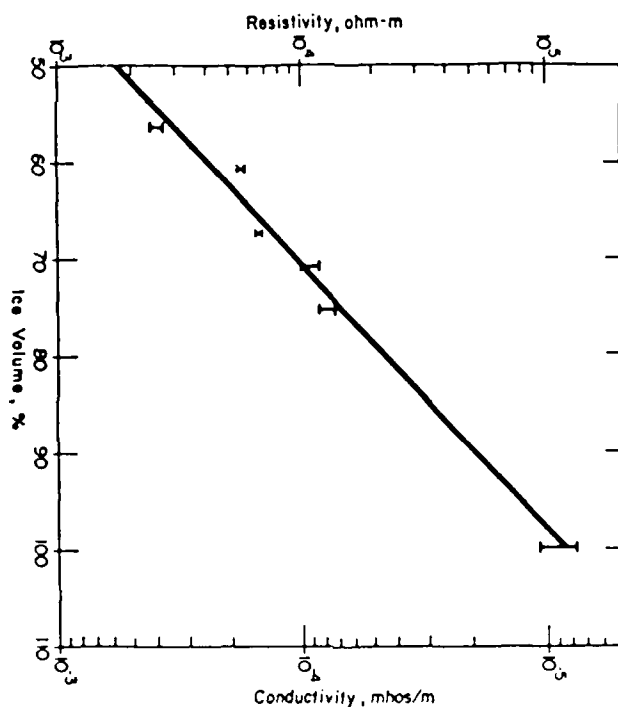


a. Conductivity vs temperature (Hoekstra et al. 1975).



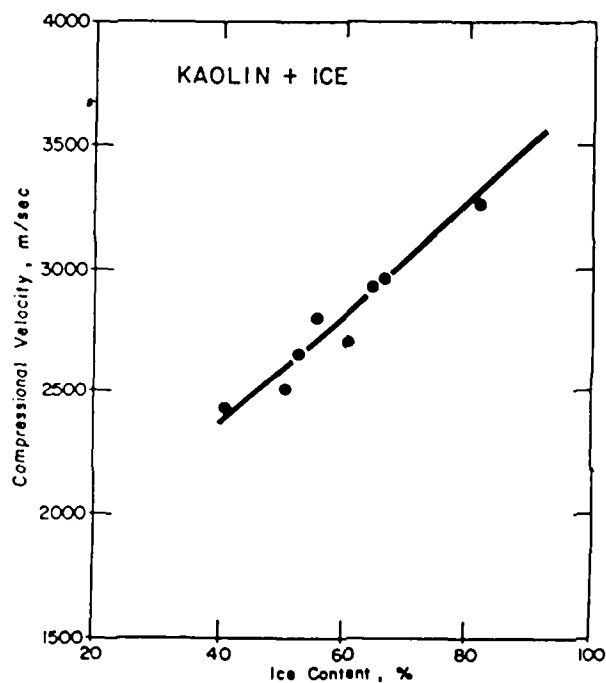
b. Velocity vs temperature (F.F. Aptikaev 1964).

Figure 1. Dependence of electrical resistivity and compression wave velocity on temperature and lithology.



a. Conductivity vs ice content (Hoekstra 1975).

Figure 2. Variation in resistivity and seismic velocity as ice content changes.



b. Velocity vs ice content (Frolov and Zykov 1971).

Figure 2 (cont'd). Variation in resistivity and seismic velocity as ice content changes.

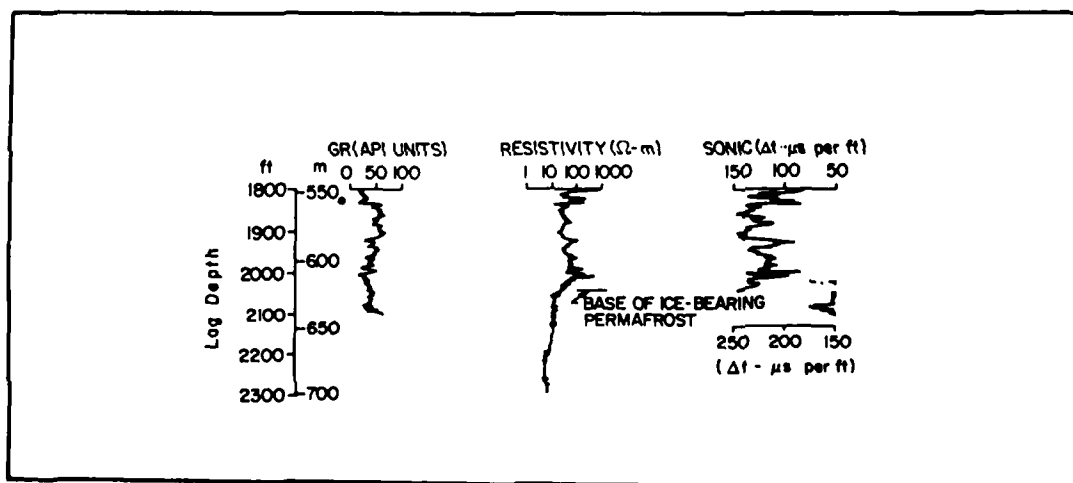


Figure 3. Resistivity and sonic logs, Prudhoe Bay (Osterkamp and Payne 1981).

Figures 1 and 2 were mainly compiled from laboratory testing of samples. Figure 3 illustrates in-situ measurements of electrical and acoustic properties performed in a well in the Prudhoe Bay area of Alaska (Osterkamp and Payne 1981). It is apparent that the substantial features of the resistivity log correlate to similar features on the sonic log. It can be concluded that:

- 1) Electrical methods may be used to delineate areas of permafrost, since the frozen state of the material alters its resistivity.
- 2) Information concerning the distribution of permafrost obtained from electrical methods may be used for the purpose of static correction to reflection seismic data, since both the electrical and elastic properties appear to be affected in similar manners by the presence of permafrost.

CASE HISTORIES

Three case histories are drawn from onshore and offshore regions in the western Canadian Arctic. One example shows the results of a TEM survey from the Alaskan North Slope.

All of the surveys described were performed using the Geonics EM-37 transient system. A nongrounded square loop was used as a transmitter. Figure 4 shows the survey arrangement. The survey in Alaska was carried out using a transmitter loop of 500 m by 500 m. The Canadian surveys were conducted with two transmitter loop sizes (400 m by 400 m and 100 m by 100 m) centered at a measurement station. Additionally, TEM data in the Canadian Arc-

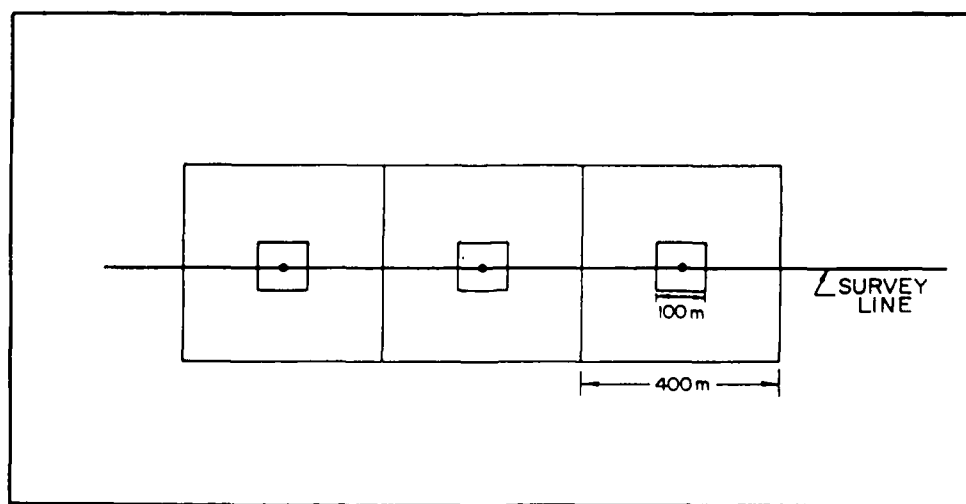


Figure 4. Survey array.

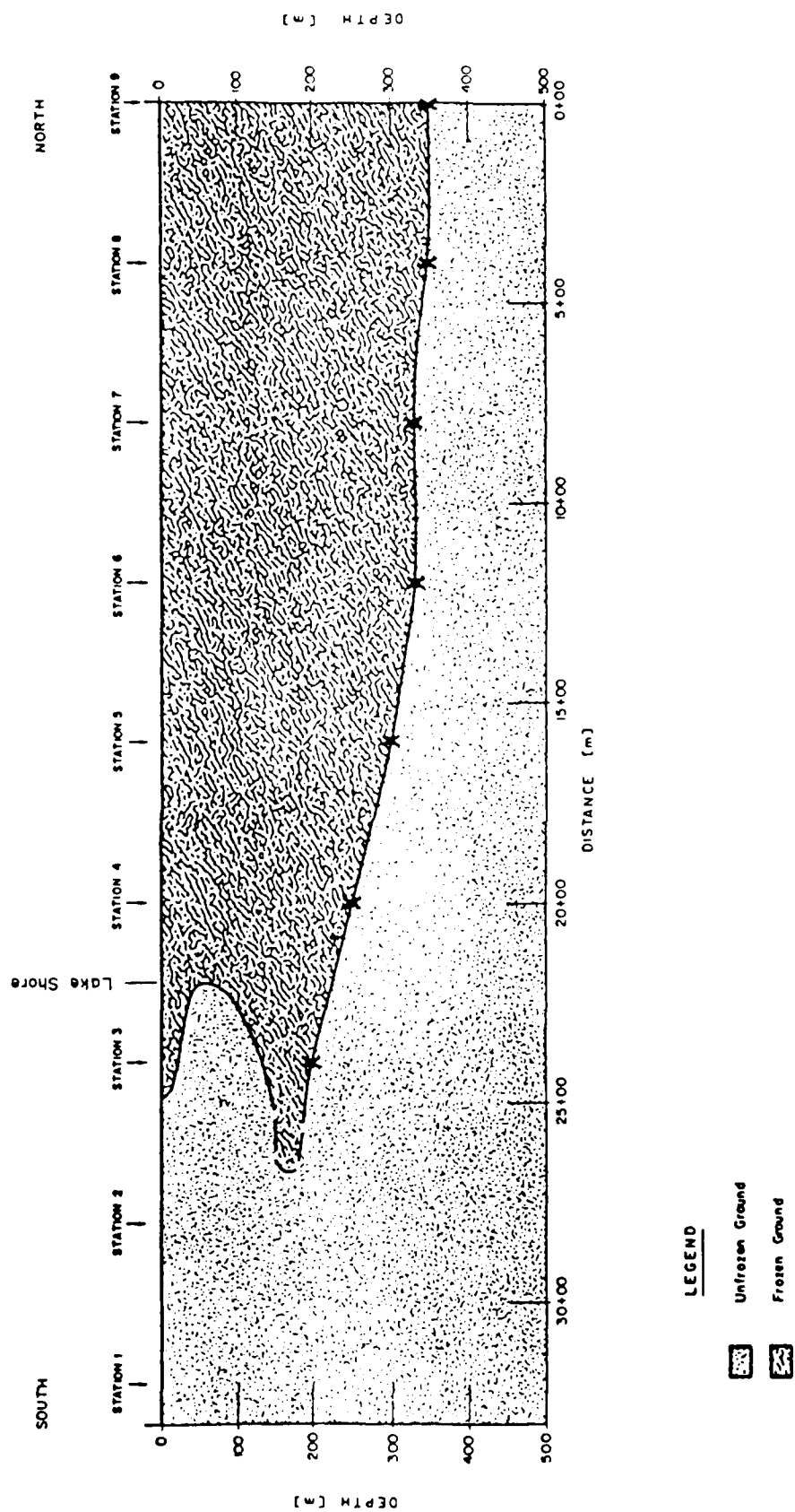
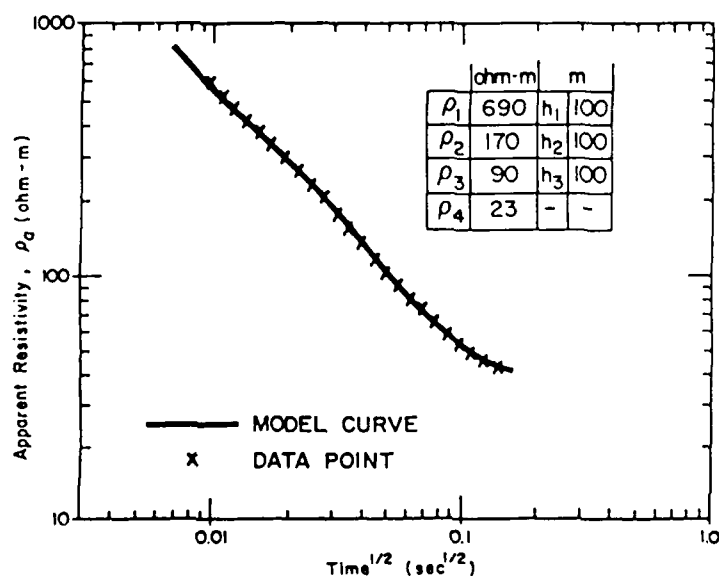


Figure 5. Interpreted section, case history 1.

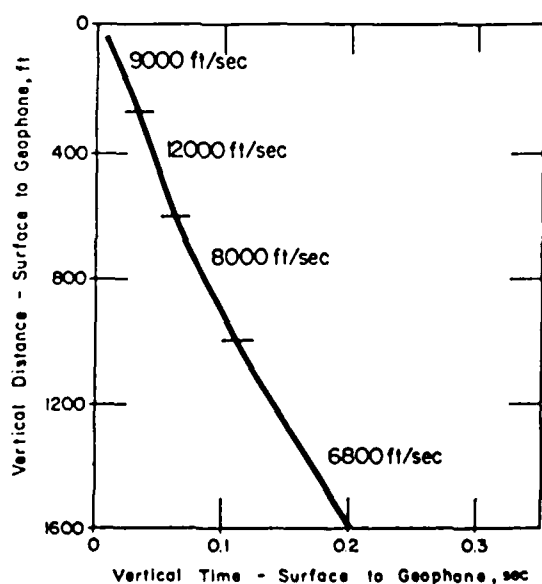
tic were supplemented by fixed frequency (EM) magnetic induction measurements, performed using the Geonics terrain conductivity meters, the EM31 and EM34-3.

Case History 1

Figure 5 shows the section interpreted from geophysical measurements along a survey line over part of a large lake and the uplands to the north of the lake. The lake shore is located between stations 3 and 4, as indicated on the profile.



a. Measured and modeled curves.



b. Near-surface velocity data.

Figure 6. Data for case history 1.

Measurements for stations located north of the lake indicate that the terrain is frozen to the ground surface. Although the objective of the survey was to map only the top and bottom of permafrost, an attempt was made to differentiate layering within the frozen materials. Figure 6a presents an example of the quantitative interpretation. The figure shows the measured apparent resistivities superimposed on the best fit model curve. Three layers with different resistivity are apparent within the permafrost at this site. The resistivity layering is expected to be due to variations in lithology, ice content, temperature, etc. It could also be expected that sonic velocity will vary similarly within the permafrost.

Figure 6b shows the crystal cable velocity log from a nearby well. Compared to the interpretation of the TEM data, it shows that a resistivity boundary is also a velocity boundary. The layers of different resistivity are characterized by different values of velocity.

The permafrost structure near the lake shore has been determined using a synthesis of both EM and TEM data. This was required to reliably map changes in the section occurring both in the shallow subsurface and at greater depth.

No frozen ground is expected beneath the lake. However, calculations do show that, if a frozen layer with a thickness of about 20 m occurred at depths of about 150 m, its presence would not be detectable with the TEM configuration used.

Case History 2

Figure 7 shows the section interpreted from TEM data along a survey line in the high Arctic. The portion of the survey line on shore is frozen to the ground surface. The interpretation of the onshore TEM data indicates that permafrost is not electrically homogeneous throughout its thickness. Figure 8a shows the interpretation of the apparent resistivity curve for station 7. Four distinct layers are recognizable within the permafrost. The variation in the thickness and resistivity of these layers suggests that a gradual change of resistivity with depth may take place. The electric log from a nearby well (Fig. 8b) illustrates the gradual change of resistivity with depth.

For survey stations located offshore the TEM data indicate that the section consists of a conductive zone overlying resistive materials. The resistivity of the conductive materials is about 0.5 ohm-m. The conductor is essentially composed of sea water.

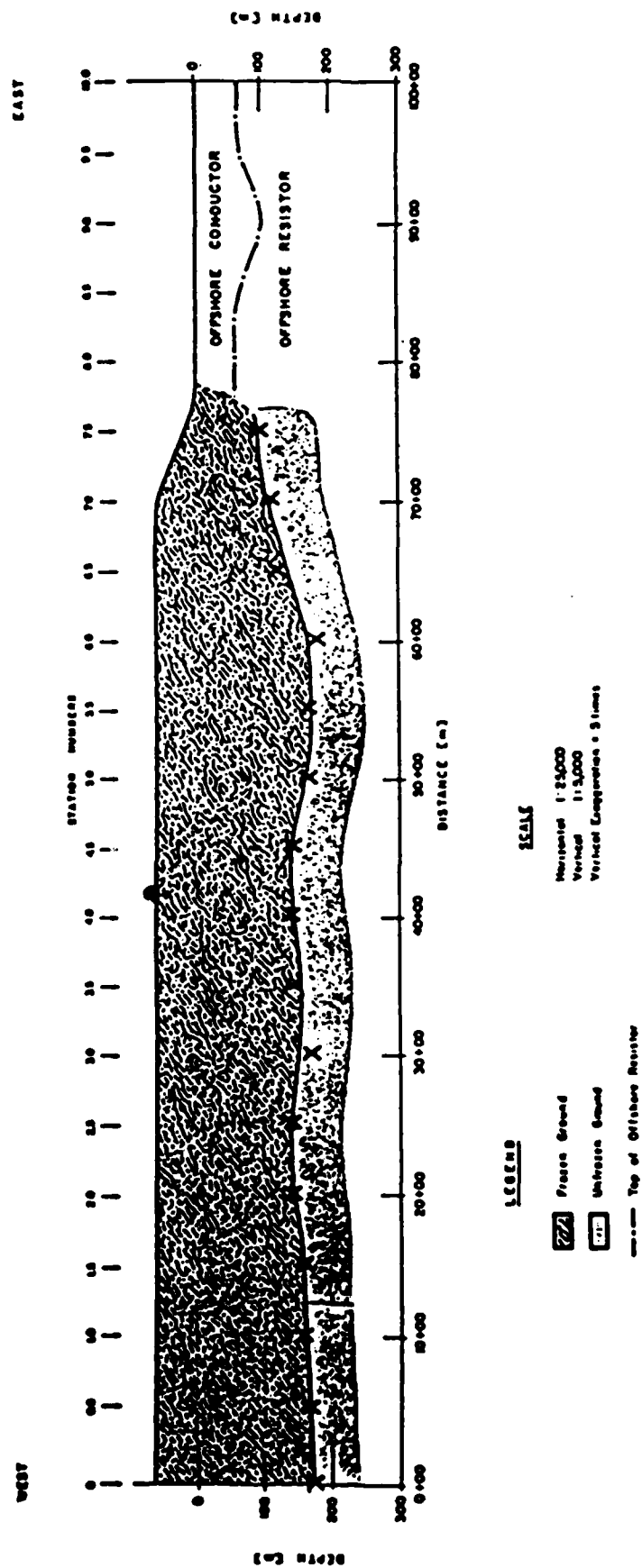
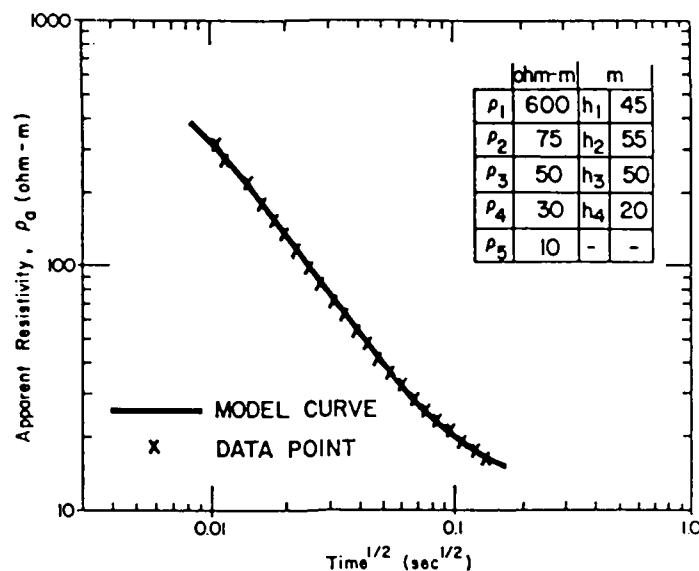
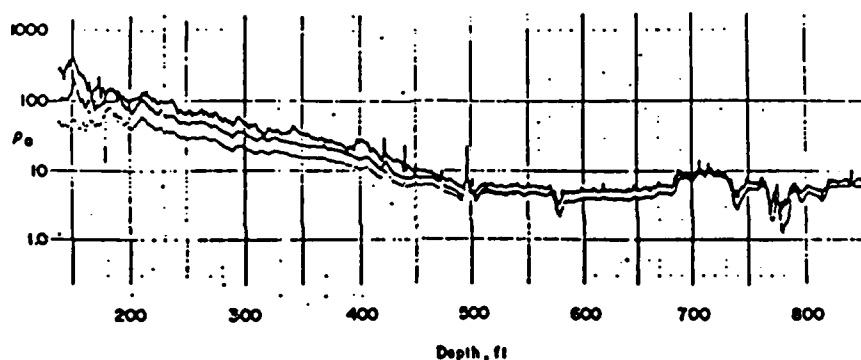


Figure 7. Interpreted section, case history 2.



a. Measured and modeled curves.



b. Resistivity log.

Figure 8. Data for case history 2.

The interpretation of the TEM data for offshore stations at this site indicates that water depth varies between 70 and 100 m. Since moderately resistive material (about 6 ohm-m) underlies the sea water, a resistivity contrast of up to 15 occurs at this interface. The occurrence of permafrost beneath the moderately resistive materials cannot be determined from data obtained using the present operation mode. The limits of detectability of permafrost beneath sea water depend mainly upon the resistivity and thickness of both the sea water and underlying unfrozen sediments.

Case History 3 (Ehrenbard et al. 1983)

Figure 9 shows a section interpreted from TEM data at a site on the North Slope of Alaska. Unlike the previous case history, it is possible to map offshore permafrost in this region. The data do not reveal as large a resistivity contrast with underlying unfrozen sediments so that the presence of permafrost and its thickness can be determined. The factors which allow the delineation of permafrost in this case are the shallower water (less than 10 m), the greater resistivity of sea water, the lower resistivity of unfrozen sediments, and the presence of a substantial thickness of permafrost.

Case History 4

Figure 10 shows a section interpreted from TEM and EM data along a survey line located in the Mackenzie Delta. In general, the section exhibits a four-layered structure: surface frozen sediments, intermediate unfrozen sediments, the main body of permafrost, and underlying unfrozen materials. At various locations along the survey line the four-layered structure degrades into a three-layered structure in which the upper frozen zone is absent, or a two-layered structure in which the intermediate unfrozen sediments are absent. Figure 11a shows the results of quantitative interpretation of sounding.

Figure 11b shows a crystal cable velocity log for a drill hole located close to station 1. It can be seen that electrical boundaries of permafrost correlate to the seismic boundaries. Figure 11c gives another example of a crystal cable velocity log to a greater depth.

This example illustrates the most complex distribution of permafrost encountered to date with TEM soundings. The role of data acquisition over such complicated sections is extremely important. Measurements taken with only one loop size, large enough to sense the bottom of permafrost, could not delineate the upper frozen zone. The use of two loop sizes, however, unambiguously indicates the presence or absence of this zone. Apart from the small-loop data, EM measurements have allowed the detection of a near-surface talik between stations 3 and 4 and the unfrozen "pockets" between stations 10 and 13.

Where the section is frozen to the ground surface and no intermediate unfrozen ground occurs, it is possible to differentiate between layers of different resistivity within the permafrost. Figure 11d shows that at least two distinct layers are present.

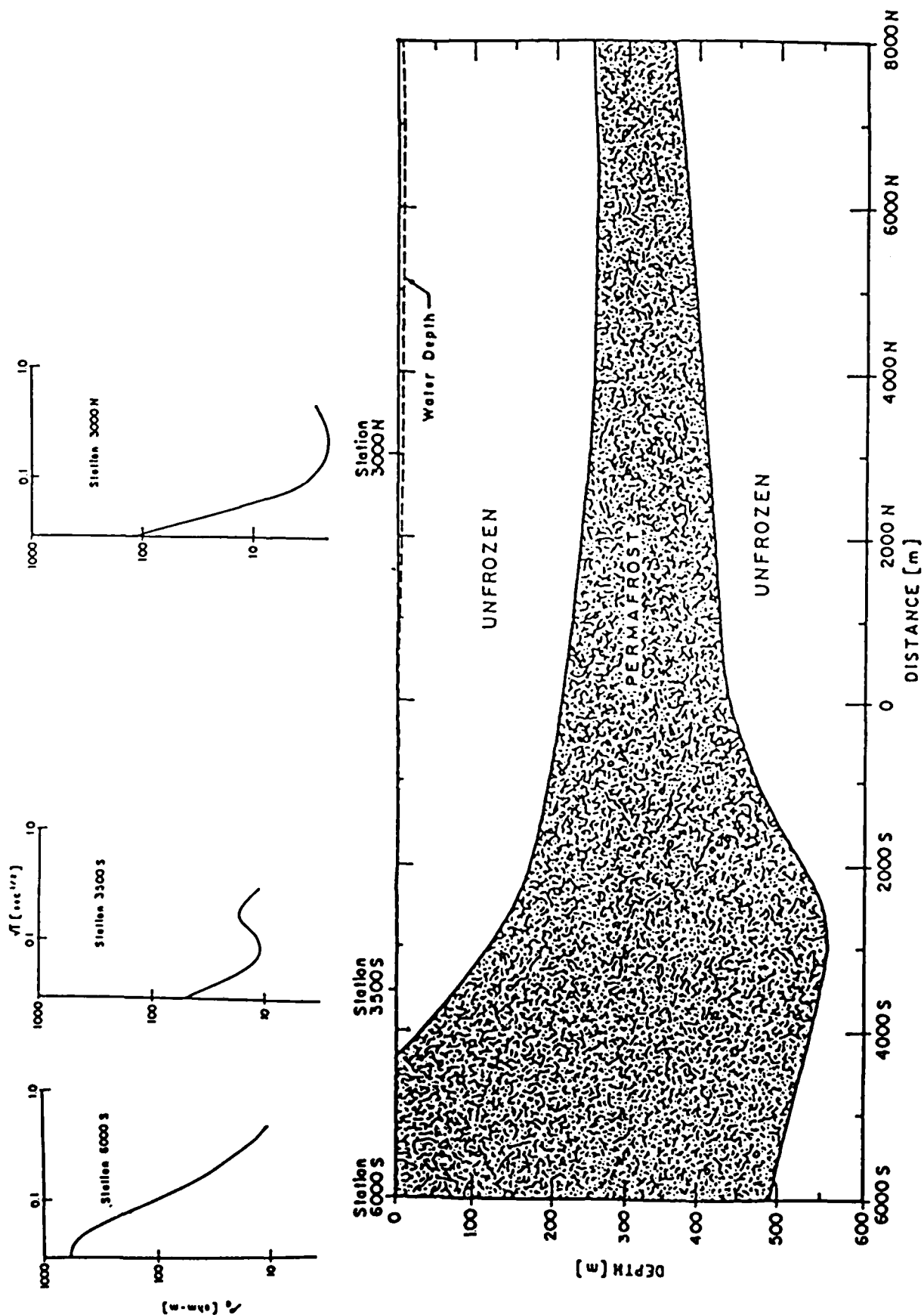


Figure 9. Interpreted section, case history 3.

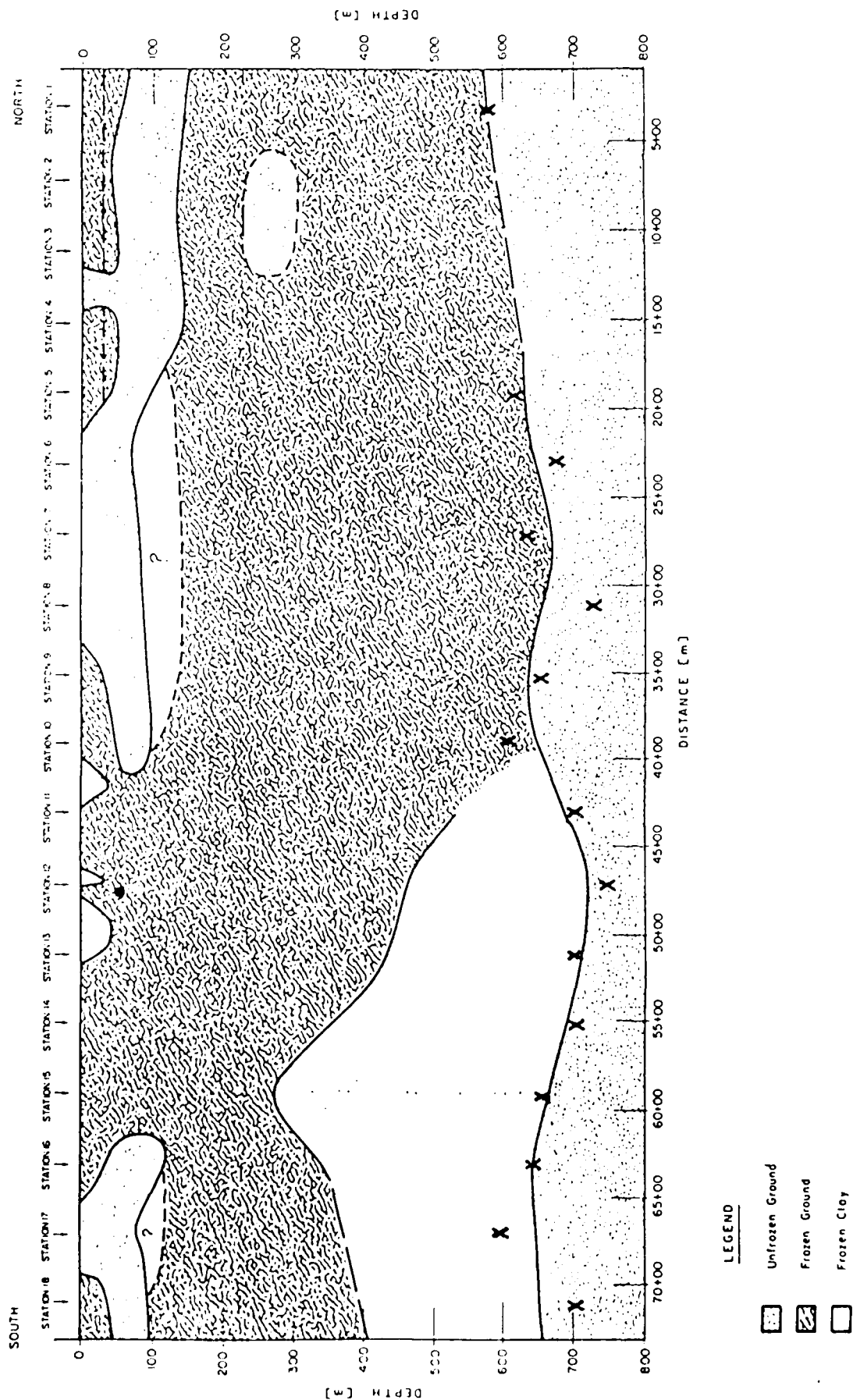
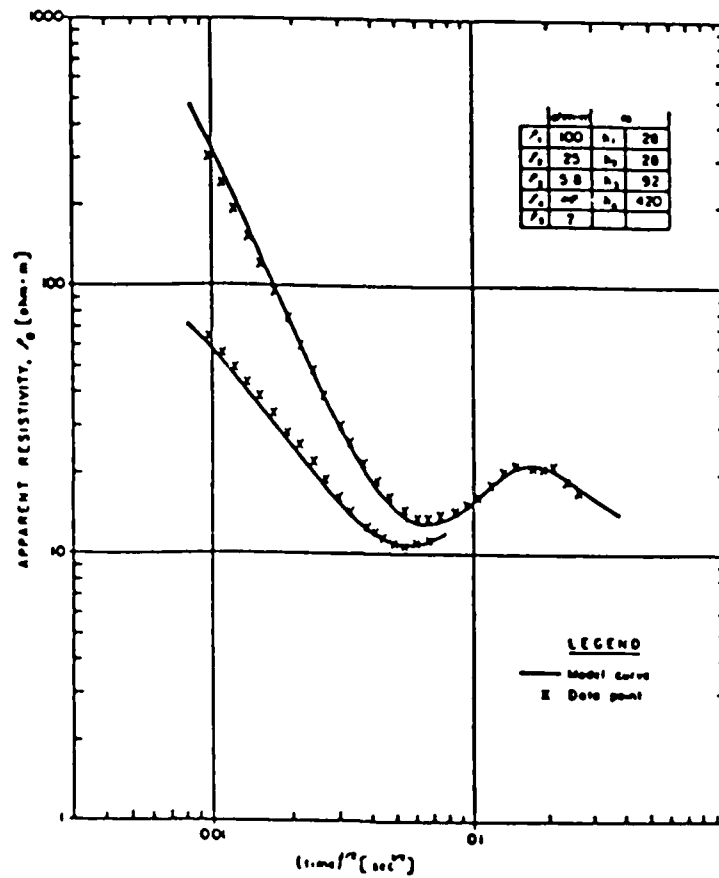
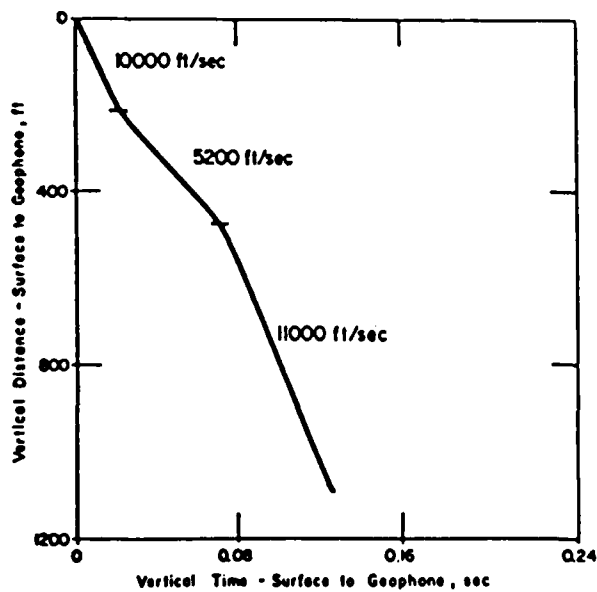


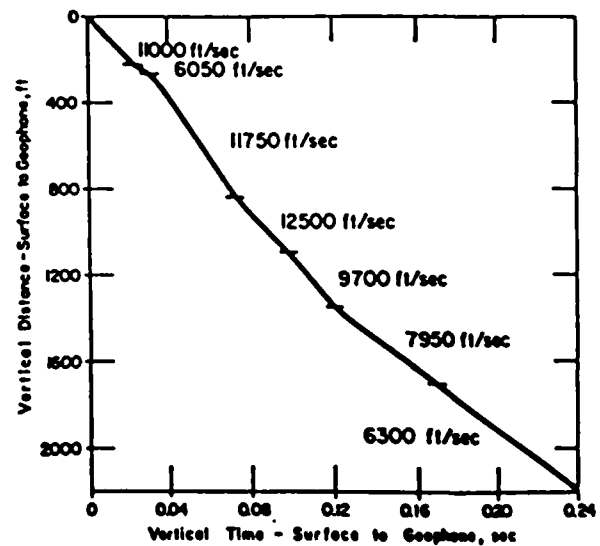
Figure 10. Interpreted section, case history 4.



a. Quantitative interpretation of sounding.

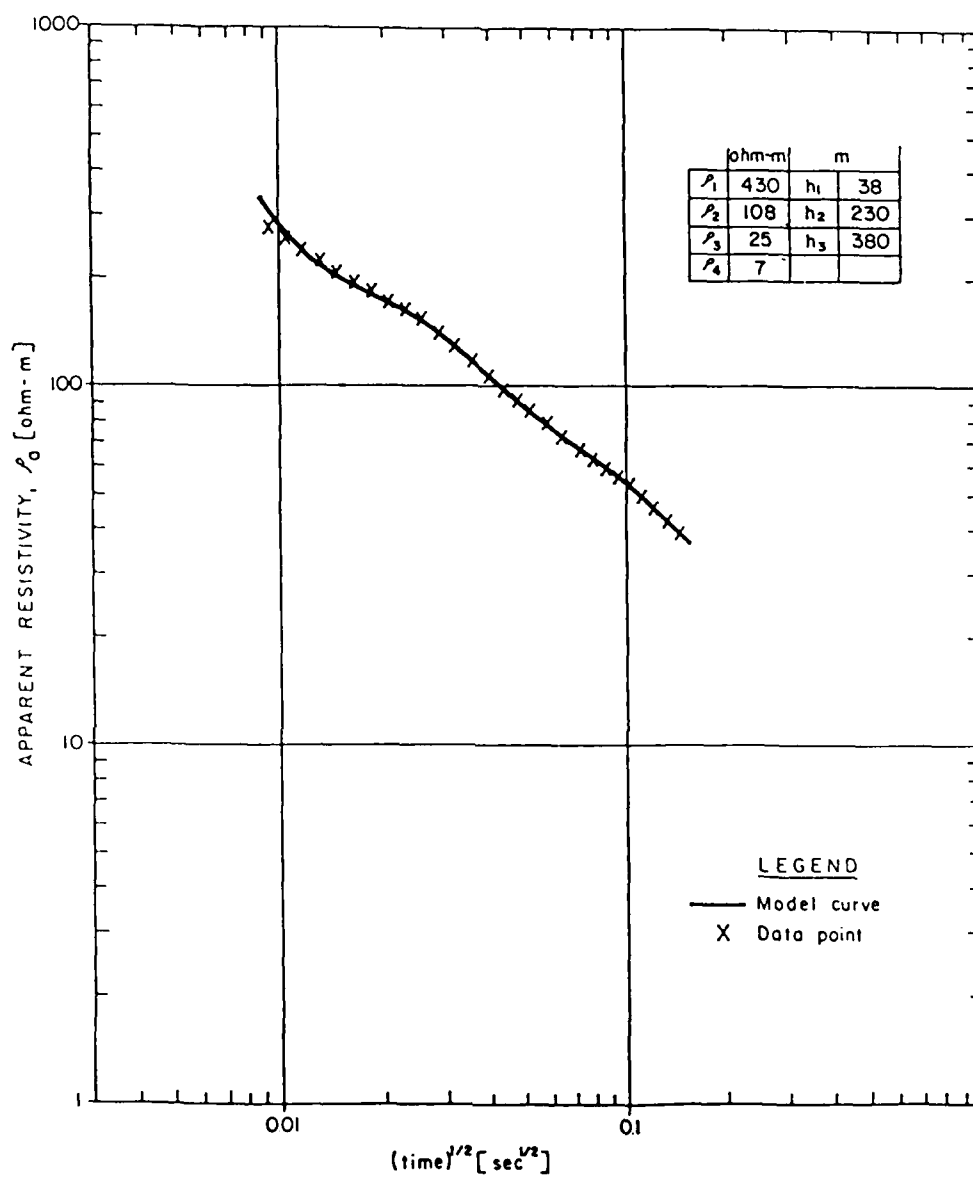


b. Near-surface velocity data.



c. Near-surface velocity data.

Figure 11. Data for case history 4.



d. Measured and modeled curves.

Figure 11 (cont'd). Data for case history 4.

The large "wedge" of material occurring south of station 10 is characterized by a resistivity of 25 ohm-m. This resistivity can represent, for example, frozen clay or unfrozen silt. Therefore, it is difficult to determine definitely the frozen state of material within this "wedge." Additional subsurface information is required to resolve this problem.

CONCLUSIONS

The case histories presented illustrate the flexibility of the TEM method to determine the presence and extent of permafrost under widely different geologic, geographic and geocryologic conditions. This flexibility is the result of two strong advantages of the TEM method over other electrical and electromagnetic techniques:

- 1) The method possesses strong vertical resolution, due to its high sensitivity to the geoelectric section.
- 2) The lateral resolution of the method is good, since the measurement array is small compared to the depth of investigation.

In many cases the method can not only map the top and bottom of permafrost, it can also detect the major variations of resistivity within the permafrost body. The comparison of TEM data with downhole sonic measurements has shown that changes in resistivity correlate to variations in sonic velocity.

In areas where there is a large variation in the upper portion of the geoelectric section, additional independent measurements with good resolving power at shallow depth should be gathered. It is our experience that TEM data at a smaller transmitter loop size and EM data at fixed frequencies can do much to complement the large-loop TEM data.

In marine environments the delineation of the extent of permafrost beneath sea water and unfrozen brine-saturated sediments can be a very complex problem. The important parameters are the thickness and resistivity of sea water conductive sediments, and the relative thickness of underlying permafrost. The limits of current resolution of the TEM method for this objective are known.

It has been shown that the frozen state of earth materials affects their electric and elastic properties in similar manners. This fact, along with the shown correlation between the resistivity and velocity layering, creates a good potential for using the electrical data at the stage of processing seis-

mic reflection data to make a reliable static correction for permafrost influence.

The information obtained by the TEM method can also be used for geotechnical and construction purposes, and in well planning.

ACKNOWLEDGMENTS

The authors express their deep gratitude to the scientific officers of the Gravity, Geothermics and Geodynamics Division, Earth Physics Branch, Department of Energy, Mines and Resources, Canada, for financial and moral support.

REFERENCES

- Aptikaev, F.F. (1964) Temperature field effect on the distribution of seismic velocities in the permafrost zone. Akad. Nauk SSSR Sibirskoe Otd-ie. Inst. Merzlotovedeniia. Teplovye Protsessy v Merzlykh Porod.
- Ehrenbard, R.L., P. Hoekstra and G. Rozenberg (1983) Transient electromagnetic soundings for permafrost mapping. Proceedings, Fourth International Conference on Permafrost. Washington, D.C.: National Academy Press, p. 272-277.
- Frolov, A.D. and Y.D. Zykov (1971) Peculiarities of the propagation of elastic waves in frozen rocks. Izv. Vysh. Ucheb. Zaved., Geol. Razvedka, no. 10, p. 89-97.
- Hatlelid, W.G. and J.R. MacDonald (1982) Permafrost determination by seismic velocity analyses. J. CSEG, 18(1): 14-22.
- Hoekstra, P., P.V. Sellmann and A. Delaney (1975) Ground and airborne resistivity surveys of permafrost near Fairbanks, Alaska. Geophysics, 40(4): 641-656.
- Kaufman, A.A. and G.V. Keller (1983) Frequency and Transient Soundings. Amsterdam: Elsevier.
- Osterkamp, T.E. and M.W. Payne (1981) Estimates of permafrost thickness from well logs in northern Alaska. Cold Regions Science and Technology, 5: 13-27.
- Rozenberg, G.S. and P. Hoekstra (1982) Transient electromagnetic soundings. Society of Exploration Geophysicists Technical Program, Abstracts, Dallas, Texas, p. 376-378.

- Sartorelli, A.N. and R.B. French (1982) Electromagnetic induction methods for mapping permafrost along northern pipeline corridors. Proceedings, Fourth Canadian Permafrost Conference, National Research Council, Canada, p. 283-295.
- Scott, W.J., P.V. Sellmann and J.A. Hunter (1978) Geophysics in the study of permafrost. Proceedings, Third International Conference on Permafrost, National Research Council, Canada, vol. 2, p. 93-115.
- Walker, J.M.D. and A.M. Stuart (1976) Determining extent of permafrost. Oil-week, May 31.

GALVANIC METHODS FOR MAPPING RESISTIVE SEABED FEATURES

P.V. Sellmann, A.J. Delaney and S.A. Arcone
Cold Regions Research and Engineering Laboratory
Hanover, New Hampshire

Field observations were made under controlled conditions to aid interpretation of future marine resistivity data and to assess the sensitivity of this technique for determining the top of shallow ice-bonded subsea permafrost.

Detailed observations at two coastal sites in Maine provided field data on the effect of water depth for both floating and sea floor cables. The influence of water depths ranging from 0-6 m was observed over unchanging bottom conditions by collecting data through tidal cycles. The observations and model data illustrate the importance of considering water depth in data analysis since it can influence results more than variations in resistivity at shallow depth in the seabed. A sample of resistivity data obtained with a short stationary bottom cable in a Wenner configuration (11 m maximum electrode spacing) beneath 0 to 6.3 m of water is shown in Figure 1.

Based on preliminary observations and available equipment, the Wenner electrode configuration with "a" spacings up to 70 m was selected for a field cable that could be used on the bottom or floated. A survey area near New Haven, Connecticut, was selected because of the large amount of control data available on depth to bedrock, and the fact that seabed conditions in this area were analogous to subsea permafrost conditions. The rock (approximately 25 ohm-m) represented warm, saline, ice-bonded sediment, and the mud over the rock (approximately 2.0 ohm-m) represented a surface thaw zone. The water depth varied from 5 to 16 m and the top of rock from 11 to 55 m below sea level. Our survey was based on sounding and profiles. Data from the profiling agreed extremely well with control from drilling and high-resolution seismic studies (Fig. 2). Profiles made with electrode spacings of 50 to 60 m and an input current of only 1.25 amperes provided data on depth to the bedrock as great as 55 m below sea level in 7 m of water. Data were also obtained in areas where seismic methods were unable to extract subbottom information due to the gas content of local organic sediments.

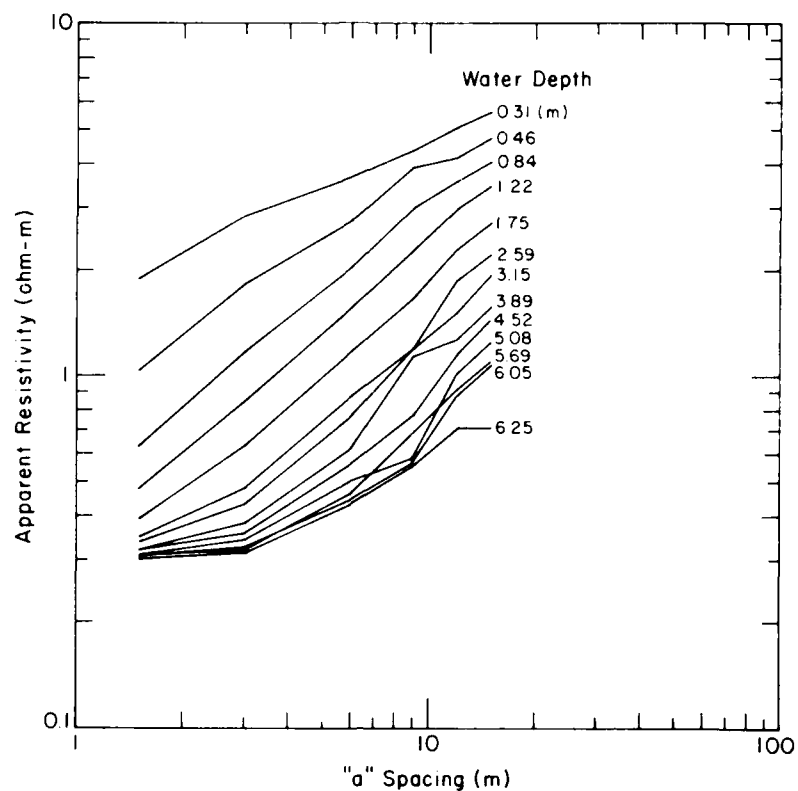


Figure 1. The influence of the depth of seawater on resistivity data obtained with a bottom cable with electrodes placed in a Wenner configuration.

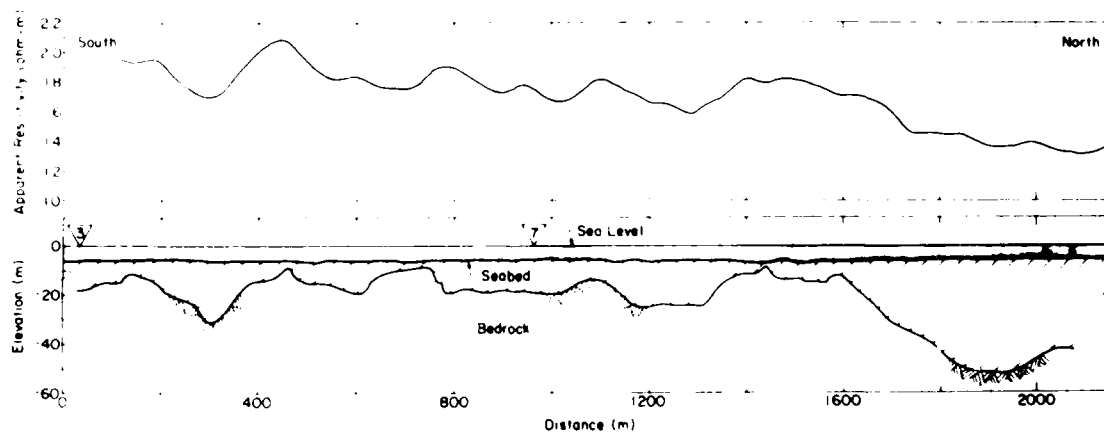


Figure 2. Resistivity profile obtained with a floating cable. Electrodes were in a Wenner configuration with an "a" spacing of 50 m. Control data are shown below for comparison. Sea water salinity was 25⁰/₀₀. The inverted triangles represent the locations of channel markers. Control was obtained from the Corps of Engineers New Haven Harbor study and feasibility report, 1981.

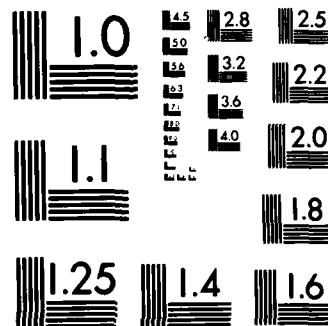
WORKSHOP ON PERMAFROST GEOPHYSICS HELD AT GOLDEN
COLORADO ON 23-24 OCTOBER 1984(U) COLD REGIONS RESEARCH
AND ENGINEERING LAB HANOVER NH J BROWN ET AL. MAY 85
CRREL-SR-85-5 F/G 8/12

UNCLASSIFIED

F/G 8/12

NL

END



MICROCOPY RESOLUTION TEST CHART
NBS-1963-A

DEEP TRANSIENT EM SOUNDING IN THE MACKENZIE DELTA, N.W.T., CANADA

Ajit K. Sinha
Geological Survey of Canada
Ottawa, Ontario, Canada

In the last three years, a number of deep electromagnetic (EM) soundings have been carried out at several locations in the Mackenzie Delta, N.W.T., Canada. Several locations were near deep drill holes that had been surveyed earlier with geophysical logs. Both multifrequency and transient EM methods were used and the results were compared with those from borehole logs. The main purpose of the experiments was to develop a relatively inexpensive and environmentally acceptable geophysical technique for detecting horizontal layers at great depths, especially the contact between the ice-bonded permafrost and the underlying unfrozen sediments. This contact occurs at depths varying from 250 m to 650 m in the Mackenzie Delta as determined by borehole temperature measurements.

Both multifrequency and transient systems detected several conductive horizons in the experiments, including the contact of the frozen and unfrozen sediments. The multifrequency system, by virtue of its greater resolving power, detected many minor features, such as clay lenses and coal beds (known from lithological logs), which made the determination of the depth to the unfrozen layer somewhat difficult. Transient EM methods, on the other hand, generally detected only thicker strata, making the task of determining the depth to the unfrozen layer somewhat easier.

Additional surveys were carried out southwest of the Big Lake in Richards Island, N.W.T., in the spring of 1984 using the transient EM system. Borehole temperature logs in that area had indicated a rather sharp drop in the thickness of permafrost from about 650 m south of the lake to 150 m or less within 20 km to the west. The purpose of the investigation was to determine the thickness of the permafrost at regular intervals along a profile about 30 km long running WSW, beginning at a point 3 km south of Big Lake. It was hoped that the EM soundings would indicate whether the decrease in permafrost thickness was gradual or abrupt at any point and also indicate the cause of this decrease in thickness.

A Geonics EM-37 transient system was used for our experiments. The transmitter was a square loop, with sides varying in length from 75 m to 450 m. Smaller loop sizes were used to characterize the shallower sediments;

larger loops were used for deep sounding. Square wave pulses were transmitted with two base frequencies of 3 and 30 Hz. The decay of the induced voltages was recorded at the center of the loop at 20 discrete time channels for each base frequency.

Interpretation of the data to date has revealed very shallow permafrost (100-150 m) at the western edge of the profile, with the thickness increasing to the east. The data are complex towards the eastern end of the profile, indicating the possible presence of two- and three-dimensional bodies. This makes the application of interpretation methods developed for layered models rather difficult, with a consequent increase in the uncertainty of such interpretation.

OBTAINING PRECISE TEMPERATURE MEASUREMENTS IN ABANDONED OFFSHORE PETROLEUM EXPLORATION WELLS

Alan Taylor and Allan Judge
Department of Energy, Mines and Resources
Ottawa, Ontario, Canada

Precise deep ground temperatures find widespread application in the earth sciences and engineering. Geophysicists use geothermal temperatures to calculate the terrestrial heat flux in the study of the geology and tectonics of a region. Petroleum engineers use the present and past ground thermal regimes to assess petroleum maturation possibilities in the quest for exploration targets. Geothermal energy as a resource is manifested by high ground temperatures; permafrost lies at the opposite extreme, reflecting unusually low ground temperatures. Being a temperature phenomenon, the distribution and thickness of permafrost is best studied through measured ground temperatures. Today, precise temperature profiles, to several hundredths of a degree accuracy and to depths of a thousand meters or so, have been acquired at a good number of wells or boreholes on land (Taylor et al. 1982). Few, if any, measurements of this accuracy and detail have been made to depths of hundreds of meters in offshore areas. Precise measurements of sea floor sediment temperatures to depths of a few meters have been made at a broad distribution of offshore sites using traditional oceanographic techniques.

This paper describes a fully integrated system, currently under development, for the acquisition of precise temperatures from abandoned offshore petroleum exploration wells. Our design target was a system that would measure and record a dozen to 20 temperatures in the upper 1000 m of an offshore well in up to 400 m of water, at intervals of a day or less for at least two years. It was assumed that permission to omit the surface plug could be obtained or that an acceptable plug penetrated by the cable could be designed. The instrumented depth need only be limited by the location of the next, deeper regulatory plug.

Because of the highly technical nature of deployment of such a system from an offshore drill rig and the variety of data acquisition systems currently available, we decided at the outset to contract the entire concept development and equipment selection to consulting companies that had the specialized experience of working with petroleum exploration companies in the offshore environment.

EBA Engineering Consultants Ltd., Edmonton, Alberta, were selected through a competitive bidding procedure to survey the available technology and to propose a methodology (EBA 1982). For offshore areas with a substantial open water season, a multiconductor thermistor cable and data acquisition equipment would be deployed from the drill ship or platform at completion of drilling, using the guide wire and sling system to reenter the hole. The cable would be threaded into the well; the electronics packages would remain on the guide base at the sea floor. An acoustic release system would be used to recover the electronics and the stored data, but not the cable, at a later date. An optional acoustic data telemetry system might be incorporated to check the operation upon deployment and to recover the accumulated data periodically. In ice-covered areas, the telemetry mode would be an integral part of the system, as later recovery of the system and its data by ship might be impractical and not cost-effective. The consultants recommended in this case that a seabed acquisition unit would telemeter data to a recording system left on the ice surface (Fig. 1). This is practical for wells currently being drilled from ice platforms in the channels of the central Canadian Arctic Islands, where the open water season is limited, at best, to July to September, and where ice drift for the remainder of the year is minimal (often less than 1 km). The sea floor unit would be written off; the surface

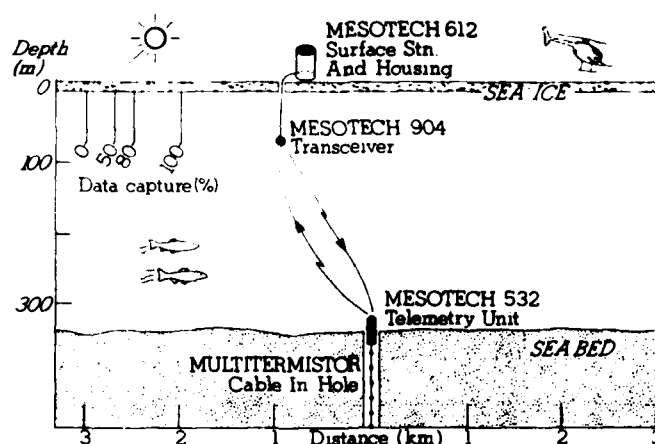


Figure 1. The acoustic telemetry system for measuring precise temperatures in an offshore well, using a technique originally proposed by EBA Engineering Consultants Ltd. The hardware was procured by Do-brocky Seatech Ltd. and tested in the Arctic; up to 2 km of ice drift can occur before data loss is experienced (Fig. 2).

station would be removed for the open water season, and data recovery could be undertaken at any time. Recognizing an immediate need for precise temperature data in offshore arctic areas, this system design for arctic wells has been further developed as a prototype phase.

Following this conceptual philosophy, the consultant assessed the data acquisition systems currently available or under development as to suitability to the task and operating environment. It was clear that the cable would be custom-manufactured. The engineers suggested a 20-conductor, multi-sheathed cable with a Kevlar stress member sufficient to support the cable's own weight in air. The ability of the cable to withstand freeze-in in permanent frost areas was inherent in this design specification.

The next phase was the procuring of the cable and the electronics, followed by thorough bench and field testing of individual components and the integrated system. Government contracting regulations required us to hold another competition before awarding a contract for this next phase.

Dobrocky Seatech of Sidney, B.C., won the competition and undertook to order the system. They worked closely with the suppliers during the manufacturing phase, as most components were custom built, using generally proven subsystems, to specifications developed in the first phase. For the 1000-m, 16-thermistor cable, the consultant recommended an extensive suite of electrical, hydrostatic and pull tests, and participated in these with Custom Cable Corp. and Maloney-Envirocon, the American manufacturers. All the electronics components were purchased from Mesotech Systems Ltd. of Port Coquitlam, B.C. Testing both on the bench and in water off the Canadian west coast was part of the acceptance procedures. The tests are described in their report (Dobrocky Seatech 1984).

As the demonstration deployment is planned for the Canadian Arctic Islands, EMR requested that an extensive arctic trial be undertaken. In May of this year, Dobrocky Seatech tested the complete data acquisition and telemetry system from the sea ice in 330 m of water (Dobrocky Seatech 1984). A dummy load containing precision resistors was used in place of the cable. We wanted to assess the effect on data telemetry of the thermocline, halocline and ice drift. Following a cycle of different sea bottom and under-ice transducer depths, the surface recording unit was moved in increments of 500 m along the ice to a final range of 3 km. Full and repeatable data capture was attained to 2 km range, with some channels lost at 2.5 km, and essential-

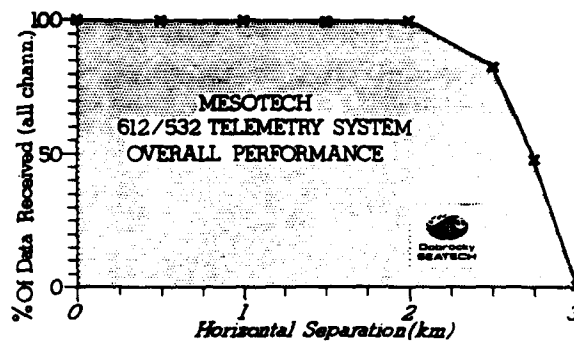


Figure 2. Performance of the Mesotech Systems Ltd. data acquisition modules for various horizontal separations in 330 m of water.

ly complete loss by 2.75 km (Fig. 2). For ranges under 2 km, the heights of the underwater transponders were immaterial; for greater ranges, however, the surface station transponder should be lowered beneath the thermocline. The recording medium in the surface station is bubble memory; during the arctic trial, the unit was cycled several times below 0°C with no apparent loss of memory. For deployment, a specially designed, propane-heated housing will be used.

The first demonstration deployment is currently being planned for the winter of 1985 in an offshore Arctic Island well. For the completion envisaged for that well, we plan to run the cable and underwater station through the riser before all subsea well equipment is removed. The electronics package will be enclosed in a steel cylinder/cage and landed at the top of the well casing, about a meter above the sea floor.

This demonstration project is supported through funding from the Office of Energy Research and Development, Department of Energy, Mines and Resources, Canada. We thank the two consulting firms and the manufacturers for their innovative ideas and excellent work on our behalf. Panarctic Oils Ltd. contributed its expertise to the methodology of deployment, and Cominco Ltd. provided logistic support at its Polaris Mine during the arctic field trials.

REFERENCES

Dobrocky Seatech Oceanographic Services Ltd. (1984) Acquisition and field testing of an integrated system to instrument an offshore well for the purpose of recording wellbore temperatures. Earth Physics Branch, De-

partment of Energy, Mines and Resources, Ottawa, Open File 84-25, 43 pp.
plus 16 appendices.

EBA Engineering Consultants Ltd. (1982) Acquisition of geothermal data in
offshore wells - Phase I. Earth Physics Branch, Department of Energy,
Mines and Resources, Ottawa. Open File 82-14, 142 pp.

Taylor, A.E., M. Burgess, A.S. Judge and V.S. Allen (1982) Canadian geother-
mal data collection: Northern wells 1981. Earth Physics Branch, Depart-
ment of Energy, Mines and Resources, Ottawa, Geothermal Series, no. 13,
153 pp.

MARINE PERMAFROST STUDIES RELATED TO DEVELOPMENT
OF THE ALASKAN BEAUFORT SEA

L.J. Toimil
Harding Lawson Associates
Novato, California

Information on the depth, thickness, and areal distribution of subsea ice-bonded soils is needed for engineering design and to determine static corrections for the processing of seismic reflection data. In recent years, accelerated development offshore in northern Alaska has resulted in the acquisition of considerable new knowledge on the marine permafrost regime of the inner Beaufort Sea shelf. Information has been obtained from both test boring programs and electrical surveys. These studies have confirmed the presence of ice-bonded subsea soils, approximated their total thickness, and shown that the depth to bonded soils is not a function of inundation time. The depth below the mudline of bonded soils in many cases is seen to decrease with increasing distance offshore. In addition, the results of recent studies indicate that zones of well-bonded soils may be overlain by marginally or partially ice-bonded zones.

During 1983/84 on-ice boring programs, visible ice was recovered from samples obtained 6.5 ft below the mudline in 58 ft of water within Harrison Bay. Previous boring programs conducted in the vicinity have repeatedly encountered bonded soils at a depth of approximately 30 ft below the mudline. The presence of bonded soils at such shallow depth, together with overlying zones of marginally bonded materials, poses important constraints on the design of offshore facilities.

In the face of the evidence recently obtained offshore in northern Alaska, intuitive models representing the offshore permafrost regimens as a seaward-thinning wedge of bonded materials do not appear valid. The design of offshore facilities for operation in water depths of 50 to 110 ft offshore in northern Alaska will require more information than now exists on the deep water permafrost regime.

UNFROZEN PERMAFROST AND OTHER TALIKS

R.O. van Everdingen
National Hydrology Research Institute, Environment Canada
Calgary, Alberta, Canada

The "Permafrost Terminology" prepared by Brown and Kupsch (1974) identified a major semantic problem, i.e. the ambiguity of the words frozen and unfrozen, and of several related terms. On the one hand, the word frozen is often taken to imply only that the temperature of the material described is below 0°C; on the other hand, the term is also widely used to imply that at least some of the total water content of the material exists in the form of ice. Misunderstanding often arises when a supporter of the one usage tries to communicate with a supporter of the other. Moreover, widespread inconsistency in the use of the word frozen tends to add further to the confusion in the literature. Similar confusion is apparent in the use of other terms, e.g. active layer, freezing front, seasonal frost and permafrost.

The basic problem arose from the fact that no separate terms were available to distinguish "below 0°C" and "above 0°C" as compared to "containing ice" and "not containing ice." It is by now common knowledge that the initiation of the phase change from water to ice requires temperatures somewhat below 0°C in many soil materials, as a result of freezing-point depression. The associated changes in mechanical and physical properties will not start occurring until these lower temperatures are reached. Hence, for the purpose of geophysical exploration, drilling, excavation and foundation engineering the prime question is not whether the temperature is above or below 0°C, but whether or not an ice phase is present. In thermal studies, however, and for the purpose of delineating permafrost (ground with temperature remaining below 0°C for two or more years), the occurrence of below-zero temperature remains of prime interest.

In 1976 the author proposed that the adjective cryotic (from the Greek κρυος (krios)--cold) be adopted to indicate that the temperature of a material so described is lower than 0°C, and the negative form noncryotic to indicate that the temperature is above 0°C. The terms frozen and unfrozen could then be reserved for materials containing ice, and materials not containing ice, respectively.

Early in 1983 the Permafrost Subcommittee of the National Research Council of Canada established a working group to prepare an up-to-date glossary

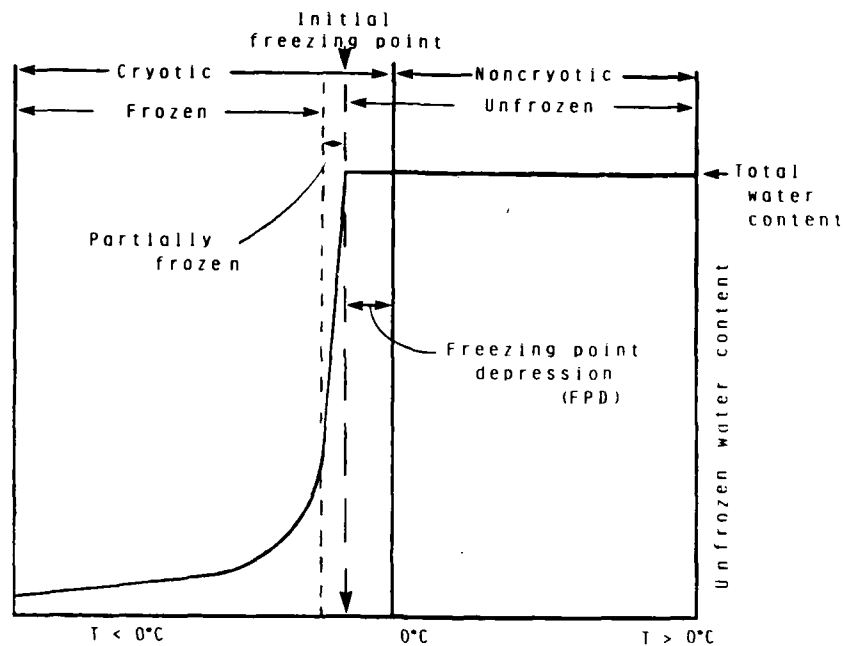


Figure 1. Terms used to describe the temperature relative to 0°C, and the state of the water, in soil materials subjected to freezing temperatures.

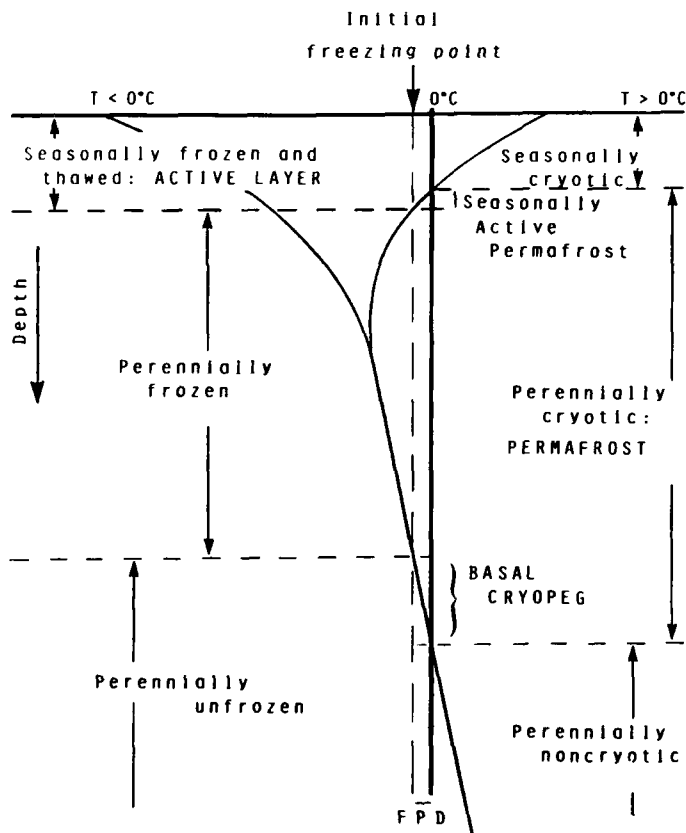


Figure 2. Terms used to describe the temperature relative to 0°C, and the state of the water, versus depth in a permafrost environment.

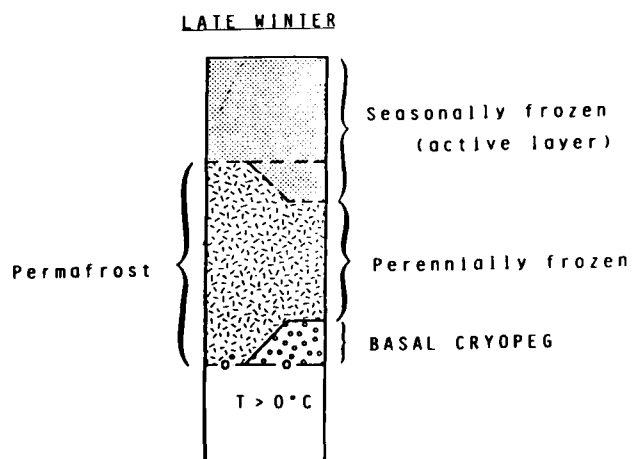
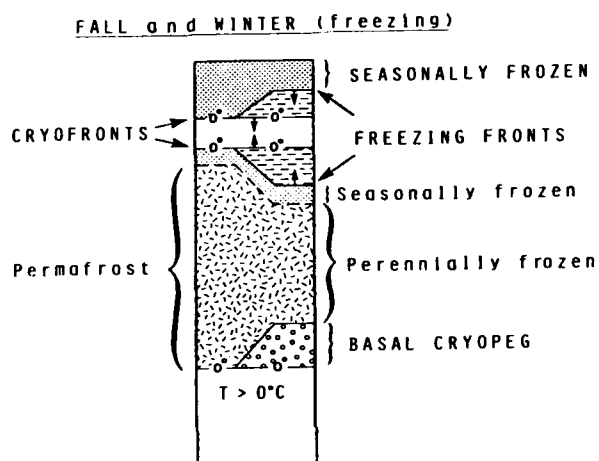
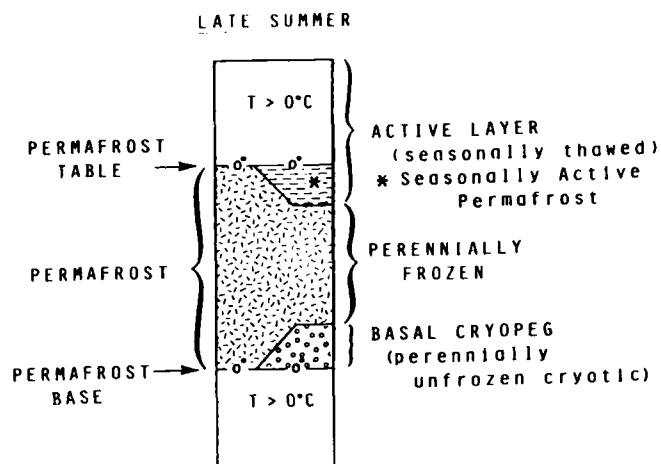


Figure 3. Terms used to describe seasonal changes in the temperature relative to 0°C , and in the state of the water, versus depth in a permafrost environment.

SPRING and SUMMER (Thawing)

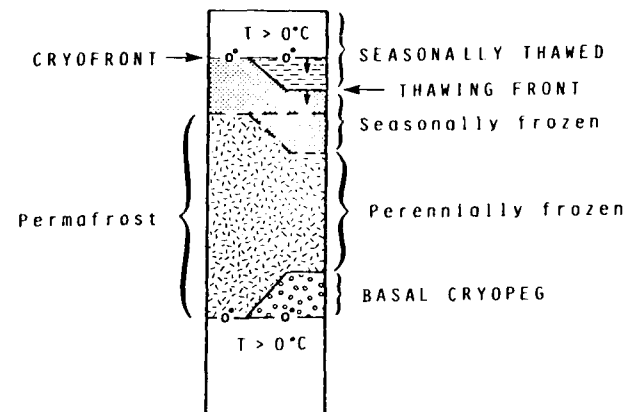


Figure 3 (cont'd). Terms used to describe seasonal changes in the temperature relative to 0°C, and in the state of the water, versus depth in a permafrost environment.

H ₂ O transport to freezing front	Yes	FROST SUSCEPTIBLE: SEGREGATED ICE will eventually form, causing HEAVE and making material ICE-RICH (initially THAW STABLE, eventually becoming THAW SENSITIVE).	FROST SUSCEPTIBLE: SEGREGATED ICE will likely form within one winter, causing HEAVE and making material ICE-RICH (THAW SENSITIVE).
	No	FROST STABLE no HEAVE (THAW STABLE).	POSSIBLY FROST SUSCEPTIBLE: HEAVE in one winter may equal up to 9% of pore volume (THAW SENSITIVE).
		$S_0 < 91\%$	$91\% < S_0 < 100\%$

Figure 4. Stability of ground during freezing and thawing, with respect to initial degree of saturation and potential movement of pore water.

of permafrost and related ground-ice terms. After an extensive review of the permafrost literature the working group has selected a list of over 500 terms to be included in the glossary. At least 200 of those terms are to be provided with definitions (existing, revised or new). The terms cryotic and noncryotic will be included in the draft glossary, as will several other related terms (Fig. 1-5). Although the adoption of these new terms makes it possible to remove the earlier ambiguity from a number of other terms in common use, some of the terms and their implications may sound disturbing or

NONCRYOTIC $T > 0^{\circ}\text{C}$	$A \approx 1.0$ $U + I \approx 0$ DRY	UNFROZEN $I = 0$	$0 < U < 0.9$ $1.0 > A > 0.1$ MOIST to WET	$0.9 < U < 1.0$ $0.1 > A > 0$ WET to SATURATED	$U > 1.0$ $A \approx 0$ SUPERSATURATED (only temporarily, upon THAWING of ICE-RICH ground)
CRYOTIC $T < 0^{\circ}\text{C}$	FPD } DRY (1)	FROZEN = ICE-BEARING $I > 0$	$0 < I < 1.0$ $0.9 > (A+U) > 0$ May be ICE-BONDED (2, 3)	$I > 1.0$ $A \approx 0 ; U \approx 0$ ICE-RICH (3)	

FPD = freezing-point depression

A = fraction of pore volume filled with air and/or other gases.

I = " " " " " " ice.

U = " " " " " " unfrozen water.

(1) Term applies to both *seasonally cryotic ground* and *permafrost*.

(2) I generally increases from low through medium to high with increasing total water content and decreasing temperature.

(3) Terms apply to both *seasonally frozen ground* and *permafrost*.

Figure 5. Terms describing temperature relative to 0°C , and relative air, water and ice contents in permafrost and seasonally frozen ground.

confusing at first glance. Examples are unfrozen permafrost, and seasonally thawed ground, which includes the uppermost (seasonally active) portion of the permafrost.

Unfrozen permafrost (reflecting high salinity or high clay content, or both) has become of increasing concern to engineers and geophysicists, especially those dealing with subsea permafrost as delineated on the basis of temperature measurements. Saline permafrost will commonly be unfrozen unless its temperature is below the initial freezing point of the pore water. If the permafrost is ice-bearing, its presence may be detectable by electrical or electromagnetic methods; it will presumably be detectable by seismic or acoustic methods only if the material is ice-bonded.

Seasonally active permafrost can also be expected to occur where high salinity causes significant freezing point depression.

REFERENCES

- Brown, R.J.E. and W.O. Kupsch (1974) Permafrost terminology. National Research Council of Canada, Ottawa, NRCC 14274, 62 p.
- van Everdingen, R.O. (1976) Geocryological terminology. Canadian Journal of Earth Sciences, 13: 862-867.

TRANSIENT ELECTROMAGNETIC DETECTION OF SUBSEA PERMAFROST

G.G. Walker, K. Kawasaki and T.E. Osterkamp
Geophysical Institute, University of Alaska
Fairbanks, Alaska

For the past year, we have been investigating the occurrence and thickness of permafrost along a north-south transect of Alaska from Prudhoe West Dock to Glennallen. During the spring of 1984, this transect was extended offshore from Prudhoe West Dock to Reindeer Island. Eleven sites were sound-ed using a Geonics EM-37 Transient Electromagnetic (TEM) system; eight of the sites were over sea ice. Most of the sites used square transmitter loops 250 and 500 m on a side. Each transmitter loop was driven at two frequencies to extend the apparent resistivity curves. The two loop sizes produce comple-mentary curves which aid interpretation.

The unusually conductive environment of subsea, saline saturated, and unfrozen sediments produces apparent resistivity curves which are not repre-sentative of late stage behavior. Therefore, ramp time corrections based on a time decay of $t^{-2.5}$ could not be used. Instead, corrections were comput-ed using the full field expression for a homogeneous half space. The resis-tivity of the half space was determined using the definition of early stage apparent resistivity, ρ_E :

$$\rho_E = \frac{\pi r^5 V}{3000 M_r 2^N M_t} \quad (1)$$

where r is radius of transmitter loop in meters, V is measured voltage in millivolts, M_r is the receiver moment defined as the effective area of the receiver coil times preamplifier gain, N is gain setting of the receiver electronics, and M_t is the transmitter magnetic dipole moment defined as the driving current times the transmitter loop area in ampere-meters squared.

The resistivity found from the early stage definition should be the same resistivity as the first layer and, indeed, the f found from curve matching using the Soviet theoretical curves (Rabinovich 1977) agrees very well with that for the early stage. Additionally, the forward modeling program devel-oped by Anderson (1981) produces single-layer curves which, when matched to the experimental curves, have a best fit resistivity that agrees with the early stage values of resistivity.

Once the first-layer resistivity is found, it is used to correct the data for a ramp time turn-off. The full field expression for the voltage measured in a receiver coil over a homogeneous half space of resistivity f is (adapted from Kaufman and Keller 1983):

$$V = \frac{3000 M_r M_t \rho}{\pi r^5 2^{-n}} \left| \theta(u) - (2/\pi)^{1/2} \left(u + \frac{u^3}{3} \right) \exp\left(-\frac{u^2}{2}\right) \right| ,$$

$$u = r \left| \frac{2 \pi}{\rho t 10^7} \right|^{1/2} \quad (2)$$

where $\theta(u)$ is the probability integral, t is time measured after turn-off, and V is once again the measured voltage in millivolts. The other quantities are as defined in equation 1.

If the earth is a linear transform system, there exists a simple relationship between the theoretical response due to a step drive and the response due to a drive with a finite ramp turn-off. If the step response is designated $s(t)$ and the measured response is designated $m(t)$, then the relationship is:

$$m(t_0) = \frac{1}{T} \int_{t_0}^{t_0 + T} s(t) dt, \quad (3)$$

where t_0 is gate time, t is time after turn-off, and T is the duration of the ramp. The correction factors are determined by evaluating the full field expression of eq 2 for $s(t)$ using the early value of resistivity from eq 1, producing the expected measured values of $m(t)$, and taking the ratio at each gate time for the correction factor at that gate time. The correction factors produced above are multiplied by the actual measured signal at each gate to produce the corrected curve. The corrected apparent resistivity curves differed only slightly from the uncorrected curves. Generally, curve matching using two or more layers produced models which were the best fit to both the corrected and uncorrected curves.

First-layer resistivities ranged from 1.6 to 5 ohm-m over the sea ice sites. The values were highest near shore and decreased with distance offshore. The thickness of the unfrozen layer increased with distance offshore. Permafrost thickness, when discernible, appears to decrease with distance offshore. Permafrost resistivity, although not as precisely determined as the first-layer resistivity, appears to be about 200 ohm-m throughout the

transect. Curve-matching often seems to require third-layer resistivities to be even less than the first-layer resistivity.

The interpreted results are presented and compared to available ground truth. Although the results seem reasonable, they do not always compare well to the analytic work of Osterkamp (unpublished), which predicts the depth to permafrost from an analytic solution to a thermal model. Consistently, the TEM data predict a thicker layer of unfrozen material than the thermal model. The TEM work of Ehrenbard et al. (1983), while not along the exact time line, is comparable to this work, and apparently predicts even larger unfrozen layer thicknesses while predicting permafrost to be somewhat thinner than found in this investigation.

REFERENCES

- Anderson, W.L. (1981) Calculation of transient soundings for a central induction loop system (Program TCILoop). U.S. Geological Survey Open File Report 81-1309.
- Ehrenbard, R.L., P. Hoekstra and G. Rozenberg (1983) Transient electromagnetic soundings for permafrost mapping. Proceedings, Fourth International Conference on Permafrost. Washington, D.C.: National Academy Press, p. 272-277.
- Kaufman, A.A. and G.V. Keller (1983) Frequency and transient soundings. Amsterdam: Elsevier.
- Rabinovich, B.I. and R.G. Stepanova (1972) Album of three-layer curves for transient sounding in the near zone (type Q). ISIG SO AN SSSR and SNIIGTMSA, issue 5, Novosibirsk.
- Rabinovich, B.I. (1977) Two-layer sounding curves for the transient horizontal magnetic component of the field in the near-zone. Geol. Geofiz., 11:148-152.

APPENDIX A: PARTICIPANTS

Sherburn Abbott
Staff Polar Research Board
2101 Constitution Avenue NW
Washington, DC 20418

Duwayne M. Anderson
Associate Provost for Research
Texas A&M University
East Bizzell Hall, Room 305
College Station, TX 77843

Steve A. Arcone
CRREL
72 Lyme Road
Hanover, NH 03755

Nolan B. Aughenbaugh
University of Alaska
School of Mineral Sciences
Fairbanks, AK 99701

Gerard Beaudain
Amoco Production
P.O. Box 800
Denver, CO 80201

Robert J. Bisdorf
U.S. Geological Survey
MS964 Box 25046
Denver Federal Center
Denver, CO 80225

Steve M. Blasco
Bedford Institute
Geological Survey Canada
Dartmouth, N.S., Canada B2Y4A2

Mark Blohm
Earth Technology Corporation
2801 Youngfield, Suite 390
Golden, CO 80401

Max C. Brewer
U.S. Geological Survey
4200 University Drive
Anchorage, AK 99508

Jerry Brown
CRREL
72 Lyme Road
Hanover, NH 03755

Kerry J. Campbell
McClelland Engineers
2140 Eastman Avenue
Ventura, CA 93003

L. David Carter
U.S. Geological Survey
4200 University Drive
Anchorage, AK 99508

Douglas R. Choromanski
Mineral Management Service
800 A Street
Anchorage, AK 99501

Robert Corwin
Harding Lawson Associates
7655 Redwood Blvd.
Novato, CA 94948

Louis De Goes
17215 N.E. 8th Street
Bellevue, WA 98008

David Esch
Alaska Dept. of Transportation
and Public Facilities
2301 Peger Road
Fairbanks, AK 99701

Lauren Evans
Earth Technology Corporation
2801 Youngfield, Suite 390
Golden, CO 80401

Oscar J. Ferrians
U.S. Geological Survey
345 Middlefield Road
Menlo Park, CA 94025

David Fitterman
U.S. Geological Survey
Box 25046
Denver Federal Center MSG64
Denver, CO 80225

Guy Fortin
Geoterrex Ltd.
2060 Walkley Road
Ottawa, Ontario, Canada K1C3P5

Hugh French
Department of Geology
University of Ottawa
Ottawa, Ontario, Canada KLN6N5

R.B. French
Sohio Petroleum Company
1 Lincoln Center, Suite 1300
5400 LBJ Freeway
Dallas, TX 75240

Kevin J. Freeman
Earth Technology Corporation
200 W. Merrer, Suite 502
Seattle, WA 98119

L.C.M. Haakmeester
516 Wilderness Drive
Calgary, Alberta, Canada T2J1Z2

James S. Hagihara
Bureau of Land Management
Bldg. 50, Denver Federal Center
Denver, CO 80225

Stuart Harris
Geography Department
University of Calgary
Calgary, Alberta, Canada

J.A. Heginbottom
Geological Survey of Canada
601 Booth Street
Ottawa, Ontario, Canada K1A0E8

J. Henderson
Geo-Physi-Con Ltd.
5810 2nd Street SW
Calgary, Alberta, Canada T2H0H2

Chris Heuer
Exxon Production Research
P.O. Box 2189
Houston, TX 77001

Pieter Hoekstra
Earth Technology Corporation
2801 Youngfield, Suite 390
Golden, CO 80401

Jim A. Hunter
Geological Survey of Canada
601 Booth Street
Ottawa, Ontario, Canada K1A0E8

Mark Jennings
Sohio Petroleum Company
50 Fremont Street
San Francisco, CA 94105

Douglas Kane
University of Alaska
Institute of Water Resources
Fairbanks, AK 99701

Koji Kawasaki
Geophysical Institute
University of Alaska
Fairbanks, AK 99701

George V. Keller
Colorado School of Mines
Geophysics Department
Golden, CO 80401

David L. Klein
Sohio Petroleum Company
5400 LBJ Freeway
Dallas, TX 75240

Austin Kovacs
CRREL
72 Lyme Road
Hanover, NH 03755-1290

Ray A. Kreig
R.A. Kreig and Associates
1503 West 33rd Avenue
Anchorage, AK 99503

John Kretzschmar
Sohio Petroleum Company
5400 LBJ Freeway
Dallas, TX 75240

Arthur H. Lachenbruch
U.S. Geological Survey
345 Middlefield Road
Menlo Park, CA 94025

Dan Lawson
CRREL
72 Lyme Road
Hanover, NH 03755

M.G. Loudin
MEPSI
Mobil North Alaska Exploration
P.O. Box 900
Dallas, TX 75221

C.W. Lovell
Purdue University
School of Engineering
Grissom Hall
W. Lafayette, IN 47907

J. Ross Mackay
Department of Geography
University of British Columbia
Vancouver, B.C., Canada V6T 1W5

Frank Maxwell
Hardy Associates
221-18th Street SE
Calgary, Alberta, Canada

Jorge A. Mendiguren
Chevron
P.O. Box 446 L
La Habra, CA

Michael C. Metz
GeoTec Services, Inc.
14379 W. Ellsworth Avenue
Golden, CO 80401

Bob Miller
TSA Systems, Inc.
P.O. Box 1920
Boulder, CO 80306

John Morack
Physics Department
University of Alaska
Fairbanks, AK 99701

Leslie A. Morrissey
Ames Research Center MS 242-4
Technicolor Graphic Services
Moffett Field, CA 94035

K. Gerard Neave
Northern Seismic Analysis
R.R. #1
Echo Bay, Canada POS1C0

Warren H. Neff
Phillips 66
166 Geosciences Blvd.
Bartlesville, OK 74004

J.F. Neuenschwander
Standard Oil Company (Ohio)
Engineering Department
Midland Building (1420 CEI)
Cleveland, OH 44115

Robert J. Neukirchner
GeoTec Services Inc.
1626 Cole Blvd. #201
Golden, CO 80401

Gary Olhoeft
U.S. Geological Survey
P.O. Box 25046 MS 964
Denver Federal Center
Denver, CO 80225

Thomas E. Osterkamp
University of Alaska
Geophysical Institute
Fairbanks, AK 99701

R.M. Otis
MEPSI
Mobil North Alaska Exploration
P.O. Box 900
Dallas, TX 75221

Samuel I. Outcalt
University of Michigan
Department of Geography
Ann Arbor, MI 48104

Donald R. Palmore
MEPSI
Mobil North Alaska Exploration
P.O. Box 900
Dallas, TX 75221

John K. Petersen
University of Alaska
Geophysical Institute
Fairbanks, AK 99701

Troy L. Péwé
Arizona State University
Department of Geology
Tempe, AZ 85281

Loren Phillips
Colorado State University
Department of Earth Resources
Ft. Collins, CO 80526

Jean A. Pilon
Earth Physics Branch
1 Observatory Cres.
Ottawa, Ontario, Canada K1A0Y3

Susan Pullan
Geological Survey of Canada
601 Booth Street
Ottawa, Ontario, Canada K1A0E8

Stuart E. Rawlinson
Alaska Dept. of Nat. Resources
Div. of Geol. & Geophy. Surveys
794 University Avenue
Fairbanks, AK 99701

David J. Roberts
Chevron USA Alaska Division
2003 Diamond Blvd.
Concord, CA

Jim C. Rogers
Dept. of Electrical Engineering
Michigan Technical University
Houghton, MI 49931

Gregory Rozenberg
Geo-Physi-Con Co., Ltd.
5810 2nd Street SW
Calgary, Alberta, Canada T2H0H2

Rodney D. Schlecht
Phillips 66
8055 E. Tufts Avenue Parkway
Denver, CO 80231

Paul Sellmann
CRREL
72 Lyme Road
Hanover, NH 03755

A.K. Sinha
Geological Survey of Canada
601 Booth Street
Ottawa, Ontario, Canada K1A0E8

Charles W. Slaughter
Institute of Northern Forestry
308 Tanana Drive
Fairbanks, AK 99701

Richard P. Standish
Earth Technology Corporation
2801 Youngfield, Suite 390
Golden, CO 80401

A.F. Stirbys
Frontier Development Division
P.O. Box 130
Calgary, Alberta, Canada T2PH7

Al Taylor
Energy Mines and Resources
Earth Physics Branch
1 Observatory Cres.
Ottawa, Ontario, Canada K1A0Y3

D.H. Thorson
MEPSI
Mobil North Alaska Exploration
P.O. Box 900
Dallas, TX 75221

Ken Thomas
Esso Resources Canada Ltd.
237-4 Avenue SW
Calgary, Alberta, Canada T2P0H6

Larry Toimil
Harding Lawson Associates
7655 Redwood Blvd.
Novato, CA 94948

James N. Towle
Phoenix Geophysics Inc.
5590 Havana Street
Denver, CO 80302

R.O. van Everdingen
NHRI Environment Canada
101-4616 Valiant Drive NW
Calgary, Alberta, Canada T3A0X9

Ted Vinson
Oregon State University
Department of Civil Engineering
Corvallis, OR 97331

D.A. Walker
INSTAAR
University of Colorado
Boulder, CO 80309

David Walker
Sohio Petroleum Company
2 Lincoln Center, Suite 801
5420 LBJ Freeway
Dallas, TX 75240

H.J. Walker
Department of Geography
Louisiana State University
Baton Rouge, LA 70802

Gerald G. Walker
Geophysical Institute
P.O. Box 82036
University of Alaska
Fairbanks, AK 99708

A.L. Washburn
Quaternary Research Center
(AK-60)
University of Washington
Seattle, WA 98159

John R. Watterson
U.S. Geological Survey
Denver Federal Center MS 955
Denver, CO 80225

Jeffrey Weaver
Sohio Petroleum Company
2 Lincoln Center
5420 LBJ Freeway
Dallas, TX 75240

Ron Weaver
World Data Center for Glaciology
University of Colorado
Boulder, CO 80309

Jerry Wickham
McClelland Engineers
2140 Eastman
Ventura, CA 93003

David S. Woodroffe
Dobrocky Seatech
9865 West Saanich Road
Sidney, B.C., Canada V8L4M7

Stephen R. Young
Mobil Oil Corporation
P.O. Box 5444
Denver, CO 80217

J.R.N. Zinkhan
Shell Canada Resources, Ltd.
P.O. Box 100 STN "M"
Calgary, Alberta, Canada T2P2H5

Permafrost Research: An Assessment Of Future Needs

7 Exploration Geophysics

PREVIOUS PAGE
IS BLANK

INTRODUCTION

As stated earlier in this report, permafrost underlies approximately three quarters of the land area of Alaska, most of the continental shelf of the Beaufort Sea, parts of the shelf in near-shore areas of the Chukchi and Bering seas, and some of the alpine areas of the contiguous 48 states and Hawaii. Where permafrost contains massive ice or is ice rich, severe environmental and engineering problems can result if it is thawed. These problems have been illustrated during the design and construction of the trans-Alaska pipeline system. In addition, Alaskan highways, railroads, airports, public and private buildings, and houses show the disastrous results that can occur when ice-rich permafrost soils thaw. Avoidance of such sites and use of specialized construction techniques are two ways of dealing with these problems. Both approaches require knowledge of the permafrost distribution and of the precise position and extent of massive ground ice and ice-rich soils. Detection of the presence of permafrost and ground ice is a problem for exploration geophysics, a field in which airborne, surface, and borehole methods are applied to:

- o Detecting the presence or absence of permafrost, massive ground ice, and ice-rich soils.
- o Measuring their physical and mechanical properties in situ.
- o Determining the distribution (horizontal and vertical extent) of permafrost, with emphasis on the position of its upper and lower boundaries (equivalently, its thickness).

Committee on Permafrost
Polar Research Board
Commission on Physical Sciences, Mathematics, and Resources
National Research Council

NATIONAL ACADEMY PRESS
Washington, D.C. 1983

- o Establishing the properties and thickness of the active layer on a seasonal basis.

- o Solving such environmental and engineering problems as locating groundwater in permafrost regions, detecting thawed zones for electrical grounding, and selecting pipeline and highway routes through permafrost terrain.

Demand for simple, efficient, and reliable detection methods and measurement techniques has increased with the level of resource exploration and recovery in Alaska. Recently proposed large construction projects (e.g., the gas pipeline, paving of part of the Alaska Highway in Canada, and hydroelectric power projects) will require detailed knowledge of permafrost and ground-ice conditions. Geophysical methods for detecting and establishing the properties of permafrost and ground ice should reduce the costs of such projects while ensuring a structurally sound design. Unfortunately, many of the methods and procedures for interpreting data that are currently available are not yet adequate. In addition, their effectiveness or limitations when applied to permafrost terrain consisting of nonhomogeneous, nonisotropic, and widely varying soil types containing varying quantities of ice have not been established.

RESEARCH NEEDS

The international and national conferences on permafrost have produced a number of papers on the application of the methods of exploration geophysics to permafrost problems. One of the most troublesome problems in evaluating the application of geophysical instruments to permafrost studies is that of determining the subsurface conditions in sufficient detail to understand what an instrument may be detecting. This ground truth can be provided by using sites where the subsurface conditions are well known from drilling and the application of other geophysical instruments. Construction projects, particularly highway road cuts, offer unique opportunities for defining subsurface conditions. More recently, the University of Alaska has constructed on its campus an artificial buried ice mass in permafrost terrain. This buried ice mass is to be used to evaluate geophysical instruments for their effectiveness in detecting it. There is need to develop and maintain

such sites for studies of the active layer, ground-ice detection, permafrost thickness, and permafrost properties.

Application of most geophysical instruments to permafrost problems is based on detecting contrasts between unfrozen soils, permafrost, and ground-ice masses. These contrasts depend on material type, water and ice content, temperature, and other parameters, so that no one method will work for all problems. One of the major difficulties in exploration geophysics is to select the proper instrument for the problem and conditions being investigated. Also, because of variations in permafrost properties, the successful use of a method at one site does not mean that it can be used at all sites.

Electrical Methods

The direct current (dc) resistivity method is relatively inexpensive for investigating the horizontal and vertical distribution of permafrost. It has been used for estimating material types, ground-ice concentrations, and permafrost thickness and for mapping permafrost distribution. In recent years, attempts have been made to extend the method to subsea permafrost in marine areas having water salinities lower than normal seawater. However, additional information is needed both to evaluate the application of dc resistivity methods in offshore areas and to investigate their use in detailed mapping of massive ground ice and ice-rich permafrost. Problems with electrode contact in frozen soils need to be resolved.

Measurements of spontaneous polarization (SP) effects in permafrost are not adequate to assess its application as a surface method. The presence of freezing potentials during the freezing of the active layer may present an opportunity for further investigation of this method.

For the induced polarization (IP) method, the degree of polarization of frozen soil varies with temperature, unfrozen water content, and salinity of the pore water. Field measurements have proved the utility of the technique for permafrost studies. Present understanding of the method is limited, and future progress will depend on a greater understanding of the response of frozen soils to induced polarization.

Magnetotelluric (MT) methods involving both natural

and artificial fields have been used to determine material type and permafrost thickness and distribution and to detect ground ice. Airborne radio wave methods have also been used to map permafrost on a large scale. Studies are needed to evaluate further the usefulness of MF methods for mapping permafrost and measuring its thickness.

Inductive electromagnetic (EM) methods, employing both ground and airborne systems, have been used increasingly to map permafrost distribution, thickness, and material type and to obtain information on ground ice. These methods require further evaluation in permafrost terrain. New transient EM methods appear to be capable of determining permafrost thickness in the onshore environment and possibly in shallow water offshore. Although their use has been limited, they appear to be promising and should be investigated.

With ground-probing radar systems, information on the depth and geometry of massive ground ice and changes in material type has been obtained, although penetration is greatly restricted in fine-grained soils with high moisture contents. These radar systems have potential applications to engineering problems in coarse-grained permafrost, in active layer studies, and in ground-ice investigations. Research should focus on additional evaluation of these systems in permafrost terrain and on improved methods of data handling and interpretation.

Time-domain reflectometry (TDR) methods have been used for studies of the active layer. However, the requirement for a probe installation and the limited depth of penetration restrict them to very shallow levels. Further research is needed.

Radiofrequency interferometry (RFI) methods have not been commonly used in permafrost studies in North America.

Measurements of magnetic susceptibility in permafrost terrain containing magnetic material have shown that ice wedges can be associated with magnetic anomalies.

Seismic and Acoustic Methods

Seismic refraction methods have been used for permafrost studies, both on land and offshore. This technique is well suited for determining the position of the top of ice-bonded permafrost and it has been used for mapping

the active layer and for permafrost distribution studies. It has also been used to characterize permafrost properties and material types, since velocity can be measured accurately. Interpretation techniques could be improved for shallow investigations, including greater use of amplitude and frequency information (attenuation of refraction data). Data processing could also be improved to reduce velocity-depth scatter in single-ended profiles.

Seismic reflection surveys, most commonly used on large-scale studies, have provided information on permafrost velocities and thickness based on velocity-depth functions. Computer-assisted data analysis is required. However, qualitative analysis can also be used as an indicator of subsurface variations. For example, attenuation of the high-frequency part of the signal can be an indication of changes in material properties; large-amplitude reverberations have been used to indicate ice-bonded material below the seabed.

Acoustic reflection methods are usually applied to shallow permafrost studies in the marine environment. This technique is best suited for profiling the top of the ice-bonded permafrost and for studies of the distribution of shallow permafrost. Good resolution of even fairly small features is possible due to the short wavelength of the signal source, but the lack of velocity data makes interpretation qualitative and generates requirements for supporting observations based on drilling or some other geophysical technique such as marine refractions. Improvements in noise suppression and signal penetration would be an advantage for subsea permafrost studies conducted in shallow waters.

Borehole-seismic methods have been used for permafrost investigations in shallow boreholes, mining operations, and in deep holes as part of petroleum exploration activities. Information obtained on permafrost thickness and velocity distribution can be correlated with changes in material type and properties. Wave-front diagrams obtained from surface arrays combined with arrays at depth may be used to define variations in permafrost structure and possibly for mapping zones rich in ground ice. Additional information on variations in permafrost properties could be acquired by study of shear-wave velocities by means of tube-wave analysis.

Borehole-acoustic methods are used in permafrost logging as part of petroleum exploration programs. Thawed material adjacent to the hole causes problems in

attempts to acquire permafrost data. New small-diameter sonic tools may improve application to shallow geological and engineering investigations if the transducers can be coupled directly to the undisturbed frozen walls of boreholes.

Other seismic methods might be applied in permafrost studies. With appropriate equipment and array design, surface-wave data can be acquired, providing information necessary for estimating the thickness of the thawed surface layer as well as shear velocities in ice-bonded permafrost. Shear-wave data combined with compressional-wave velocities can also be used to estimate properties of in situ material.

Under some conditions, thickness of ice-bonded permafrost can be estimated from analysis of the propagation modes and decay characteristics of seismic energy trapped in high-velocity layers.

Laboratory studies of permafrost have contributed to our understanding of the way that velocity varies as a function of material properties and temperature. Additional observations are needed to improve interpretation for a range of materials, particularly those characteristic of the saline marine environment, including saturated materials simulating gas-bearing sediments. The velocity observations should include data on both compressional and shear waves.

Other Methods

Gravity methods can provide an estimate of the amount of excess ice in a permafrost profile where ice quantities are large. Research is needed to improve interpretations by evaluating the method at sites where ground-ice volumes are well known.

Well-logging methods have been used to determine the presence or absence of permafrost and to map its horizontal and vertical extent, top and bottom (thickness), ice and water content, lithology, and properties. In addition to temperature logs, as discussed in previous sections, electrical, acoustical, and nuclear logs have been run in permafrost boreholes. Both down-hole and cross-hole methods have been employed. Direct current resistivity, SP, EM, acoustic (sonic and crystal cable), gamma ray, and neutron logs are commonly obtained in deep boreholes and can be used to investigate permafrost conditions. Direct current resistivity measurements

have been made in shallow boreholes to locate interfaces between frozen and thawed zones. Both gamma ray and neutron logs were used to determine density and moisture content in shallow boreholes drilled during construction of the trans-Alaska pipeline. Small-diameter (5 cm or less) borehole logging tools should be developed and evaluated. Tools and interpretation methods for determining ice content quantitatively are especially needed.

RECOMMENDATIONS

Two types of research are critical to exploration geophysics:

We recommend that highest priority be given to research involving the detection and quantitative determination of the position, geometry, and quantity of ground ice in permafrost.

We recommend that high priority be given to research involving the development and evaluation of equipment and methods that can be used to quantify permafrost distribution in both the onshore and offshore environments.

In addition, we recommend that research directed toward measuring in situ permafrost properties using the methods of exploration geophysics be expanded to include both onshore and offshore environments and seasonal effects on permafrost properties.

To ensure maximum benefits from application of exploration geophysical methods to permafrost problems, we recommend that research to develop new equipment, to improve data handling and processing, and to refine the techniques of interpretation and understanding of methods be encouraged.

END

FILMED

9-85

DTIC